ISTANBUL TECHNICAL UNIVERSITY ★ GRADUATE SCHOOL OF SCIENCE ENGINEERING AND TECHNOLOGY

EXPERIMENTAL STUDY OF MINIMUM QUANTITY LUBRICATION EFFECT ON COMPACTED GRAPHITE IRON MACHINING

M.Sc. THESIS

Armin Bijanzad

Department of Mechanical Engineering

Materials & Manufacturing Programme

Thesis Advisor: Doç. Dr. Mustafa BAKKAL

JUNE 2013

ISTANBUL TECHNICAL UNIVERSITY ★ GRADUATE SCHOOL OF SCIENCE ENGINEERING AND TECHNOLOGY

EXPERIMENTAL STUDY OF MINIMUM QUANTITY LUBRICATION EFFECT ON COMPACTED GRAPHITE IRON MACHINING

M.Sc. THESIS

Armin Bijanzad
(503101301)

Department of Mechanical Engineering

Materials & Manufacturing Programme

Thesis Advisor: Doç. Dr. Mustafa Bakkal

JUNE 2013

İSTANBUL TEKNİK ÜNİVERSİTESİ ★ FEN BİLİMLERİ ENSTİTÜSÜ

KOMPAKT GRAFİTLİ DÖKME DEMİRİN TORNALAMA SIRASINDA MİNİMUM MİKTARDA YAĞLAMANIN ETKİSİ

YÜKSEK LİSANS TEZİ

Armin Bijanzad
(503101301)

Makina Mühendisliği Anabilim Dalı

Malzeme ve İmalat Programı

Tez Danışmanı: Doç. Dr. Mustafa Bakkal

HAZİRAN 2013

Armin Bijanzad, a **M.Sc.** student of ITU **Graduate School of Mechanical Engineering** student ID 503101301, successfully defended the **thesis** entitled "**EXPERIMENTAL STUDY OF MINIMUM QUANTITY LUBRICATION EFFECT ON COMPACTED GRAPHITE IRON MACHINING**", which he prepared after fulfilling the requirements specified in the associated legislations, before the jury whose signatures are below.

Thesis Advisor :	**Doç. Dr. Mustafa BAKKAL** Istanbul Technical University Mechanical Engineering Department	....
Jury Members :	**Doç.Dr. Turgut GÜLMEZ** Istanbul Technical University Mechanical Engineering Department	....
	Y.Doç. Dr. Murat ÇELİK Boğaziçi University Mechanical Engineering Department	....

Date of Submission : 22 May 2013
Date of Defense : 6 June 2013

To Minoo, Yahya and Ayin,

FOREWORD

First of all, I would like to express my deep appreciation to my thesis advisor Doç.Dr. Mustafa Bakkal for giving me the chance to study in my MSc. program and for his everlasting academic support and guidance throughout this research. I have benefited from him as a role-model of an excellent researcher.

I would also like to thank ‘ Ali Taner Kuzu’ and ‘ Umut Karagüzeli’ who has never got tired of my endless questions and for their valuable comments on this thesis and being helpful during the experiments. Special thanks to all technicians of mechanical department who helped me with their useful advices during my experimental procedure.

Finally, I am so pround of being the son of Minoo and Yahya who are my living reason. I want to thank them for their neverending love of me. This work would not happen without their everlasting supports in my lifetime. I also, would like to thank my sister Ayin with all my heart for her kindness and support. I hope her success and happiness in her lifetime.

‘ Yaşasın Azarbaycan, Yaşasın Tabriz ’

June 2013

Armin BIJANZAD
(Mechanical Engineering)

TABLE OF CONTENTS

Page

ABBREVIATIONS

CGI	: Compacted Graphite Iron
MQL	: Minimum Qunatity Lubrication
SEM	: Scanning Electron Microscope
SG	: Spheroidal Graphite
CNC	: Computer Numerical control
NC	: Numerical control
PCD	: Polycrystalline Diamond
PCBN	: Polycrystalline Boron Nitride
CBN	: Cubic Boron Nitride
RE	: Rare Earth
BCIRA	: British Cast Iron Research Association
LAM	: Laser-Assisted Machining
RPM	: Revolutions Per Miniute

SYMBOLS

F_t	: Tangential Force
F_f	: Feed Force
F_r	: Radial Force
F	: Resultant Force
i	: Inclination Angle
ϕ_c	: Shear Angle
τ_s	: Shear Stress
σ_s	: Normal Stress
α_r	: Tool Rake Angle
β_a	: Average Friction Angle
h	: Uncut Chip Thickness
L_c	: Shear Plane Length
r_c	: Compression Ratio
K_t	: Tangential Cutting Force Coefficient
K_f	: Feed Force Coefficient
P_n	: Normal Plane
V	: Cutting Velocity
P	: Cutting Force Constant, Power
q	: Cutting Force Constant
K_{tc}	: Tangential Cutting Force Coefficient Relates to Cutting Condition
K_{fc}	: Feed Force Coefficient Relates to Cutting Condition
K_{te}	: Tangential Cutting Force Coefficient Relates to Cutting Edge
F_u	: Friction Force
F_v	: Normal Force
H_c	: Deformed Chip Thickness
μ_a	: Friction Coefficient On The Rake Face
θ_i	: Acute Projection Angle
θ_n	: Oblique Cutting Angle Parameter In Normal Plane
ϕ_n	: Shear Velocity In Normal Plane
ϕ_i	: Shear Velocity In Inclination Angle
η	: Chip Flow
$\mathcal{P}_t$’	: Nondimensional Power
ψ_r	: Chip Flow Angle
a, a_p	: Depth Of Cut
d	: Diameter Of Workpiece
α_f	: Side Rake Angle
α_p	: Back Rake Angle
α_o	: Orthogonal Rake Angle
α_n	: Normal Rake Angle
K_r’	: End Cutting Edge Angle

Cl_p	: End Relief Angle
Cl_f	: Side Relief Angle
dθ	: Angular Increment
K_{re}	: Radial Component of Cutting Force
$\mathcal{T}$	: Torque
Nm	: Newton Metre
W	: Watt
R_s	: Feed Mark's Amplitude
T	: Tool Life
C	: Feed Rate
C_t	: Constants of Tool-Workpiece Machinability Characteristics
p'	: Constants of Tool-Workpiece Machinability Characteristics
q'	: Constants of Tool-Workpiece Machinability Characteristics
γ_n	: Normal Rake Angle
ε	: Shear Strain
ε_B	: Shear Strain at Breaking Limit
ε_F	: Shear Strain at Fraction Point
ε_0	: Shear Strain at Zero Point
C°	: Celsius
V_B	: Flank Wear Amount
V_{cr}	: Crater Wear Amount
V_{ox}	: Oxidation Zone Length
R_a	: Surface Roughness
µm	: Micro metre
MPa	: Mega Pascal
Mm/rev	: Milimetre Per Revolution
m/min	: Metre per Minute

LIST OF TABLES

Page

LIST OF FIGURES

Page

EXPERIMENTAL STUDY OF MINIMUM QUANTITY LUBRICATION EFFECT ON COMPACTED GRAPHITE IRON MACHINING

SUMMARY

Compacted graphite cast iron (CGI) is one alternative engine material to gray cast iron. The cost effective and environmentally sensitive process improvement of compacted graphite iron (CGI) is one the major concern of today’s manufacturing world due to the allure of mechanical properties of CGI. Beneficiary properties of CGI, such as high strength, in contrast with gray cast iron, make it one of the valuable material in automotive industry. However, poor machinability of CGI increases the production costs. Many suggested ways to deal with the poor machinability of CGI had lack of sufficient results or was not favorable economically in the manufacturing industries. Despite many efforts in CGI machinability improvement to reach a level that is comparable with other type of cast irons, it is evident that much studies needs to be investigated in this area.

This study is assessed the efficiency of minimum quantity lubricant (MQL) in CGI turning when compared to the dry cutting. MQL is a sustainable method in which the mixture of oil and air sprays over cutting zone for cooling and lubrication means. There is no cost advantage only in MQL, but also has the advantages in terms of environmental and health protection. During all machining experiments MQL was applied externally to the cutting zone and depth of cut was kept constant as 1 mm. Different cutting parameters and ceramic cutting tool is selected for CGI turning. The turning test were conducted in a wide range of cutting parameters, which are three different cutting speed (100, 200, 300 m/min) and feed rates (0.1, 0.2, 0.3 mm/rev) at constant 1mm depth of cut.

The MQL efficiency is evaluated through cutting force and surface roughness measurements, optical and SEM analysis of chip formation and tool wear analysis. Cutting forces, flank and crater wear values were measured and evaluated. Results showed that MQL use provided a reduction in the amount of only 5-10% in cutting forces, whereas 25% in surface roughness and significant 30% in crater wear.

SEM analysis also revealed much more clear and smooth cutting edges on tool surfaces in MQL used tests. However no cutting forces difference was observed between dry and MQL cutting conditions.

KOMPAKT GRAFİTLİ DÖKME DEMİRİN TORNALAMA SIRASINDA MİNİMUM MİKTARDA YAĞLAMANIN ETKİSİ

ÖZET

Kompakt grafitli dökme demir (CGI), son zamanlarda mekanik özellikleri bakımından otomotiv sanayisinde artan bir şekilde kullanılmaya başlanmıştır. Bunun sebebi otomotiv sanayisinin beklentilerinden biri olan daha küçük boyutta, hafif, az tüketen ve az gaz salınımı olan motor ve aksamları üretilmesine yardımcı olmasıdır. Kompakt grafitli dökme demirler mükemmel dayanım, süneklilik, aşınma direnci gibi mekanik özelliklere sahip oldukları için iş makinelerinde ve ulaşım ekipmanlarında, krank şaftı, fren diskleri, volanlar, debriyaj parçaları, eksoz manifoltları, motor kapağı ve motor blokları gibi parçaların yapımında kullanılmaktadırlar. Kompakt grafitli dökme demirler gri dökme demirle karşılaştırıldığında, yüksek basınçlı yanma odalarının imalatına daha elverişli, daha verimli yanma ve düşük emisyon değerleri elde edilmesine olanak sağlamaktadır. Kompakt grafitli dökme demir ile daha ince et kalınlığında parça üretmek mümkün olup daha hafif motorların imalatı söz konusu olabilmektedir. İlk bulundukları yıllarda sınırlı miktarlarda üretilebilen kompakt grafitli dökme demirler, günümüzde seri üretime uygun proseslerin gelişmesi ile büyük miktarlarda da üretilebilmektedirler.

Grafit fazının şeklinden dolayı mekanik özellikleri kır dökme demir ile küresel dökme demirin arasında değerler almaktadır. Grafitlerinin sahip olduğu bu özellik nedeniyle, kompakt grafitli dökme demirlerin dayanım, özellikle de yorulma dayanımı açısından performansları kır dökme demire göre daha iyidir. Kompakt grafitli dökme demir ve gri dökme demirdeki özellik farklılıkları iç yapıyla ilgilidir. Grafit partikülleri daha kalın ve kısa olduğu için, matris ve bu partiküller arasında büyük miktarda yapışma (strong adhesion) oluşur ve çentik etkisi grafitlerin geometrisinden dolayı azalır buda daha çok çekme dayanımını sağlar.

Ayrıca, grafitin şekli ve dağıtım biçimi, yüksek mukavemetli ve çekme dayanımlı, geliştirilmiş süneklik (improved ductility) ve yüksek elastiklik modülüne (higher modulus of elasticity) neden olur.

Kompakt grafitli dökme demir geçmişte, Küresel dökme demir (SG) üretim sırasında yanlışlıkla, yetersiz düzeyde magnezyum veya seryum katılmasından dolayı üretilmiştir. Ancak, 1965 yılından sonra, farklı üretim teknolojisi gerektiren farklı özelliklere sahip bir malzeme olarak dökme demir ailesinde yerini almıştır. Kompakt grafitli dökme demir, gri dökme demir ve aluminyüma göre daha fazla yorulma dayanımı vardır ki bu özellikler onu otomotiv sanayisinde alternatif bir malzeme haline getirebilir. Grafit parçacıkları gri dökme demir de olduğu gibi rastgele dağılmıştır, ancak aradaki fark ötektik hücre içinde en yakın komşularına bağlı uzatılmış yuvarlak kenarlı, daha kısa ve daha kalın olan grafit partikülleri ile ilgilidir. Bu, grafit ve demir matrisi arasında güçlü bir bağ oluşumuna neden olur. Aynı şekilde, yüksek soğutma hızı, ince perlit ile nodüler grafit parçacıklarının oluşumuna yol açar ki mekanik özelliklerin iyileşiminin kaynağıdır. Diğer taraftan, yuvarlak kenarlı ince perlitli içyapı, kompakt grafitli dökme demirlerin işlenebilirliklerinin gri dökme demire karşı azalmasına ve gri dökme demir ile karşılaştırıldığında, kompakt grafitli dökme demirin iç yapısındaki bu sınırlamalar, üretim maliyetlerinin artmasına ve takım ömrünün azalmasına neden olur. Son yıllarda CGI malzemesine yönelik yapılan çalışmaların olumlu sonuçları, bu malzemenin kullanımını artırmaya başlatmıştır. Grafit kürelerinin yapısı ve yapıyı oluşturan fazlar, kompakt grafitli dökme demirin mekanik özelliklerinin belirlenmesinde yardımcı olabilmektedir. Yapılan çalışmaların incelenmesi sonucunda, CGI malzemesine yönelik, çalışmaların son yıllarda ivme kazandığı, işlenebilirliği açısından değişik yöntemlerin, kesicilerin ve kesme parametrelerinin denendiği görülmüştür. Bu çalışmada kompakt grafitli dökme demir işlenebilirliği tornalama işleminde kuru kesme ve minimum miktarda yağlama (MQL) şartlarında araştırılmıştır. Bu amacla, her iki köşulda takım ucu aşınma miktarı, kesme kuvvetleri, yuzey pürüzlüğü ve talaş morfolojisi kıyaslanmıştır.

Minimum miktarda yağlama sisteminde, basınçlı hava ile az miktarda yağın karışımı kesme noktasına püskürtülür böylece soğutma ve yağlama işlemi çok az miktarda yağlayıcığla yapılır.MQL uygulandığında, yağlayıcı miktarı ve performamsı kıyaslanamayacak ölçüde tasarruf edilmesini sağlar.

Bunun yanında, işlem sonrası oluşan atık ve onun bakım veya geridönüşüm maliyetleri büyük ölçüde azalır. Üstelik, çok daha temiz, sağlıklı ve güvenli çalışma ortamı yaratılır. Bu yöntem etkinliği torna, freze, raybalama ve delme gibi çoğu kesme işlemlerinde görülmüştür. Örneğin Ford motor fabrikasındaki bir araştırmaya göre MQL vasıtasıyla işlem maliyetini 13% oranında düşürmeği başarmışlar. Bu başarıyı en çok takım ömrünün çoğalması ve kesme sıvısının miktarının nerdeyse hiç kullanılmaması ile ilgili olup, makina bakım ve imalattan çıkan parçaların yüzey kaliteleri artmakta ve parça yüzeylerinde ek bir temizlik operasyonuna gerek kalmamaktadır. Kesme kenarına erişilebilirlik açısına bağlı olarak, MQL sistemleri harici ve dahili kategorilerine ayrılır. Harici besleme durumunda, yağlama aracının çemberi etrafında püskürtme nozel vasıtasıyla uygulanır. Bu sistemin standart işlemlerde (torna, freze, delme) uygulanması tavsiye edilir. Dahili beslemede, yağ, makinenin iş mili sistemi ve işleme noktasındaki kanallar aracılığıyla taşınır. Bu sistem daha çok esnek işleme merkezleri ve yüksek hızlı kesme şartları altında kullanılır. Bu çalışmada CNC tornalama işleme sırasında, tüm deneylerde harici MQL sistemi kullanılmıştır. Kesme derinliği kuru ve minimum yağlama sırasında sabit tutulmuş ve her iki prosedür için 1 mm olarak alınmıştır. Bu çalışmada, farklı kesme hızları (100, 200, 300 m.min) ve ilerleme değerleri (0.1, 0.2, 0.3 mm/rev) seramik kesici takım ucuyla kompakt grafitli dökme demir tornalamasında denenmiştir. MQL sisteminin kompakt grafitli dökme demir tornalama işlemi üzerindeki verimlik, kesme kuvvetleri, yüzey pürüzlülüğü, takım aşınma türleri (serbest yüzey aşınması, krater, çentik, oksitlenme alanı) ve değerleri, talaş şekli ve morfolojisi aracılığıyla değerlendirilmiştir. Her deney sonrası takım ucunda oluşan aşınmalar, iş parçası yüzey pürüzlülük değerleri, oluşan talaşlar ve uygulanan kuvvetler ölçülmeye çalışılmıştır. Kuru kesme ve MQL şartları altındaki kesmede bu değerleri elde etmek için optik ve SEM fotoğrafları çekilmiştir. Numunelerin iç yapısını incelemek için, temiz ve parlak yüzeyleri 2% nital ile yıkanmış ve alkolle temizlendikten sonra optik mikroskopla fotoğrafları çekilmiştir. Çekme dayanımı testleri, ISO 16112 standardı üzerinden, numune EN-GJV-450 olarak sınıflandırılmıştır. Kesme kuvvetleri üç eksenli dinamometreyle ölçülmüştür. Tüm deneylerde seramik takım ucu kullanılıp, yüzey pürüzlülüğü değerleri MITUTOYO SJ.201P cihazı kullanarak ölçülmüştür.

Yapılan çalışmaların incelenmesi sonucunda, MQL kullanılarak, kesme kuvvetinde 5-10% azalma gözetlenmiştir. Ayrıca, yüzey pürüzlülüğü açısında 25% azalma ve krater aşınması açısından 30% ölçülerde iyileşme gözükmüştür.

SEM fotoğraflarının analizi ile MQL ile işlenen takım ucu kesme kenarları daha net ve pürüzsüz olduğu açığa çıkmıştır. Ancak, kuru kesme ve minimum miktarda yağlama koşulları arasında kesme kuvveti açısında mahsus bir fark gözetlenmemiştir.

1. INTRODUCTION

As automotive industry tries to meet the expectations of the user demands for a long time, they also try to respond the scope of expanding environmental protection laws. Because of the low emission laws, engine designers are forced to improve technology in order to have more effective combustion process in engines [1].

Cast irons are the most important alloys in industrial environments due to their competitive physical and mechanical properties and beneficiary engine material in vehicles. The oldest member of this family is Gray cast iron which has flaky graphite particles. Although the tensile and strength properties of gray cast irons are lower than the other types, it has a wide range of utilizing tendency because of low price and marvelous damping capacity [2]. Lower strength properties of gray cast iron and more softness demands yield to explore new cast iron types which called ductile iron (also known as nodular cast iron) and compacted graphite iron in 1949. At that time ductile iron became manufacturing trend while CGI never was seriously utilized despite CGI's magnificent mechanical properties (75% stronger and stiffer than gray cast iron). Basic difference of these cast iron categories is due to the shape, size, nodularity, and growth mechanism of graphite particles in their microstructure [3,4].

The coral graphite masses in compacted graphite iron (CGI) and their connection's within each eutectic cell makes it's mechanical (and physical) properties between gray and ductile irons .Strong adhesion between graphite and the metal matrix, being randomly oriented and elongated, thicker and round edges of graphite particles makes CGI more resistant to crack initiation and propagation even works as crack arrestors. Graphite shape and distribution in compacted graphite iron (CGI), cause high tensile strength, improved ductility and higher modulus of elasticity. These fascinating properties of CGI make it as a gasoline engines, brake disks, exhaust manifolds, cylinder heads first candidate material to be used in the automotive industry.

CGI has more fatigue resistance than gray cast iron and aluminum that could be an alternative material for automotive industry. The graphite particles are randomly oriented in the microstructure like grey iron. The difference is related to graphite particles which are shorter and thicker with rounded edges elongated connected to nearest neighbors within the eutectic cell. This causes a strong bond between graphite and iron matrix [3]. Likewise, high cooling rates causing nodular graphite particles with finer pearlite is the source of mechanical property improvement [5]. On the other hand finer pearlitic structure with rounded edge of graphite phases in CGI microstructure makes its machinability more difficult than gray cast iron. These limitations in CGI mass production in comparison to gray cast iron increase the production costs and decrease the tool life. The pearlite phase makes the material brittle and nodular compacted graphite protects the crack initiation and consequently the strength of CGI becomes higher than gray cast iron. White parts which are around the graphite are ferrite phases.

Many investigations for machinability improvement of CGI have been conducted. Dawson et al. observed the MnS inclusions forming a lubrication or protective layer over the tool during the high speed machining which reduces the tool wear [5]. However, Mohammed stated that these improvements were for specific cutting speed or non-continuous machining operations such as milling and may not be applicable for turning machining. Their paper reported the effects of microstructure of CGI on tool wear and cutting forces by finite element analysis [3]. Also Abele et al. declared CO_2 cryogenic coolant system increase the tool life of PCD cutting inserts in CGI machining. They claimed these improvements were directly related with diamond grain size, the binder material, and the cutting parameters [6].

Gastel et al. investigate the wear mechanism of cubic boron nitride (CBN) insert during the turning of CGI. Oxidation of tool and interdiffusion of constituting elements in tool-workpiece interface were the key features of tool wear [7]. Manipulating metallurgical variables to achieve a CGI with satisfactory machining performance was another attempt for machinability improvement. But during the work, the fact that machinabilty performance of this material couldn’t be improved by the means of metallurgical manipulation has been revealed. Due to the approach, the efforts changed for innovative tooling designs which had cost and complexity disadvantages [8].

Other investigations of machinability improvement were rotary insert tools, different cutting insert materials (using 10 mm diameter solid carbide drills from class K35 with single layer coating of TiAlN) even employing laser-assisted machining (LAM) technique at low speeds (102 m/min) hope to have a material removal volume which is suitable for mass production [9,10]. However, all of these solutions seemed to work in limited circumstances like low cutting speeds or using high priced and hard to manufacture cutting tools or even sometimes the metallurgical manipulation caused a decrease in mechanical properties [3]. Machinability studies which were conducted by Moecellin et al. on compacted graphite iron (CGI) provided 83% of tool life improvement and cause to make a CGI which has machinabilty similarity to gray cast iron [11]. Most of these investigations were conducted for drilling or milling and the improvements may not be applicable for other machining processes like turning [3]. so in this study the machinability improvement was examined through external Minimum Quantity Lubrication (MQL) system.

MQL is a near dry lubrication process in which a small amount of lubricant (most of the time oil or alcohol based lubricants) blows over cutting tool-work piece interface in the means of less coolant usage. Effectiveness of This method in most of the metal cutting processes like sawing, turning, milling, drilling, and tapping propelled the Manufacturers using it due to tremendous advantages. As stated by the report of Ford Motor Compony which was related about efficiency of MQL, they had a 13% decrease in process costs by the means of MQL. Its most advantage was through increasing tool life and water mixed fluid elimination, which caused a decrease in maintenance costs, increase in machine uptime and better skin care [12]. The basic concept of MQL is to spray atomized lubricant to the cutting zone via compressed air jet. MQL can be applied externally via separated nozzeles or internally via inside of the tool. In order to achieve this mean system divides into two major categories as external supply with nozzles separated to the machine (which is going to discuss in this paper) and internal supply with channels inside the tool [8, 13]. The objective of this study is to investigate wheather the improvements in CGI turning performance can be achieved by MQL. In this study tool wear, surface roughness, power consumption, chip morphology and cutting forces are examined in dry machining and near dry machining Different cutting parameters were selected to understand the effect of MQL on CGI turning.

1.1 Purpose of thesis

This paper investigates the effect of minimum quantity lubrication (MQL) on compacted graphite iron (CGI). Beneficiary properties of CGI in contrast with gray cast iron, makes it valuable material of automotive industries. The material has been used for engine blocks with thinner wall instead of gray cast iron because of higher strength. However the machining of CGI is cumbersome and increases the overall manufacturing costs. This paper presents the machinability improvement and tool life expansion by using MQL.

MQL is a sustainable method in which the mixture of oil and air sprays over cutting zone for cooling and lubrication means. The reason of MQL using is not only because of costs, but also because of ecological and health issues. In this study cutting forces, surface roughness, tool wear and chip morphology were investigated in order to evaluate the machinability of CGI with MQL system. Cutting tests were performed under different cutting speeds and feed values. During all experiments, depth of cut was kept constant as 1 mm and MQL was applied externally to the cutting zone. Cutting forces, flank and crater wear values, oxidation zone distance on tool rake face, surface roughness, chip types and microstructures were measured and evaluated in same condition for both DRYand MQL machining conditions.

In conclusion, MQL reduces the tool wear and prolongs the tool life almost 25%. Also, parts machined by the means of MQL have better finish surface in comparison with dry machining. However, no cutting forces and chip morphology difference was observed between dry and MQL cutting conditions.

2. BACKGROUND

2.1 Introduction

This chapter provides basic information regarding the turning machining of compacted graphite iron (CGI) by the means of ceramic cutting tool. It also includes a review of published literature on minimum quantity lubrication (MQL), cutting mechanics especially for turning operation and properties of the work material (CGI). Later, tool wear, surface roughness, cutting temperature and chip formation theories will be explained.

2.2 Mechanics of Orthogonal Cutting

Turning machining operation is most of the time three dimensional and geometrically complicated to figure out the shear angle and cutting force components. As a result, theoretically two dimensional orthogonal cutting is employed to explain the turning mechanics [14].

Material removal in orthogonal cutting occurs with the cutting edge which is perpendicular to the direction of tool-work piece motion and respectively cutting velocity . Mostly, oblique cutting mechanism (three dimensional) assesses through geometric and kinematic model transformation of orthogonal cutting mechanism.

Orthogonal cutting is considered as a two-dimensional plane strain shearing deformation operation so cutting force components are in velocity and width of cut directions as tangential force (F_t) and feed force (F_f) respectively. However in oblique cutting, the inclination angle (i) causes another cutting component which is called radial force (F_r). Figure 2.1 shows a cross section of orthogonal cutting with three deformation zones during the tool-work piece interaction. When cutting tool penetrates into work piece, primary shear zone forms a chip. The primary shear zone deforms and at first sticks over rake faces which cause secondary shear zone creation. Also, tertiary zone is the area in which the tool flank rubs the newly machined surface.

Sticking region is caused when the chips sticks to the tool's rake face and eventually the chips start to slide over rake face with a sliding friction coefficient. Although after sliding chips lose their contact with the rake face, depending on cutting velocity, tool and material properties contact zone changes. Two main hypotheses about the analysis of primary shear zone are:

1) MERCHANT'S orthogonal cutting model by thin shear plane assumption.

2) LEE, SHAFFER analysis based on thick shear deformation zone and laws of plasticity to predict the shear angle.

Cutting mechanics in this paper is explained via first assumption in which the shear deformation zone is infinitely thin and cutting edge is without chamfer or radius. Shear angle (ϕ_c), shear stress (τ_s) and normal stress (σ_s) is shown in figure 2.2. Also, the resultant force ($\mathcal{F}$) which applied to the shear plane is assumed to be equilibrium with tangential and feed force components.

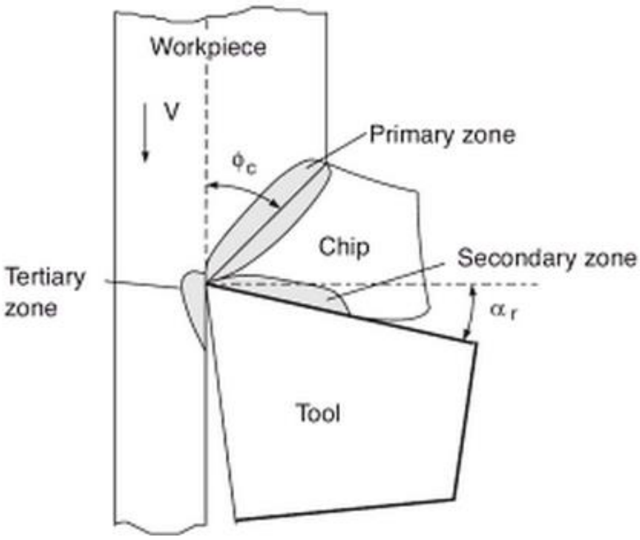

Figure 2.1 : Deformations and shear zones of chip and work piece.

As shown in figure 2.3, tangential force is in the direction of cutting velocity and feed force is in the direction of uncut chip thickness. In this section mechanics of primary and secondary shear zones will be explained.

$$\mathcal{F}=\sqrt{\mathcal{F}_t^{\,2}+\mathcal{F}_f^{\,2}} \tag{2.1}$$

2.2.1 Primary shear zone

Shear force and normal force of the shear plane derives geometrically as shown below:

$$\mathcal{F}_{\mathrm{s}} = \mathcal{F} \cos\left(\phi_c + \beta_a + \alpha_r\right) \tag{2.2}$$

$$\mathcal{F}_{\mathrm{n}} = \mathcal{F} \cos\left(\phi_c + \beta_a + \alpha_r\right) \tag{2.3}$$

$$\mathcal{F}_{\mathrm{s}} = \mathcal{F}_{\mathrm{t}} \cos \phi_c - \mathcal{F}_{\mathrm{f}} \sin \phi_c \tag{2.4}$$

$$\mathcal{F}_{\mathrm{n}} = \mathcal{F}_{\mathrm{t}} \sin \phi_c + \mathcal{F}_{\mathrm{f}} \cos \phi_c \tag{2.5}$$

α_r is the tool rake angle and β_{a} is average friction angle between chip and rake face .Also shear plane area, shear stress and normal stress in the shear plane with the assumption of uniform stress distribution could be derived coherently.

$$\tau_{\mathcal{S}} = \frac{\mathcal{F}_{\mathcal{S}}}{\mathcal{A}_{\mathcal{S}}} \tag{2.6}$$

$$\mathcal{A}_{\mathcal{S}} = \mathrm{b}\,\frac{h}{\sin \phi_c} \tag{2.7}$$

$$\sigma_{\mathcal{S}} = \frac{\mathcal{F}_{\mathrm{n}}}{\mathcal{A}_{\mathcal{S}}} \tag{2.8}$$

b in the shear area formula represents the depth of cut for turning machining , h is uncut chip thickness and (ϕ_c) is shear angle between the direction of cutting velocity and shear plane.Furthermore shear plane length (L_c) and compression ratio (r_c) derives from chip deformation geometry .

$$L_C = \frac{h}{\sin \phi_c} = \frac{h_{\mathrm{c}}}{\cos(\phi_c - \alpha_r)} \tag{2.9}$$

$$r_c = \frac{h}{h_c} \tag{2.10}$$

h is the uncut chip thickness and h_c is the deformed chip thickness components of compression ratio . So the shear angle function could be described as:

$$\phi = \tan^{-1} \frac{r_c \cos\alpha_r}{1 - r_c \cos\alpha_r} \tag{2.11}$$

2.2.2 Secondary shear zone

Two components of cutting force on the tool rake face are friction force (F_u) and normal force (F_v).

$$\mathcal{F}_u = \mathcal{F}_t \cos \alpha_r + \mathcal{F}_f \sin \alpha_r \tag{2.12}$$

$$\mathcal{F}_v = \mathcal{F}_t \cos \alpha_r - \mathcal{F}_f \sin \alpha_r \tag{2.13}$$

Although the chip at first sticks to the rake face then begins to slide with a constant friction coefficient. in orthogonal cutting theory the sticking part is removed from the calculation. The friction coefficient on the rake face (μ_a) and friction angle (β_a) equations are given as below:

$$\mu_a = \tan \beta_a = \frac{\mathcal{F}_u}{\mathcal{F}_v} \tag{2.14}$$

$$\tan(\beta_a - \alpha_r) = \frac{\mathcal{F}_f}{\mathcal{F}_t} \longrightarrow \beta_a = \alpha_r + \tan^{-1}\frac{\mathcal{F}_f}{\mathcal{F}_t} \tag{2.15}$$

Also shear force, resultant force, tangential and feed forces could be definite as a function of shear stress, shear angle, tool geometry and cutting conditions:

$$\mathcal{F}_s = \tau_s \, b \frac{h}{\sin \phi_c} \tag{2.16}$$

$$\mathcal{F} = \frac{\mathcal{F}s}{\cos\,(\phi_c + \beta\text{a} - \alpha_r)} = \tau_s \text{ b h } \frac{1}{\sin \phi_c \cos\,(\phi_c + \beta\text{a} - \alpha_r)} \quad \textbf{(2.17)}$$

$$\mathcal{F}_{\text{t}} = b\,h\ \left[\tau_s \frac{\cos\,(\beta\text{a} - \alpha_r)}{\sin \phi_c \cos\,(\phi_c + \beta\text{a} - \alpha_r)}\right] \quad \textbf{(2.18)}$$

$$\mathcal{F}_{\text{t}} = b\,h\ \left[\tau_s \frac{\sin\,(\beta_a - \alpha_r)}{\sin \phi_c \cos\,(\phi_c + \beta_a - \alpha_r)}\right] \quad \textbf{(2.19)}$$

In these equations, h is the uncut chip thickness and b is the width of cut. Moreover they are dependent to the cutting process and material properties through τ_s, β_a, α_r, ϕ_c parameters.

Figure 2.2 demonstrates the cutting force directtions and orthogonal cutting parameters. In metal cutting theory, cutting force coefficients are defined for understanding the oblique cutting and shear angle prediction. These coefficients are called specific cutting pressure or tangential cutting force coefficient ($\mathcal{K}_{\text{t}}$) and feed force coefficient ($\mathcal{K}_{\text{f}}$).

$$\mathcal{K}_t = \tau_s \frac{\cos\,(\beta_a - \alpha_r)}{\sin \phi_c \cos\,(\phi_c + \beta_a - \alpha_r)} \quad \textbf{(2.20)}$$

$$\mathcal{K}_f = \tau_s \frac{\sin\,(\beta_a - \alpha_r)}{\sin \phi_c \cos\,(\phi_c + \beta_a - \alpha_r)} \quad \textbf{(2.21)}$$

Also a dimensionless form of feed force constant ($\mathcal{K}_f$) could be shown as:

$$\mathcal{K}_f = \frac{\mathcal{F}_{\text{f}}}{\mathcal{F}_{\text{t}}} = \tan\,(\beta_a - \alpha_r) \quad \textbf{(2.22)}$$

The shear angle (α_{r}) in the equations is dependent mostly to the lubrication, tool-chip contact area, tool and workpiece material properties.

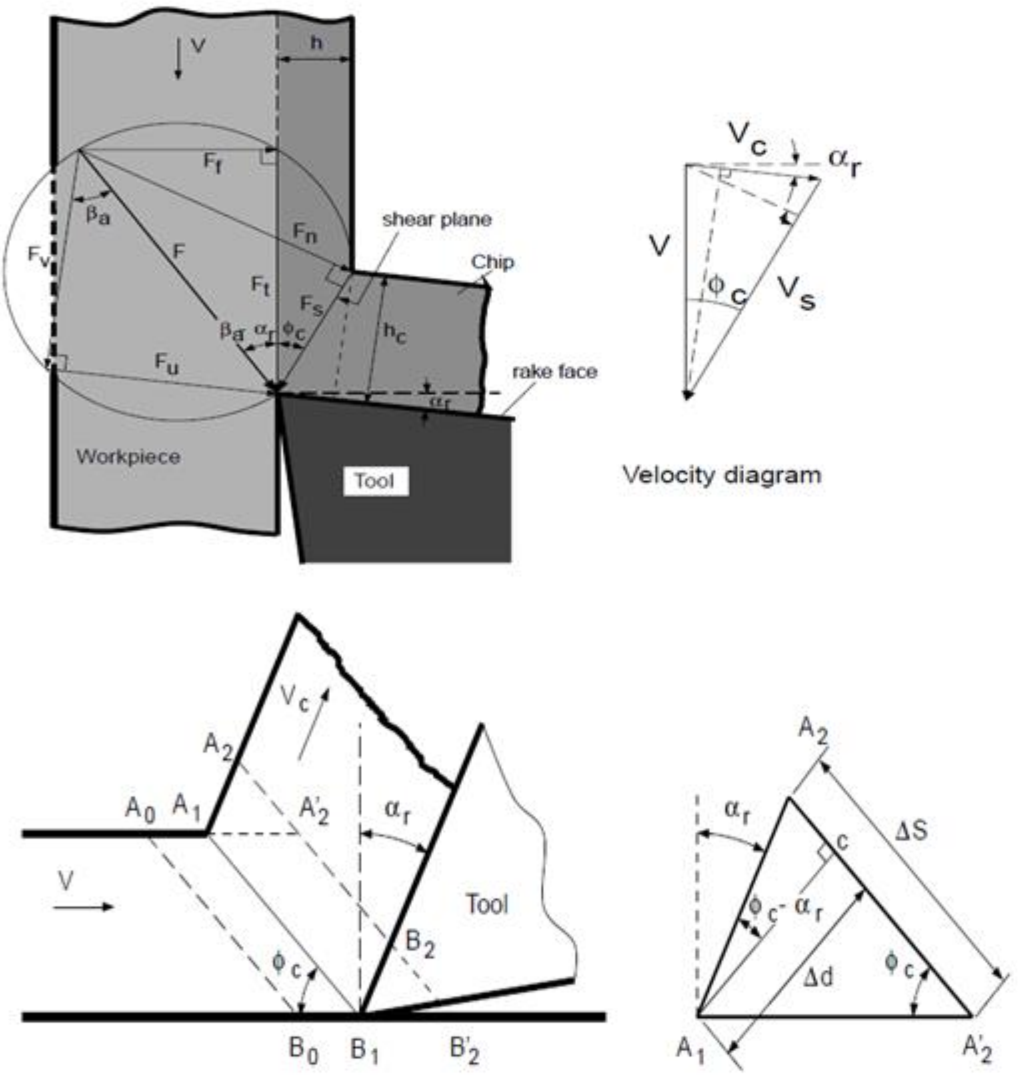

Figure 2.2 : Cutting force and shear diagrams of orthogonal cutting [14].

Although the orthogonal cutting equations give an overview on cutting mechanics, the theory is insufficient in reality circumstances because the shear plane is assumed to be thick zone in reality. Moreover work hardening and temperature variation in the shear and friction zones change the stress values of primary deformation zone. Hence, it's more preferred to use the functions which are dependent to cutting conditions and cutting constants ($\mathcal{K}_{tc}$ and $\mathcal{K}_{fc}$).

$$\mathcal{F}_t = \mathcal{K}_{tc}\, b\, h + \mathcal{K}_{te}\, b \tag{2.23}$$

$$\mathcal{F}_f = \mathcal{K}_{fc}\, b\, h + \mathcal{K}_{fe}\, b \tag{2.24}$$

The edge coefficients ($\mathcal{K}_{te}$ and $\mathcal{K}_{fe}$) are emerged from metal cutting experiments. Also, due to complex factors of thermal, deformation and chip thickness effects, nonlinear functions are introduced as:

$$\mathcal{K}_t = \mathcal{K}_T \, h^{-p} \tag{2.25}$$

$$\mathcal{K}_f = \mathcal{K}_F \, h^{-q} \tag{2.26}$$

In these nonlinear equations p and q are cutting force constants which derive from cutting experiments in different feed rates.

2.3 Mechanics of Oblique Cutting

While the cutting velocity in orthogonal cutting is perpendicular to the cutting edge, it's lean at an acute angle (i) in normal plane to the cutting edge in oblique cutting condition.

2.3.1 Oblique cutting geometry

Normal plane ($\mathcal{P}_n$) is defined as a cutting edge plane in which the direction is parallel to cutting velocity (V). Because the shear deformation is plane strain without side spreading, the shearing and chip motion are parallel to cutting velocity and perpendicular to cutting edge as shown in figure 2.3.

The cutting velocity in oblique cutting has an indication angle (i) so consequently shear, friction, chip flow and resultant cutting force have components in all three directions (x,y,z). Oblique cutting mechanics in normal plane are similar to orthogonal cutting for velocity and force vectors.

In figure 2.4, the friction force on the rake face ($\vec{\mathcal{F}}_u$) and normal force to the rake ($\vec{\mathcal{F}}_v$) are the resultant cutting force ($\vec{\mathcal{F}}$) components with a friction angle of β_a. Also ($\vec{\mathcal{F}}$) has an acute projection angle (θ_i) with the normal plane ($\mathcal{P}_n$) and eventually $\theta_n+\alpha_n$ with the normal face ($\mathcal{F}_v$).

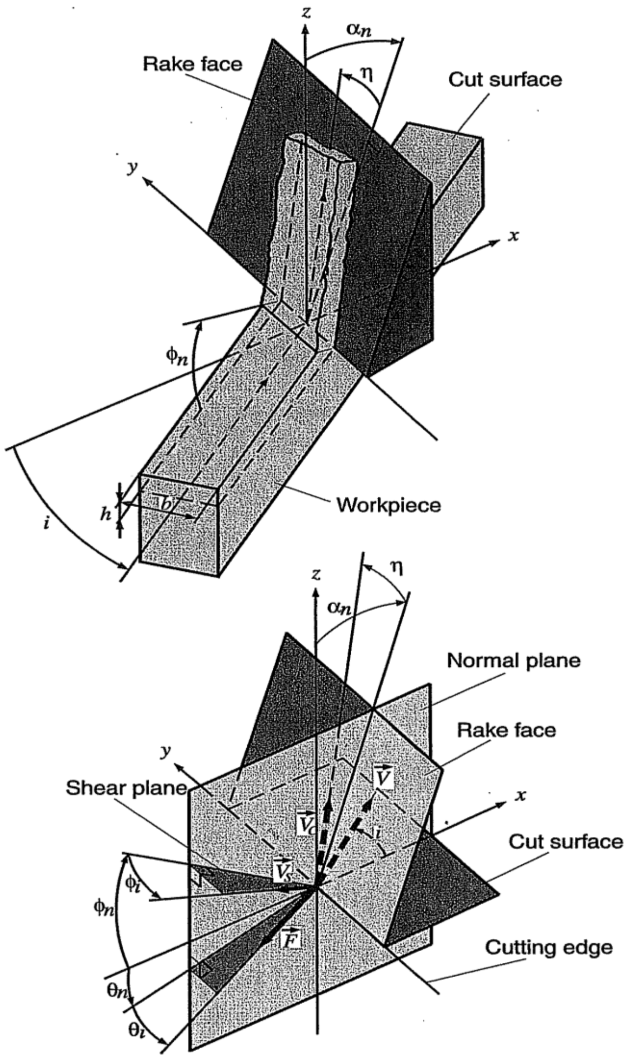

Figure 2.3 : Geometry of oblique cutting process [14].

Oblique cutting parameters, define the direction of resultant force (θ_n , θ_i) , shear velocity (ϕ_n , ϕ_i) and chip flow (η).

$$\mathcal{F}_u = \mathcal{F} \sin \beta_a = \mathcal{F} \frac{\sin \theta_i}{\sin \eta} \longrightarrow \sin \theta_i = \sin \beta_a \sin \eta \tag{2.27}$$

$$\mathcal{F}_u = \mathcal{F}_v \tan \beta_a = F_v \frac{\tan(\theta_n + \alpha_n)}{\cos \eta} \longrightarrow \tan(\theta_n + \alpha_n) = \tan \beta_a \cos \eta \tag{2.28}$$

$$\tan \eta = \frac{\tan i \cos(\phi_c - \alpha_n) - \cos \alpha_n \tan \phi_i}{\sin \phi_n} \tag{2.29}$$

2.3.2 Maximum shear stress principle

In order to predict the direction of shear angle ($\phi_n = \frac{\pi}{4} - \beta + \alpha_n$) numerous solutions by Krystof [15] and later by Lee and Shaffer [16] applied with maximum shear stress criteria and slip-line field. Both of the papers had an assumption for oblique cutting which was same as orthogonal cutting theory. The assumption was, the shear occurs in the direction of maximum shear stress in which the angle between shear velocity and resultant force is 45°.

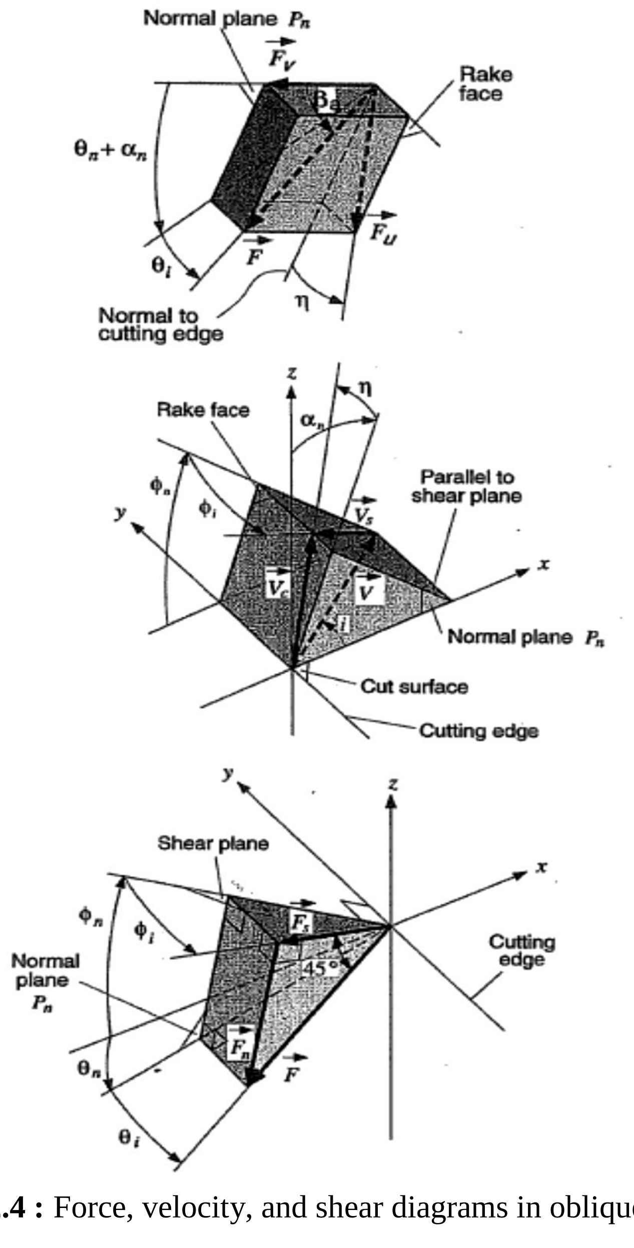

Figure 2.4 : Force, velocity, and shear diagrams in oblique cutting [14].

$$\mathcal{F}_s = \mathcal{F}(\cos\theta_i \cos(\theta_n + \phi_n)\cos\phi_i + \sin\theta_i \sin\phi_i) = \mathcal{F}\cos(45°) \quad \textbf{(2.30)}$$

Also the component of the resultant force in the normal direction to the shear is:

$$\mathcal{F}(\cos\theta_i \cos(\theta_n + \phi_n)\sin\phi_i - \sin\theta_i \sin\phi_i) = 0 \quad \textbf{(2.31)}$$

These equations occur when the shear stress in the shear direction is maximum(45°).

$$\sin\phi_i = \sqrt{2}\sin\theta_i \quad \textbf{(2.32)}$$

$$\cos(\phi_n + \theta_n) = \frac{\tan\theta_i}{\tan\phi_i} \quad \textbf{(2.33)}$$

For oblique cutting a block diagram is used to predict the (ϕ_i , ϕ_n , θ_i , θ_n) angles and consequently maximum shear stress. Friction (β_a) , rake (α_n) and inclination (i) angles are known through tool geometry and material properties.

2.3.3 Minimum energy principle

Another theory over shear angle prediction was conducted by Merchant [17]. In this theory, the minimum energy principle was applied to orthogonal cutting then extended for oblique cutting.

$$\mathcal{F}_s = \mathcal{F}(\cos\theta_i \cos(\theta_n + \phi_n)\cos\phi_i + \sin\theta_i \sin\phi_i = \tau_s \mathcal{A}_s = \tau(\frac{b\,h}{\cos i \sin\phi_n}) \quad \textbf{(2.34)}$$

In these equations $\mathcal{A}$s, b and h are shear area, the width of cut and uncut chip thickness respectively. Also, resultant force ($\mathcal{F}$) and cutting power ($\mathcal{P}_t$) in oblique cutting are:

$$\mathcal{F} = \frac{\tau\, \mathrm{b\, h}}{[\cos\theta_i\ \cos\ (\theta_n + \phi_n)\cos\phi_i + \sin\theta_i\ \sin\phi_i\,]\cos i\ \sin\phi_n} \quad \textbf{(2.35)}$$

$$\mathcal{P}_t = \mathcal{F}_t \mathcal{V} = \mathcal{F}(\cos\theta_i\, cos\ \theta_n \cos i + \sin i\ \sin\theta_i)\,\mathcal{V} \quad \textbf{(2.36)}$$

And nondimensional power ($\mathcal{P}_t$') could be derived from the above equations.

$$\mathcal{P}_t' = \frac{\mathcal{P}_t}{v\,\tau_s\,b\,h} = \frac{\cos\theta_n + \tan\theta_i\,\tan i}{[\cos(\theta_n + \phi_n)\cos\phi_i + \tan\theta_i \sin\phi_i]\,\sin\phi_n} \tag{2.37}$$

In minimum energy principle, the cutting power must be minimum, in order to find the unique shear angle. So the unknown angles (ϕ_n , ϕ_i , θ_n , θ_i , η) could be solved from equations with the usage of iteration technique.

2.3.4 Emprical approach

For this approach Armarego [18] gave a model with two assumptions of shear direction and chip length ratio.

(1): Shear velocity is collinear with the shear force

(2): The chip length ratio for both oblique and orthogonal cutting is same.

$$\tan(\phi_n + \beta_n) = \frac{\cos\alpha_n\,\tan i}{\tan\eta - \sin\alpha_n\,\tan i} \quad , \quad \beta_n = \theta_n + \alpha_n \tag{2.38}$$

$$\tan\beta_n = \tan\beta_a\,\cos\eta \quad , \quad \tan(\phi_n) = \frac{r_c\,(\cos\eta\,/\,\cos i)\cos\alpha_n}{1 - r_c\,(\cos\eta\,/\,\cos i)\sin\alpha_n} \tag{2.39}$$

2.3.5 Prediction of cutting forces

The cutting force components are projections of resultant cutting forces in different directions. As shown in following equations, they are function of shear yield stress (τ_s), oblique cutting (i), resultant force directions (θ_n , θ_i) and oblique shear angles (ϕ_i , ϕ_n).

The force components in the direction of cutting speed ($\mathcal{F}_t$), thrust ($\mathcal{F}_f$) and normal ($\mathcal{F}_r$) are shown in the equations below:

$$\mathcal{F}_t = \frac{\tau_s\;b\,h\,(\cos\theta_n + \tan\theta_i\;\tan i)}{[\cos(\theta_n + \phi_n)\cos\phi_i + \tan\theta_i\sin\phi_i]\sin\phi_n} \tag{2.40}$$

$$\mathcal{F}_f = \frac{\tau_s\;b\,h\;\sin\theta_n}{[\cos(\theta_n + \phi_n)\cos\phi_i + \tan\theta_i\sin\phi_i]\cos i\sin\phi_n} \tag{2.41}$$

$$\mathcal{F}_r = \frac{\tau_s \ b\ h\ (\tan\theta_i - \cos\theta_n\ \tan \mathrm{i}\,)}{[\cos\,(\,\theta_n\ +\phi_n\,)\cos\phi_i\ +\ \tan\theta_i\,\sin\phi_i\,]\,\sin\phi_n} \tag{2.42}$$

In order to make these equations simple, we use the cutting force coeffient terms and define them as:

$$\mathcal{F}_{\mathrm{t}} = \mathcal{K}_{\mathrm{tc}}\ \mathrm{b\ h} + \mathcal{K}_{\mathrm{te}}\ \mathrm{b}\,,\quad \mathcal{F}_{\mathrm{f}} = \mathcal{K}_{\mathrm{fc}}\ \mathrm{b\ h} + \mathcal{K}_{\mathrm{fe}}\ \mathrm{b}\,,\quad \mathcal{F}_{\mathrm{r}} = \mathcal{K}_{\mathrm{rc}}\ \mathrm{b\ h} + \mathcal{K}_{\mathrm{re}}\ \mathrm{b}\,, \tag{2.43}$$

Where the corresponding coefficients are:

$$\mathcal{K}_{tc} = \frac{\tau_s\,(\cos\theta_n + \tan\theta_i\ \tan \mathrm{i}\,)}{[\cos\,(\,\theta_n\ +\phi_n\,)\cos\phi_i\ +\ \tan\theta_i\,\sin\phi_i\,]\,\sin\phi_n} \tag{2.44}$$

$$\mathcal{K}_{fc} = \frac{\tau_s\ \ \sin\theta_n}{[\cos\,(\,\theta_n\ +\phi_n\,)\cos\phi_i\ +\ \tan\theta_i\,\sin\phi_i\,]\,\sin\phi_n\,\cos \mathrm{i}} \tag{2.45}$$

$$\mathcal{K}_{rc} = \frac{\tau_s\ \ (\,\tan\theta_{\mathrm{i}} - \cos\theta_{\mathrm{n}}\ \tan \mathrm{i}\,)}{[\cos\,(\,\theta_n\ +\phi_n\,)\cos\phi_i\ +\ \tan\theta_i\,\sin\phi_i\,]\,\sin\phi_n} \tag{2.46}$$

By employing Armarego’s [19] classical oblique model and transforming the geometrical relations, the following equations emerge. These equations could be useful for predicting the oblique cutting forces from orthogonal cutting forces. So, this prediction equations are practical for understanding forces amount in many operations like turning, milling and drilling.

$$\mathcal{F}_{\mathrm{t}} = b\hbar\ .\left[\frac{\tau_s}{\sin\phi_n}\ \frac{\cos\,(\,\beta_n - \alpha_n\,) + \tan \mathrm{i}\ \tan\eta\ \sin\beta_n}{\sqrt{\cos^2(\,\phi_n + \beta_n - \alpha_n\,) +\ \tan^2\eta\ \sin^2\ \beta_n}}\right] \tag{2.47}$$

$$\mathcal{F}_{\mathrm{f}} = b\hbar\ .\left[\frac{\tau_s}{\sin\phi_n\cos i}\ \frac{\sin(\,\beta_{\mathrm{n}} - \alpha_{\mathrm{n}}\,)}{\sqrt{\cos^2(\,\phi_n + \beta_n - \alpha_n\,) +\ \tan^2\eta\ \sin^2\ \beta_n}}\right] \tag{2.48}$$

$$\mathcal{F}_{\mathrm{r}} = b\hbar\ .\left[\frac{\tau_s}{\sin\phi_n}\ \frac{\cos\,(\,\beta_n - \alpha_n\,)\tan \mathrm{i} - \tan\eta\ \sin\beta_n}{\sqrt{\cos^2(\,\phi_n + \beta_n - \alpha_n\,) +\ \tan^2\eta\ \sin^2\ \beta_n}}\right] \tag{2.49}$$

2.4 Turning Mechanics

Turning operation is used for machining of cylindrical parts. Conventional lathe is including chuck (to hold the workpiece), spindle (for rotating), and a tool post (for holding the tool and accurate motion during the machining process). Also at the bottom part of lathe is held tail stock for long and heavy workpieces.

The power motor of conventional lathe produces a constant speed and transmitted it to spindle and feed drive via belts. Also a gear box is designed for favorable speeds during the machining operation. However, in turning CNC, stepless drives and consequently spindle speed and feed rate get controlled by programmed NC controllers. The turret could move in both directions (along and perpendicular to spindle axis) and reduce the workpiece diameter or shorten workpiece length and facing operation respectively. Moreover combination of these motions with programming in CNC could be used for chamfering, radius machining and threading operations very accurately. The direction of cutting force and cutting velocity components are very important criteria for power consumption, tool wear, surface roughness of workpiece and main cutting parameters. Figure 2.5 shows turning tool geometry with its faces. The tool nose radius, rake face, side rake, back rake and cutting edge plays an important role in tool wear and chip formation.

The orientation of rake angle is the main factor in categorizing tools as positive, neutral and negative. In orthogonal cutting back rake considered zero and only side rake is assumed to be. Positive rake angle is used because of higher shear angles which reduce the cutting force and better finish surface due to chip flow on the rake face. Negative tools create more cutting force in comparison with positive ones due to shear angle decreasement. These tools are mostly used in interrupted cutting conditions and where tools are used periodically. These tools have more shock resistance than positive ones because the weak part of cutting edge doesn’t contact with the workpiece. Figure 2.6 shows a typical cutting tool which is clamped to holder and its faces. Another advantage of negative tools is cost reduction. In positive tools, only one side could be used due to clearance angle at edges but for negative ones this angle is zero and more edges could be used.

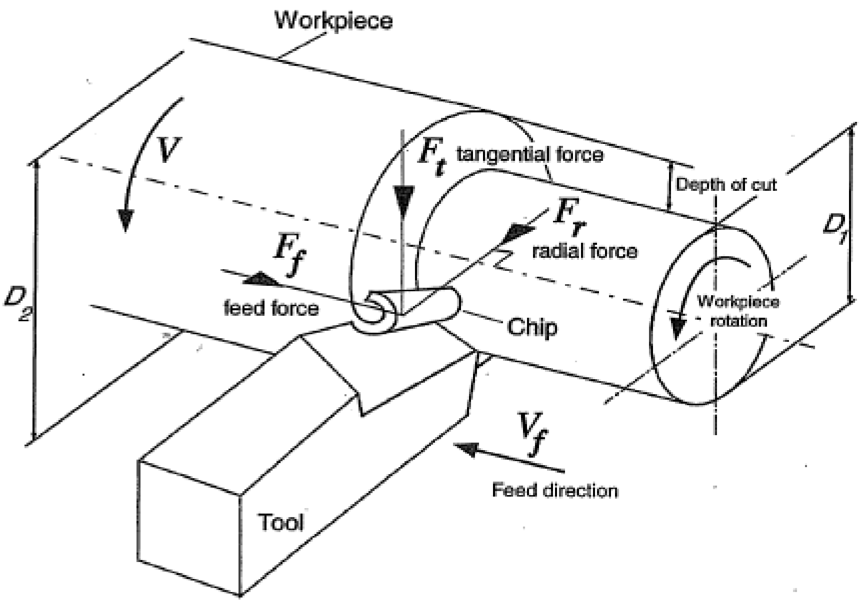

Figure 2.5 : Geometry of turning process [14].

The tool radius at the nose part is mostly zero or small amount. This is because of, the large tool nose make self-excited vibrations or chatter in machining. Oblique cutting angle equations in turning process are shown as:

$$\tan \alpha_0 = \tan \alpha_f \cos \psi_r + \tan \alpha_p \sin \psi_r \qquad \textbf{(2.50)}$$

$$\tan i = \tan \alpha_p \cos \psi_r + \tan \alpha_f \sin \psi_r \qquad \textbf{(2.51)}$$

$$\tan \alpha_n = \tan \alpha_0 \cos i \qquad \textbf{(2.52)}$$

Where i, α_0 and α_n are the oblique, orthogonal and normal rake angles, respectively. Stabler [20] suggested that the chip flow angle is assumed to be equal to oblique angle. The oblique cutting geometries in turning operation (as shown in Eq. 2.50-2.51-2.52) transform the orthogonal cutting parameters to predict the cutting forces.

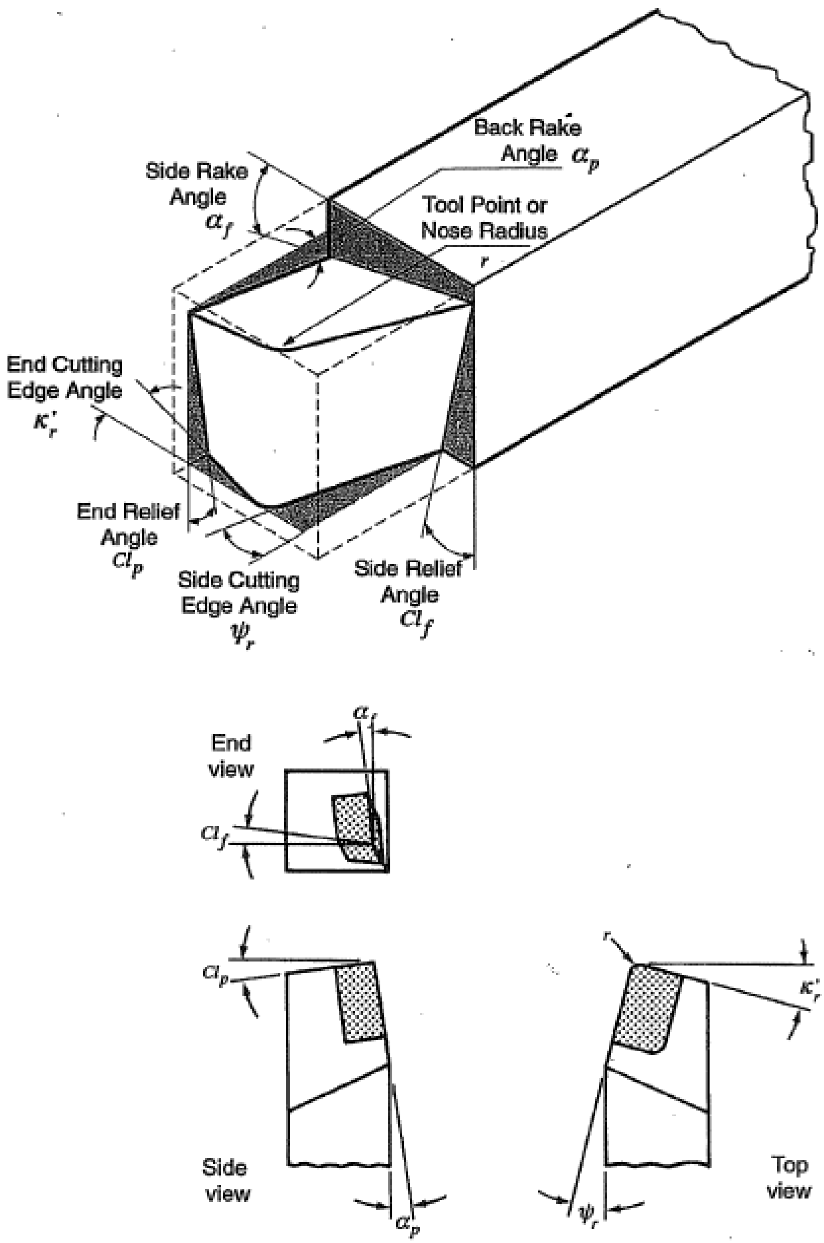

Figure 2.6 : Geometry of turning tool.

2.4.1 Prediction of cutting forces in turning

Armarego [18] proposed the classical oblique cutting transformation for two regions in which the chip thickness is the criteria. In regionI, the radial depth is less than radius (r) and chip thickness is uniform. But for regionII, the chip thickness alters owning to the corner radius of the tool. Figure 2.7 shows the corner radius (r), side rake angle (α_f), back rake angle (α_p), diameter of workpiece (d) and the radial depth of cut (a).

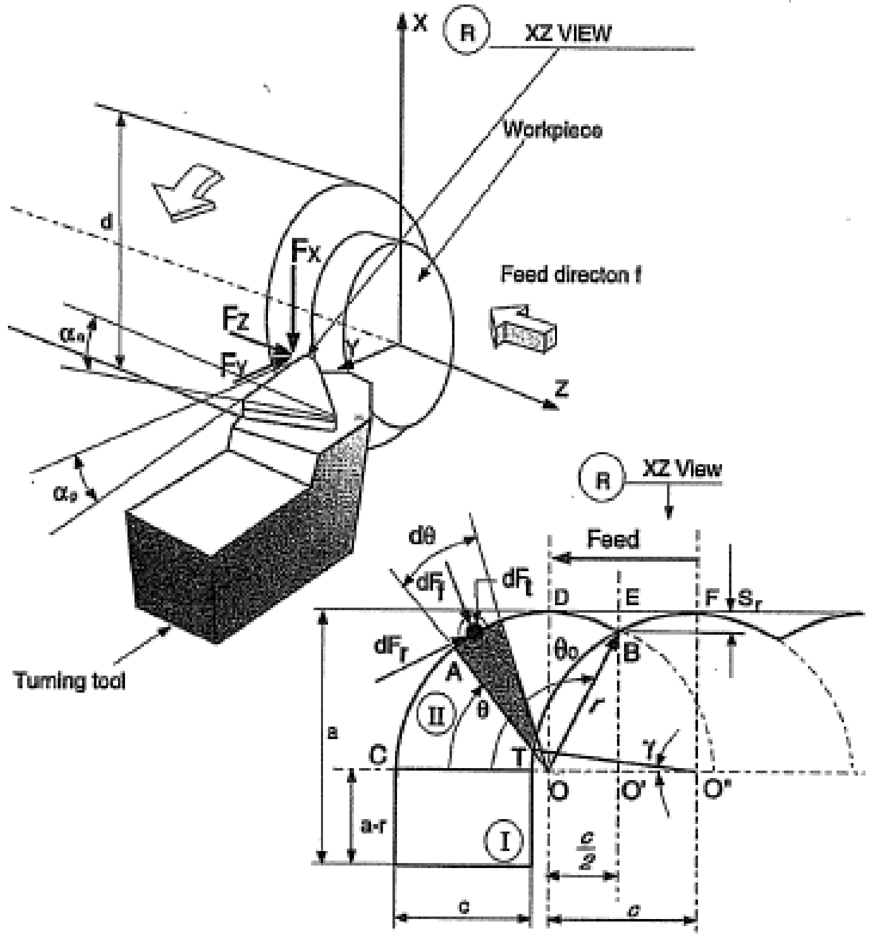

Figure 2.7 : Mechanics of turning with bull-nosed inserts.

2.4.1.1 Region I

In the first region the chip thickness is invariant and same as feed rate (h=c). Also, depth of cut is less than tool radius (0<y<r). As shown in figure 2.7, the cutting force components in x,y,z directions, are parallel to oblique cutting forces $\mathcal{F}_t$, $\mathcal{F}_r$, $\mathcal{F}_f$, respectively.

$$\mathcal{F}_{x,I} = \mathcal{F}_{t,I} = K_{tc}\, c\, (a-r) + \mathcal{K}_{te}\, (a-r) \tag{2.53}$$

$$\mathcal{F}_{y,I} = \mathcal{F}_{r,I} = K_{rc}\, c\, (a-r) + \mathcal{K}_{re}\, (a-r) \tag{2.54}$$

$$\mathcal{F}_{z,I} = \mathcal{F}_{f,I} = K_{fc}\ c\ (a\text{-}r) + \mathcal{K}_{fe}\ (a\text{-}r) \quad \textbf{(2.55)}$$

The cutting constants ($\mathcal{K}_{tc}$, $\mathcal{K}_{rc}$, $\mathcal{K}_{fc}$) could be derived from orthogonal cutting parameters (ϕ_n , β_a , τ_s) by oblique angle (i) and normal rake angle (α_n) considerations. The normal friction angle is calculated from:

$$\beta_n = \tan^{-1}(\tan\beta_a \cos i) \quad \textbf{(2.56)}$$

2.4.1.2 Region II

In second region, the directions of oblique cutting change around the chip segment and chip thickness consequently changes. So the calculations are through angular increment (dθ). The cutting force component equations are as:

$$dF_{t,II} = K_{tc}\,(\theta)\ dA + K_{te}\ dS \quad \textbf{(2.57)}$$

$$dF_{r,II} = K_{rc}\,(\theta)\ dA + K_{re}\ dS \quad \textbf{(2.58)}$$

$$dF_{f,II} = K_{fc}\,(\theta)\ dA + K_{fe}\ dS \quad \textbf{(2.59)}$$

Also, the cutting constants at each element must be considered as a function of approach angle (θ). Furthermore, in second region the radial component of the cutting force is assumed to be zero (K_{re} = 0).

Because of direction change in second region, the x,y,z components of turning machining cutting forces are as below:

$$dF_{x,II} = dF_{t,II} \quad \textbf{(2.60)}$$

$$dF_{y,II} = dF_{f,II}\cos\theta - dF_{r,II}\cos\theta \quad \textbf{(2.61)}$$

$$dF_{z,II} = dF_{f,II}\cos\theta + dF_{r,II}\cos\theta \quad \textbf{(2.62)}$$

The total cutting forces in second region is calculated by integral function for each component.

$$F_{q,II} = \int_0^{\theta_0} d\mathcal{F}_{q,II} \qquad q = \text{x, y, z} \tag{2.63}$$

The approach angle limit in integrating function is $\theta_0 = \pi\text{-}\cos^{-1}(c/2r)$. Another approach for cutting force calculation is numerically gathering the segmental forces are explained individually.

$$F_{q,II} = \sum_{k=0}^{k} d\mathcal{F}_{q,II} \qquad q = \text{x, y, z} \tag{2.64}$$

The chip is divided into segments as $\mathcal{K} = \theta_0 / \Delta\theta$. The total cutting forces are the sum of two region's force.

$$\mathcal{F}_q = F_{q,I} + F_{q,II} \qquad q = \text{x,y,z,} \tag{2.65}$$

Also the torque ($\mathcal{T}$) and power ($\mathcal{P}$) for spindle revolution can be explained as:

$$\mathcal{T} = \mathcal{F}_x \left(\frac{d-a}{2}\right) \ [\mathcal{N}m] \qquad \mathcal{P} = \mathcal{F}_x \mathcal{V} \ [\mathcal{W}] \tag{2.66}$$

Where d is shaft's diameter [m] and $\mathcal{V}$ is cutting velocity [m/s] .

Feed mark's amplitude is:

$$\mathcal{R}_s = r\left(1 - \cos\left(\sin^{-1}\left(\frac{c}{2r}\right)\right)\right) \tag{2.67}$$

The cutting force prediction is an important attitude for cost saving, tool breakage foresight, chatter vibration preventing, power consumption and main cutting parameters selection (cutting speed, feed, depth of cut).

2.5 Tool Wear and Breakage

In order to produce parts with desired surface finish and dimensional tolerances, the cutting tool edges must be in favorable life cycle with monitoring the tool wear and breakage. Otherwise, if the tool reaches its life limit, it should be replaced with new one. Tool wear describes the gradual failure of tools material in contact with workpiece at contact zones [21]. Figure 2.8 shows the tool wear types and tool-workpiece contact area.

The chip which erodes the rake face of the cutting tool causes the crater wear. The crater wear does not seriously degrade the use of tool until it reaches serious amounts and cause the cutting edge failure.

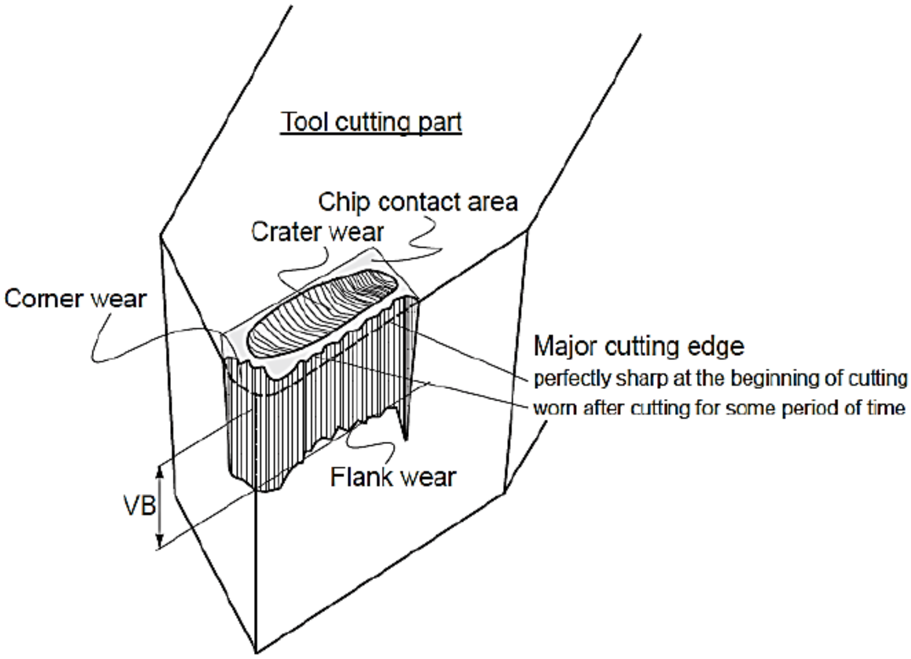

Figure 2.8 : Types of tool wear and breakage [14].

The flank face of the tool in contact with wotkpiece starts to rub against the finish surface and cause flank wear as shown in figure 15. The flank wear is one the most important criteria's for tool life prediction. Notch wear occurs by rubbing the finish surface and cutting tool at the border in which the chip does not contact the tool. This kind of wear causes poor surface finish and risk of edge breakage. Also, other kinds of tool wear like plastic deformation and thermal cracks occur in the cutting edge of the tool but for our paperwork these wear categories have not seen during the machining of CGI via ceramic cutting tool. Tool breakage occurs mostly due to thermal and mechanical overloading of cutting edge or increased cutting force through tool wear growth.

The tool wear mechanism understanding and optimization purpose is to find out the economical machining time with desired surface finish and dimensional tolerance accuracy by the usage of same tool and with all factors consideration to reduce the costs.

2.5.1 Tool wear

In this part, the most known wear known wear mechanism will be introduced and will be tried to explain. These mechanisms could occur simultaneously or just one of them could affect the cutting operation.

2.5.1.1 Abrasion wear

Abrasion wear occurs when a hard rough material slides across a softer workpiece and cause particle removal in both materials. Also, the hard tool particles between the tool and workpiece are include of carbides, oxides, and nitrides with hard microstructure characteristics so consequently abrasion wear starts during the machining operation.

2.5.1.2 Adhesion wear

Adhesion wear is the result of micro-junctions caused by workpiece particles and they weld and adhere to the cutting tool. Adhered particles stick to the contact edge of tool and because of unstableness, they take small fragments of cutting tool edge with themselves and wear occurs. At low cutting speed, part of a chip sticks to cutting edge and the build-up edge occurs. This phenomena cause the cutting forces decrease or increase due to changing the rake angle. At low cutting speed the interface temperature is low and it’s hard for chip to slide over the rake face but as the temperature increases, the chip becomes softer and slides easier. Also, as the cutting speed increases, the length of build-up edge decreases and becomes non effective.

2.5.1.3 Diffusion wear

Atoms of the tool migrate to the chip at high temperature in the contact zones due to the same atom concentration in chip and tool microstructure. This progressive behaviour is explained via diffusion wear mechanism and gradually may cause the tool breakage.

2.5.1.4 Oxidation wear

At contact area, the affecting atoms in exposure with air (oxygen) form new molecules and corrosion starts to act. This kind of wear is so dependent to work materials, tool geometry and cutting conditions.

2.5.1.5 Crater wear

At high temperature, heavy loads or high feed rate circumstances, the crater wear on the rake face of the tool with cut chip rub action occurs. The crater wear in the cutting edge, weakens the rake and the contact area which could cause chipping. The use of lubricant and its penetration between the chip and tool reduces the friction and cutting temperature and eventually the crater wear reduces. In general, crater wear is in small concern in tool life dependency.

2.5.1.6 Flank wear

This kind of wear occurs as a result of friction between the tool flank and machined surface of workpiece. The tool particles adhere to the primary clearance face of workpiece and periodically shear off. It's measured by the width of wear land. The flank wear affects the mechanics of cutting drastically. At high temperatures in the contact area, beside the adhesion mechanism, the abrasion and diffusion occurs in the flank face by the means of escaped tool particles and work material scratching. The critical limit for flank wear in industrial machining environments is 0.3 mm, (V_B = 0.3 mm). The higher amount of V_B could cause the tool failure and high surface roughness due to cutting force growth.

2.5.1.7 Notch wear

This is a special type of combined flank and rake face wear which occurs adjacent to the point where the major cutting edge intersects the work surface. The gashing (or grooving, gauging) at the outer edge of the wear land is an indication of a hard or abrasive skin on the work material. Such a skin may develop during the first machine pass over a forging, casting or hot-rolled workpiece. It's also common in machining of materials with high work-hardening characteristics, including many stainless steels and heat-resistance nickel or chromium alloys.

2.5.2 Tool breakage

Fracture can be the catastrophic end of the cutting edge. The bulk breakage is the most harmful type of wear and should be avoided as far as possible. The loss of a major portion of the tools cutting edge, make the cutting ability loss in tools. The feed rate and cutting forces have an important role in tool breakage.

Theoretically, when the feed rate increases until it reaches the tensile strength of the cutting tool, the crack starts and grows in the cutting edge. Eventually, brittle tool deforms a little bit plastically and after that by loading the cutting force, the tool breakage occurs. Effects of the tool wear on technological performance measures are:

1. Increasing the cutting force,
2. increasing the surface roughness,
3. increasing the cutting temperature in both tool and workpiece,
4. decreasing the dimensional accuracy,
5. vibration causing,
6. lowering the production efficiency, and part quality.

2.5.2.1 Influence on cutting force

Crater and flank wear on the cutting edge, affect performance of the performance of the cutting tool in various ways. The cutting forces are normally increased by the wear of the tool. Crater wear may, however, under certain circumstances, reduce forces by effectively increasing the rake angle of the tool. Clearance –face (flank or wear-land) wear and chipping almost invariably increase the cutting forces due to increased rubbing forces.

2.5.2.2 Influence on finish surface

The surface finish produced in a machining operation usually deteriorates as the tool wears. This is particularly true of a tool worn by chipping and generally the case for a tool with flank-land wear. Also, there are circumstances in which a wear land may polish the workpiece and produce a good finish.

2.5.2.3 Influence on dimensional accuracy

Flank wear influences the plan geometry of a tool, this may affect the dimensions of the components produced in a machine with set cutting tool position or it may influence the shape of the components produced in an operation utilizing a form tool. Also, if tool wear is rapid, cylindrical turning could result in a tapered workpiece.

2.5.2.4 Influence on chatter or vibration

Vibration or chatter is another aspect of the cutting process which may be influenced by tool wear. A wear land increases the tendency of a tool to dynamic instability.

A cutting operation which is quite free of vibration when the tool is sharp may be subjected to an unacceptable chatter mode when the tool wears.

2.5.3 Tool life

As the cutting process proceeds gradually, the tools wear value increases. In tool life expectancy theories, the flank wear amount (V_B) is mostly considered. The critical limit for V_B in machining operation is about 0.3 mm. The cutting time in which the flank wear (V_B) reaches this limit is called tool life (T) which is a basic parameter during the machining operation. Figure 2.9 shows the cutting time –flank wear diagram. Taylor [22] showed the tool life as a function of cutting speed $\mathcal{V}$ [m/min], feed rate $\mathcal{C}$ [mm/rev] and tool-workpiece material behaviour.

$$\mathcal{T}_t = \mathcal{C}_t\, \mathcal{V}^{-p'}\, \mathcal{C}^{-q'} \tag{2.68}$$

$\mathcal{C}_t$, $\mathcal{P}$’, and q’ are constants of tool-workpiece machinability characteristics. The slope of the wear curve depends on the cutting speed and cutting temperature mostly. Also, properties of work material and cutting tool geometry are effective factors in tool life predictions. Figure 2.10 shows the parameters which effect the tool wear.

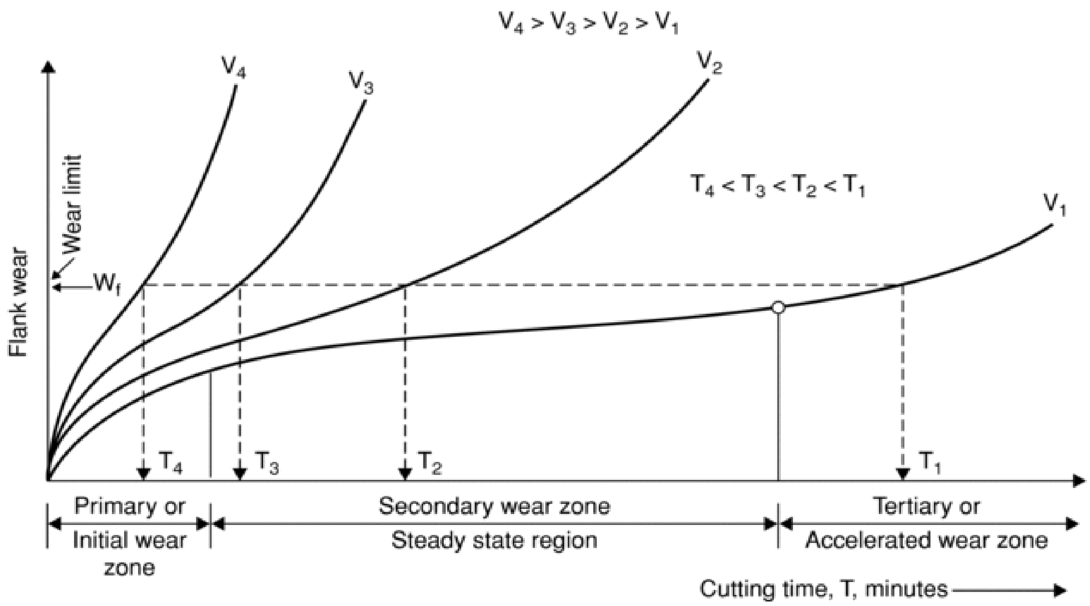

Figure 2.9 : Tool life (T) curves at different cutting speeds (V) [14].

2.6 Chip Formation

Chip formation process begins with tool penetration at the cutting zone which causes the work material to deform elastically and plastically. When shear stress surpasses material's yield shear stress the chip begins to flow over rake face of cutting tool. The produced stress is dependent to feed rate ($\mathcal{F}$), cutting velocity ($\mathcal{V}_c$) and depth of cut (a_p). Also, the cutting edge angles in the tool as normal rake angle (γ_n), tool cutting edge angle ($\mathcal{K}_r$) and cutting edge inclination ($\imath$) is concerned [23].

Although, cutting parameters (cutting speed, feed rate and depth of cut) influence the amount of stress, the direction and amount of stress could change the materials behavior during the cutting operation as brittle or tough. Figure 2.10 shows plastomechanical deformation process during chip formation [24]. The continuous plastic deformation zone in the chips could be divided into five parts as shown in figure 2.11.

a) The transition part of the uncut chip to the cut one

b) Sheared zone

c) Strong deformation on the rake face of tool

d) Cut surface

e) First detachment of material

This kind of representation is mostly for the materials with the tendency of continuous chip production. However, other types of chips including lamellar chips, segmented chips and discontinuous chips could be produced depending on material properties. Chip types is mostly related to shear strain (ε) as shown in figure 2.12 In addition, the description of chip formation is as below:

If the work material has significant deformability ($\varepsilon_B > \varepsilon_0$), continuous chips form. Deformation stress does not make brittleness and the chips do not crack simultaneous. These kinds of chips are not wanted for manufacturing production.

Lamellar type of chips form when $\varepsilon_B < \varepsilon_0 < \varepsilon_F$ theoretically. Also, the vibrations during the machining process and materials with non uniform microstructure could have this kind of chips. Furthermore the cutting conditions like high cutting speed and feed rate makes these kinds of chips.

A chip which has high and low shear energy in the shear plane and is separated with crack growth along the shear plane is called segmented chips. They form when ε_F < ε_0 . Also, during the machining of materials like cast iron with brittle properties or at very low cutting speed (1-2m/min) conditions or in the cases of deformation embrittlement during the operation, segments form. Discontinuous chips form during the cutting operation of hard materials.

These chips are not detached and for mass production are favorable. However, they could cause tool wear at high rate or tool and some time work material breakage at finish surface. When cutting brittle materials with uneven microstructures such as certain types of cast iron and stone. The chips are not detached, but are torn off the surface, often causing damage due to small breakings from the workpiece surface [25].

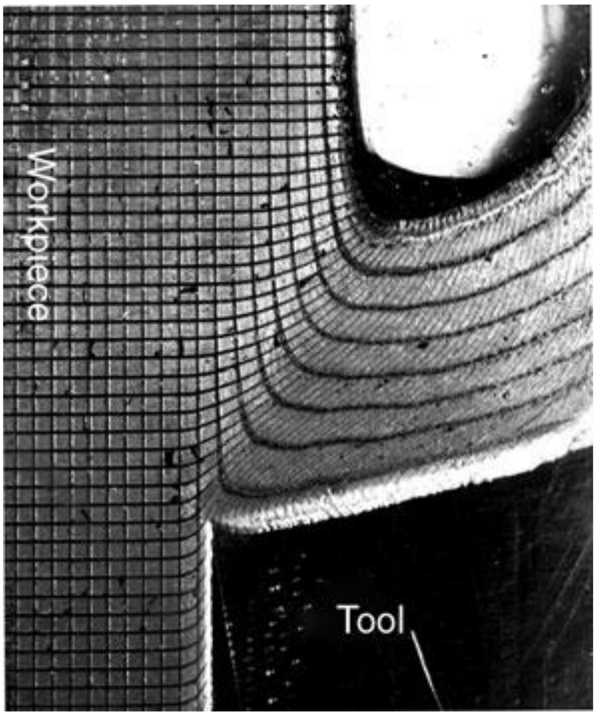

Figure 2.10 : Deformation representation of workpiece.

Two basic mechanisms in chip formation are:

-Yielding: generally for ductile materials

-Brittle fracture: generally for brittle materials

During the machining operation, at the tool tip a small crack cracks and because of stress concentration, it grows.

Although, in ductile materials yielding and plastic deformation reduces stress concentration and prevent crack propagation with the result of continuous chips, in brittle materials crack initiation and propagation acts quickly with the result of discontinuous chips. Also, strain localization in machining of cast irons could cause separated regions of high and low strains which led to segmented chip formation. The segmented chips are not homogenously deformed and mostly form at high cutting velocity [26]. Furthermore, crack growing mechanism in segmented chips beside the shear localization mechanism could cause this kind of chips.

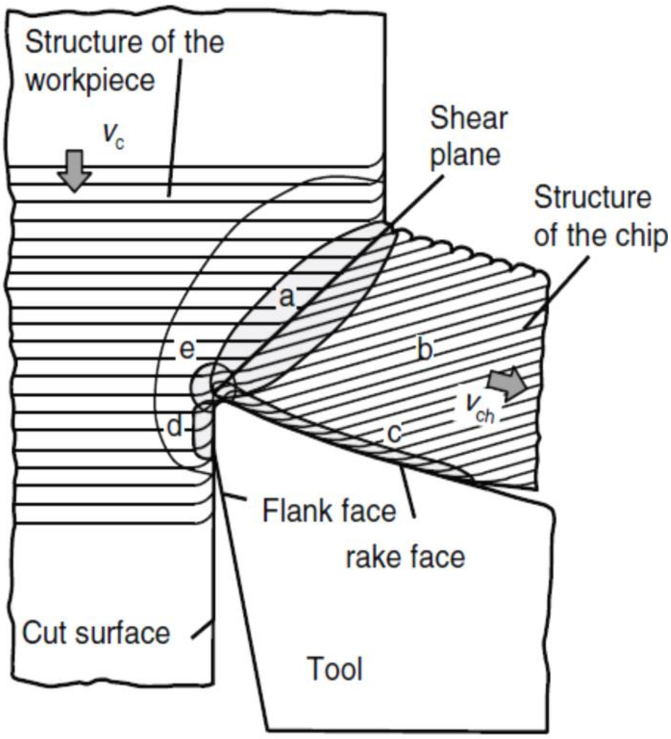

Figure 2.11 : Chip initiation and deformed zones [14].

The production process of serrated chips include of two stages. At first deformation energy and cutting temperature rises until it reaches a certain value after that the stage of shear localization starts. During the machining, local high cutting temperature will soften the material and consequently plasticity increases which causes shear localization.

This action repeats during the machining operation and make serrated (tooth-shape) chips. Also other cutting factors like cutting speed and feed increasing, tool rake angle decreasing and material characteristic change depending on cutting temperature rising can cause serrated chip formation.

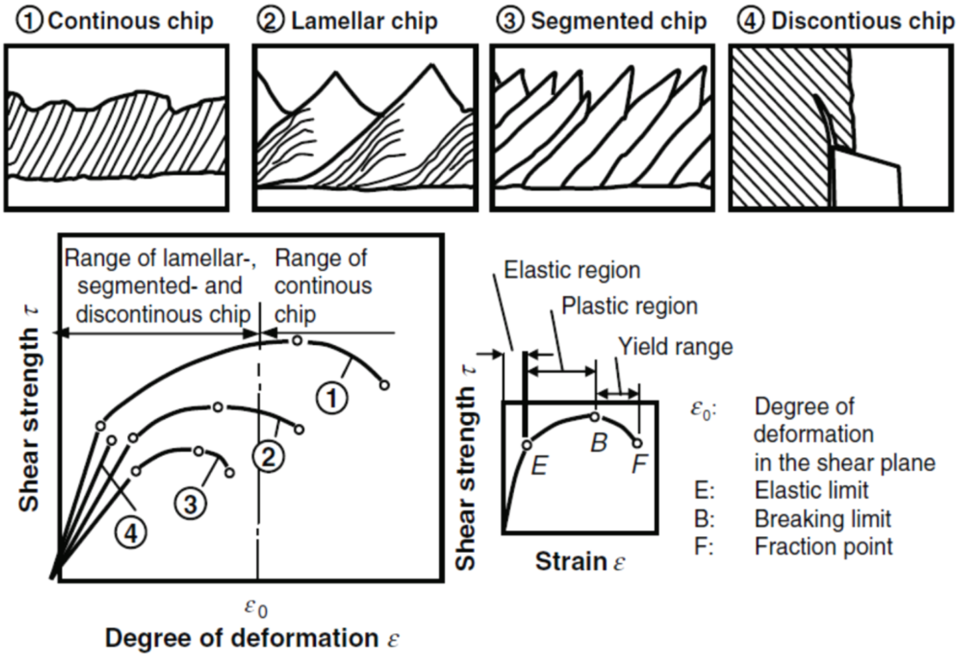

Figure 2.12 : Types of chip depending on material properties [14].

2.7 Properties of Compacted Graphite Iron: CGI

Compacted (vermicular) graphite has been produced heedlessly during the spheroidal graphite iron production process as a result of magnesium or cerium lacking. However, during the 1960's, this type of cast iron took its place with valuable mechanical properties in manufacturing technologies [27].

Although, the origin of compacted graphite iron is related to a research by Morrogh at British cast iron research association (BCIRA), the first patent in U.S was conducted by R.D.Schellerg (U.S patent 3,421,886, May 1965). This kind of cast irons is characterized by graphite particle shapes and consequently physical properties between grey flake-graphite irons and spheroidal graphite (SG) cast irons [28]. Figure 2.13 shows the microstructure of different types of cast irons.

This type of graphite shape originates higher strength and ductility than cast irons containing flake graphite. Also, the solidification of flake and compacted graphite irons are similar to each other which show better castability of CGI in comparison with ductile iron.

Even more, the interconnected graphite particles cause better thermal conductivity and damping capacity than ductile iron. Figure 2.14 shows the mechanical properties of CGI in contrast with grey cast iron.

Compacted graphite irons can be replaced by grey cast iron where the strength of grey iron is insufficient like gearbox housings, turbocharger housings, connecting forks, bearing brackets, pulleys for truck servo drives, sprocket wheels, and eccentric gears. However, the change for ductile iron is mostly undesirable because of less casting properties of latter. The compacted graphite particles restrict crack initiation and growth in the microstructure which is the main reason for mechanical properties improvement [27].

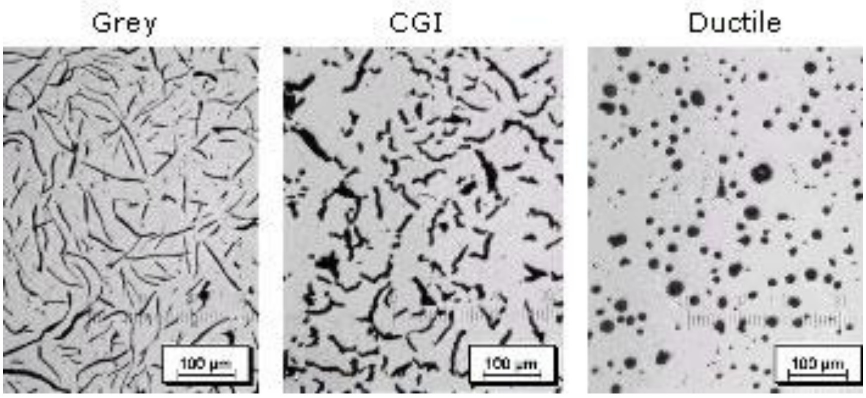

Figure 2.13 : Microstructure of (a) grey iron, (b) CGI and (c) ductile iron [77].

Compacted graphite iron is produced when near-eutectic molten iron de-sulphurised and thermal treated at about 1400 c° with alloy containing magnesium (as a nodulizing element), titanium (as anti-nodulizing element) and cerium. Although, magnesium tends to produce spheroidal graphite during the process, titanium controls this behavior to the amount which is less critical [28].

The amount of magnesium usually is about 0.01-0.015 % in weight to guarantee the flakes would not form in the microstructure but not enough for full nodularity [29]. The graphite's heat resistance characteristic in cast irons is more than iron matrix and compacted graphite particles make this specific type of cast iron attractive as a heat-resisting material for automotive industry [28].

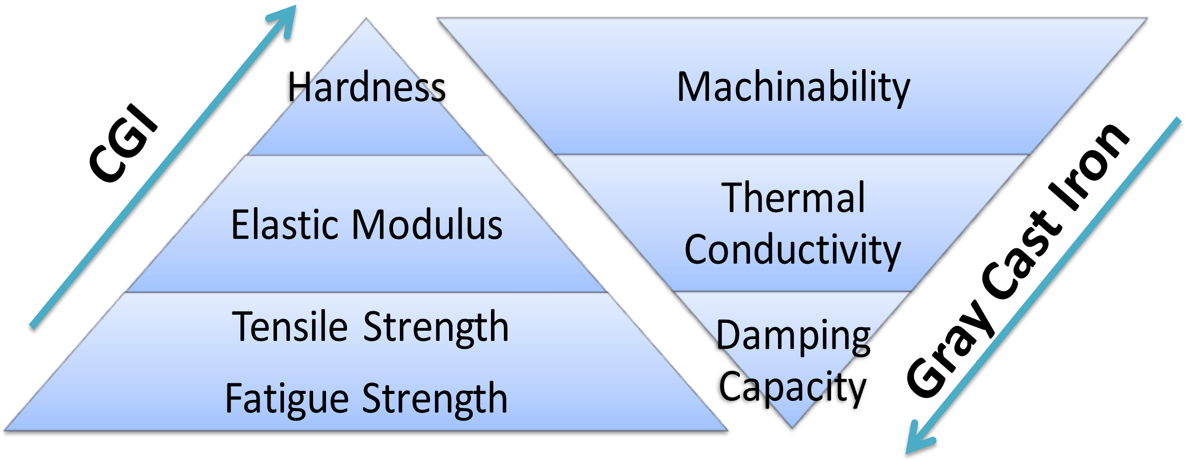

Figure 2.14 : Mechanical properties of different cast iron types.

Table 2.1 shows comparative mechanical and physical properties of different types of cast irons. The index 100% was assigned to compacted graphite iron for comparison purposes (SAE J1887/2002).

Table 2.1 : A comparison of mechanical properties in different types of cast irons [11].

Property	Gray Iron	CGI	Ductile Iron
Ultimate Tensile Strength	55%	100%	155%
Yield Strength	-	100%	155%
Elastic Modulus	75%	100%	110%
Fatigue Strength	55%	100%	125%
Hardness	85%	100%	115%
Damping Capacity	285%	100%	65%
Thermal Conductivity	130%	100%	75%

The ISO 16112 standard for CGI grades ranging from 300 MPa to 500 MPa of tensile strength is showed in Table 2.2. In this categorization the EN-GJV-300 grade is fully ferritic and the GJV 500 grade is fully pearlitic due to application demands. All the grades are in the nodularity range of 0-20% in their microstructure. Also, specific alloying elements for high temperature resistance, wear resistance or other properties could be added to CGI as shown in Figure 2.15.

Table 2.2 : CGI Grades – German Standard VDG Merkblatt W50 (2002) [37].

Grade	UTS (MPa)	YS (MPa)	E (%)	HB 30 (typical results)
EN-GJV-300	300-375	220-295	1.5	140-210
EN-GJV-350	350-425	260-335	1.5	160-220
EN-GJV-400	400-475	300-375	1.0	180-240
EN-GJV-450	450-525	340-415	1.0	200-250
EN-GJV-500	500-575	380-455	0.5	220-260

Figure 2.16 shows the micrographs of worm-shaped graphite particles in compacted graphite iron by usage of optical microscope and scanning electron microscope (SEM). The graphite particles are randomly oriented in the microstructure like grey iron.

Grade	Pearlite (%)	Chemical Analysis (%)								
		C	Si	CE	Mn	S	Mg	CeMM	Cu	Sn
GJV 400	~ 70	3.6-3.8	2.1-2.5	4.4-4.7	0.2-0.4	0.005-0.022	0.006-0.014	0.01-0.03	0.3-0.6	0.03-0.05
GJV 450	> 90	3.6-3.8	2.1-2.5	4.4-4.7	0.2-0.4	0.005-0.022	0.006-0.014	0.01-0.03	0.7-1.0	0.08-0.10

Figure 2.15 : Typical element contents for CGI with 0-20% nodularity [5].

The difference is related to graphite particles which are shorter and thicker with rounded edges elongated connected to nearest neighbors within the eutectic cell. This action causes a strong bond between graphite and iron matrix [30]. likewise, high cooling rates cause nodular graphite particles with finer perlite phases and this action is the source of mechanical property improvement as shown in Table 2.3.

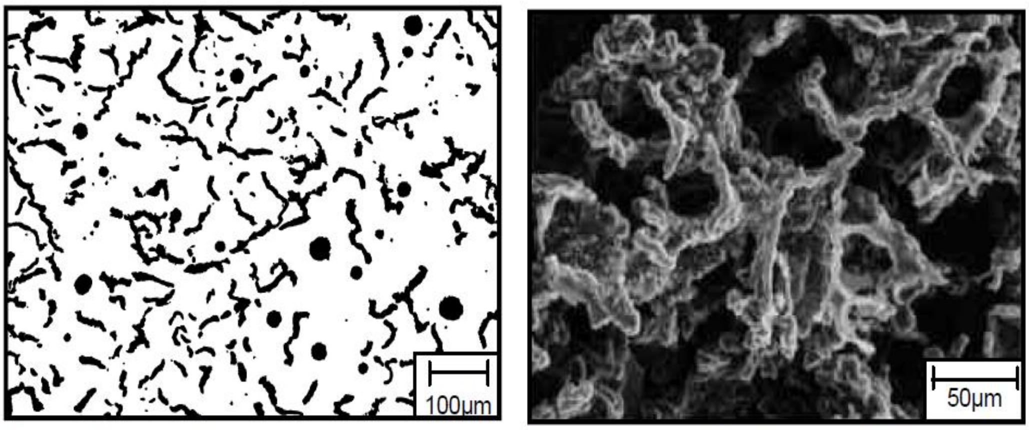

Figure 2.16 : CGI microstructue a) with 10% nodularity b) SEM micrograph [37].

Table 2.3 : Typical properties of ISO Grade GJV 450 as a Function of Nodularity [5].

Property (25°C)	Nodularity %				
	10	30	50	70	90
Tensile Strength (MPa)	465	520	590	640	700
Yield Strength (MPa)	350	370	390	420	470
Elastic Modulus (GPa)	145	150	155	155	160
Elongation %	1-2	1-3	2-4	2-5	3-6
Thermal Conductivity (W/m- K)	36	33	31	28	25

2.7.1 Important factors effecting CGI formation

The main factors affecting the formation of CGI are the following:

- Sulphur content
- Oxygen content
- Active Magnesium
- Nucleation status
- Cooling rate

A close balance between these five variables is required. Unlike grey and ductile irons, the sensitivity of CGI to Magnesium and inoculants prevent foundries from adopting the traditionally conservative philosophy of overtreatment. Therefore, reliable CGI production requires simultaneous control of active Magnesium and inoculation throughout the process.

2.7.1.1 Control of Magnesium

After Magnesium reacts in the melt with Sulphur and Oxygen, the residual Magnesium is classed as active Magnesium. Active Magnesium content needs to be controlled to suit the section or modulus (cooling rate) of the chosen casting to ensure that suitable CGI structures are produced. Too high an active Magnesium content results in a high proportion of nodules, reducing thermal conductivity and decreasing mechanical damping. Too low an active Magnesium results in the formation of flake iron, reduced mechanical strength and ductility. Fast cooling promotes nodule formation and slow cooling promotes flake iron.

2.7.1.2 Control of inoculation

Inoculation levels need to be tightly controlled to minimize the formation of flake or carbides but limited to prohibit the formation of excessive nodules. The only reliable method available to monitor nucleation levels and performance of different Ferro Silicon inoculants is with the use of thermal analysis.

2.7.1.3 Titanium method of CGI production

A wide window of opportunity is available if the titanium method of CGI production is utilized and complete CGI structures can be produced in castings with wide cross sectional variation. The downside is reduced machineability. This method is usually limited to ingot moulds, brake discs (the cuboids enhance the brake disc wear properties) or parts requiring limited machining. However for general engineering castings, requiring extensive machining, alternative methods are required.If the titanium method is not applicable, very tight control of base iron metallurgy is necessary. Active Sulphur, Oxygen, Magnesium levels and nucleation status need to be measured and controlled.

The main obstacle in CGI's mass production and replacement with grey cast iron is its poor machinability. Investigations for machinabilty improvement was through manipulating metallurgical variables [8], innovative tooling designs as rotary insert tools [31], different cutting insert materials even employing laser-assisted machining (LAM) technique at low speeds [10], hope to have a material removal volume which is suitable for mass production. However, all of these solutions seemed to work in limited circumstances like low cutting speeds or using high priced and hard to manufacture cutting tools or even sometimes the metallurgical manipulation caused a decrease in mechanical properties [3].

Machinability study which was conducted by Moecellin et al. on drilling of CGI provided 83% of tool life improvement and cause to make a CGI which has machinabilty similarity to gray cast iron [11]. Most of these investigations were conducted for drilling or milling and the improvements may not be applicable for other machining processes like turning [11] by the means of CGI's machinability development.

2.7.2 Factors influencing machining performance of CGI

The percentage of nodularity in CGI workpieces has extensive influence on machining performance and more nodularity could cause less tool life. Also, the pearlite content could affect the machinability of CGI depending on the type of operation. Although, an increase of pearlite during the milling operation improved the tool life, for turning and boring operations (continuous cutting) it has reverse effect and decreased the tool life.

It is assumed that the CGI with low content of pearlite is too soft for chip formation during the milling operation; however the high content is too abrasive for turning and decreases the tool life. Furthermore the addition of titanium for controlling the magnesium and spheroidal graphite preventing, influences the machining performance of CGI negatively (causing 50% reduction in tool life). Magnesium bonds with oxides, silicate and sulphide which affect the machining performance of CGI negatively. However, Dawson et al. [5] observed the MnS inclusions forming a lubrication or protective layer over the tool during the high speed machining which reduces the tool wear.

2.8 Minimum Quantity Lubrication: MQL

The investigations for the usage of less harmful cutting fluids and wet machining elimination induced many researchers to work on near-dry machining processes as like minimum quantity lubrication (MQL). As stated by the report of Ford Motor Company which was related about efficiency of MQL, they had a 13% decrease in process costs by the means increasing tool life, water mixed fluid elimination, decrease in maintenance cost and better skin care via MQL [12]. Also, in the reports of Chalmers (1999) [32] more than 100 million gallons of metalworking fluids are used in the U.S. each year and 1.2 million employees are exposed to these fluids which could have serious health issues and economy damage [33]. Furthermore, the chips which are produced during the wet machining, should be dried before recycling which incurs additional costs. Besides, MQL produces almost dry chips with easier maintence,recycling, cleaning and waste organizing so the cost reduces. Also, during the MQL process the basic functions of cooling, lubrication and chip removal occurs.

MQL is a near dry lubrication process in which a small amount of lubricant blows over cutting tool-workpiece interface by the means of compressed air jet so it cause less coolant usage. Effectiveness of this method in most of the metal cutting processes like sawing, turning, milling, drilling, and tapping propelled the manufacturers using it due to tremendous advantages. The oil droplets reduce the friction and adhesion of chips between tool and workpiece so the cutting temperature in the contact area reduces and tool life improves. The basic types of MQL delivery systems are external spray with a nozzle blows over tool-workpiece interface, and internal by the means of channels inside the cutting tool to bring the mixture in the contact area.

The external system is consists of compressor, coolant tank, coolant delivery system, tubes and nozzle that are not integrated into machine's design. Therefore the nozzle must be adjusted to the respective application. This relatively rigid system is suitable for machining operations where the tools and work piece contours do not change. It can also be used for series-produced parts. The advantage of external MQL system is simplicity and low cost. Also, there is no complex parts in the system and easily could be changed or serviced. The problem of this system is while the mixture of oil and air travel to nozzle and tool-workpiece interface it could be seprated which affect the performance of lubrication and cooling.

With internal MQL, the aerosol is transported by either the rotating spindle or turret through the tool holder and tool. The metered oil quantity is completely dispersed when adjusted properly. This system has less sepration of oil and air in comparison with external and during the tool change less lag time is the benefits of system. However, the maintence and service of parts because of complexcity is much more difficult and costly. Figure 2.17 shows the component of MQL system for external and internal applications. During the MQL operation the lubricant evaporates and mixes with air and blows over too-workpiece interface. Then, the chips, workpiece and tool remain in near-dry statue which is beneficiary for mass production in environmentally friendly manufacturing. Therefore, better surface finish and tool life occurs during the operation [34].

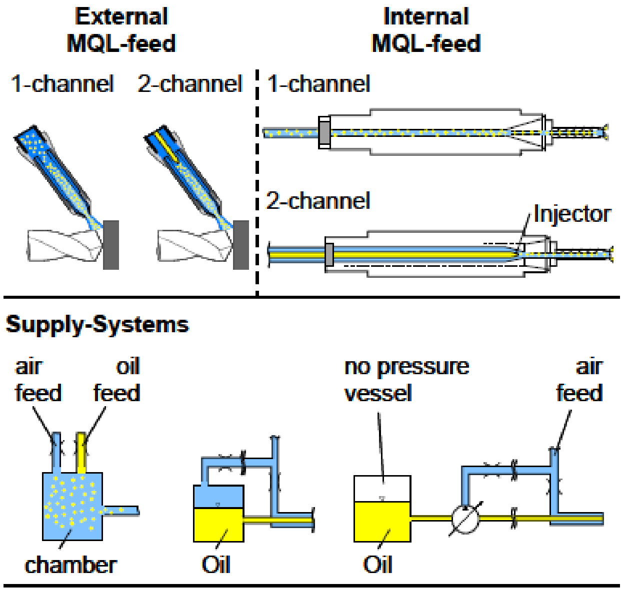

Figure 2.17 : MQL feed system [13].

Lugscheider et al. reported that by the usage of MQL in reaming process of gray cast iron and aluminum alloy by the means of coated carbide tools, tool wear reduces in comparison with dry machining and consequently, the surface roughness of holes reduces [35]. Oil and other wastes present significant disposal impacts and implications to our environment. While legislation and regulation specify mitigation to the environment, enforcement of this legislation is challenging, expensive, and difficult. Metal chips produced during MQL machining are nearly dry and much cleaner than conventional approaches. Near-dry chips are easier to recycle and more valuable as a recycled material.

2.8.1 Advantages of MQL

Financial

- Through the elimination of nearly all supply and waste disposal systems for the metalworking fluid produce large savings.
- With streamlined processes longer service life can be expected.
- In individual cases can be reduced with optimized processes, the process time by up to 30%.
- Purchase, storage, transport and disposal of cutting fluids are greatly reduced or dropped.
- The cost of checking and maintaining the coolant is gone.

- Depending on the application consuming subsequent, processes for the cleaning and washing of the workpieces can be reduced or saved.
- Dry chips can be sold as recycled material but, wet chips must be disposed of hazardous waste.

Ecological

- Accidents by leaking coolant in large quantities are not possible.
- There are no environmentally harmful emulsions.
- Through a dry machine environment, the risk of accidents will be reduced.

2.8.2 Disadvantages of MQL

- Depending on the circumstances, there is high investment in the upgrading of machinery. By more expensive special tools in optimization, a very careful tuning of the workpiece, machine parameters, and tool lubrication is needed.
- Because of extra costs, for individual and small series production a minimum quantity lubrication is therefore sometimes not profitable.
- The change to minimum quantity lubrication is not practical for all machining processes, machines and workpieces, so usually the coolant supply is required in the company.

3. LITERATURE REVIEW

The oldest and most famous member of cast iron categories is Grey cast iron with graphite flakes. Despite high compression strength of gray cast iron, it has less tensile strength and low cost is the main reason for common usage. Since 1950's, spheroidal graphite cast iron (SG iron), has been replaced with most cast iron types due to its higher strength and elongation. Higher mechanical properties of SG iron compared to other types are via nodular graphite particles with better iron matrix continuity in contrast with flaky graphite of gray cast iron [1]. Different mechanical and physical properties of cast iron types are mostly related to dissimilar shape, size and growth mechanism of graphite particles in the microstructure. Ductile iron and compacted graphite iron was first patented in 1949. Although, ductile iron became a favorable material in manufacturing industry, CGI was considered as a curiosity at the time. It can be said that Compacted Graphite Iron is a denigrated or spoiled Ductile Iron and its invention was probably an accident when the base metal for producing Ductile Iron was unintentionally under-treated with magnesium and the resultant metal was found to have certain characteristics very near to that of Ductile Iron and certain characteristics very near to that of Grey Iron. But the advantages of CGI in application do not stem from its mechanical properties. If a superior mechanical property compared to Grey Iron is the only criteria, then the natural choice would be Ductile Iron due its ease of manufacturing compared to CG Iron. The most important fact about CG Iron is that, while it has much higher mechanical properties compared to Grey Iron, its thermal and damping characteristics are very near to Grey Iron [2,3]. In order to describe the graphite shape in CGI microstructure, the term "vermicular" has been used. However, the term "compacted" is more preferable which shows three-dimensional structure of this cast iron type. Moreover, the term "vermicular" refers to the worm-like graphite structure in irons of very low sulfur content and differs from compacted graphite [36]. These properties have been found to make CGI ideally suited for engine manufacturing, where lighter and stronger materials are needed which can absorb more power. An assembled automotive engine can be made nine percent lighter with CGI.

The engine block weight alone can be reduced by 22 percent. This corresponds to a 15 percent reduction in length and 5 percent reduction in height and width. It can be easily understood why CGI is continually gaining popularity in automobile industry [37]. The reason that CGI has not yet been widely adopted for production by foundries is that the stable range of compacted graphite is too narrow to ensure risk-free production which necessitates very strict process control involving heavy investment on control equipments. While not quite as strong as Ductile Iron, CGI is 75 percent stronger and up to 75 percent stiffer than Grey Iron. The thermal conductivity and damping characteristics of CGI are 80% and 60% respectively of Grey Iron. It is five times more fatigue resistant than aluminum at elevated temperatures, and twice as resistant to metal fatigue as grey iron [3]. CGI standards for different grades have been developed and published by several international organizations and countries. These standards are categorized mostly due to nodularity percentage and mechanical properties as shown in table 3.1 [37]. Several methods have been adopted to produce CGI. The simplest method would have been to under-treat the metal with magnesium so that the residual magnesium is within the specified range. But the treatment process adopted by most of the foundries are not very consistent with respect to Mg recovery, besides Mg recovery is also dependent on the base metal chemistry and thermal conditions. Other method is treating the molten metal with both spheroidizing and anti-spheroidizing elements, mainly Ti.

Table 3.1 : CGI standards.

Country	Issuing body	Number	Year
International	ISO	ISO 16112	2006
International	SAE	J 1887	2002
Germany	VDG	W 50	2002
USA	ASTM	A 842-85	1997
China	JB	4403-87	1987
Romania	STAS	12443-86	1986

This process can provide optimum results in many applications. Indeed, the Ti process appears to be a reliable CGI production method with repetitive results. However, one important factor impedes the general application of this treatment: titanium has a strong carbide, and nitrocarbide formation tendency. TiC and complex Ti nitrocarbides are very hard phases that diminish machining tool lifetime.

Using a 0.015 to 0.025 percent sulfur addition (after magnesium additions) in the form of iron sulfide or iron pyrites, which contained nominally 49 percent sulfur and is approximately 100 mesh by down to denodulize magnesium treated iron, is other production method of CGI with less than 20 percent nodularity [38,39]. As a result, three main methods for CGI manufacturing, are by treatment of the liquid iron with alloys containing both nodularizing elements (Magnesium and RE elements) and denodularizing elements (Titanium or Aluminum) [40,41] and the second primary method is treatment of liquid iron with RE elements and the last basic method is based on extensive desulphurization of cast iron with high casting solidification cooling rate and possibly inoculation with Zr [42].

Murthy et al. [1] on their work studied the production methods and growth mechanism of graphite particles in CGI microstructure. Although, the study contained a comprehensive overview of production methods and different mechanical properties of compacted graphite iron, some methods were not suitable for mass production.

Ecob et al. [43] studied CGI production method route and mechanical properties optimization with different treatment methods for improving poor machinability of CGI. In order to achieve this mean they develop an alloy that contained 5-6% Mg and 5.5-6.5% Rare Earth (RE) in a normal ferrosilicon nodularising base alloy. By the means of this alloy they have reduced production costs and suppress CGI's machinability.

Machinability improvement of CGI is a favorable goal in automotive industry for replacing parts such as cylinder block with traditional cast irons because of higher strength and thermal shock resistance. Machinability studies of compacted graphite iron in turning, milling, drilling and other manufacturing operations have been conducted by many researchers, hoping to achieve a desired rate in contrast with gray cast iron. Also, in continuous cutting processes of CGI, tool life decreases dramatically and production costs arise [44]. Although, experimental studies on CGI machining have been few at invention times, in 1980's by developing the production process of CGI and obtaining desired mechanical properties, researches propelled to develop poor machinability of this material.

Poor machinability of CGI in comparison with other cast iron types is mostly related to the absence of manganese sulfide (MnS) layer as a lubricator and protector during CGI machining in the contact area of material and cutting tool [5, 45]. Because of lower sulfur content in CGI (0.005-0.025%) in comparison with gray cast iron (0.08-0.12%), this phenomenon happens despite other cast iron types during their continuous cutting operations. Generally, during the production process of CGI sulfur minimization applies to prevent flake graphite formation [46]. Aside from the absence of the protective and lubricating layer of manganese sulfide (MnS) in CGI machining, the presence of a low percentage of titanium in CGI effects cutting tools wear [47]. Large amounts of titanium (0.1 – 0.25%) have been used to prevent spheroid graphite formation which increases the stable magnesium range for CGI production. Higher percentage of titanium in CGI causes titanium carbonitride (TiCN) inclusion formation which are harder than tungsten carbide.

This microstructure behavior makes more cutting wear during CGI machining. It was found that a slight increase of trace level of titanium from 0.01 to 0.02% is sufficient to reduce the tool life by about half [5]. Continuous turning tests on ferritic and pearlitic grades of CGI, first was conducted by Phillips [48]. He used different types of cutting tools (coated and uncoated tungsten carbide, ceramic cutting tools) and examined the operation in both dry and wet machining circumstances. From the tests, it was found that the machinability of CGI was intermediate to that of gray and spheroidal/ductile irons. Furthermore, it was found that ferritic CGI was more machinable than pearlitic CGI. Although, usage of cutting fluid provided an improvement during CGI machining, it wasn’t in sensible rate.

Dawson et al. [5] studied the effect of the metallurgical variables on the machinability of compacted graphite iron and mostly exposed the effect of pearlite contents in CGI machining based on machining process and cutting tool chemistry. Increasing the pearlite percentage of <5% nodularity CGI from (70-80%) to (>95%), was found to have a negative effect on turning at (150, 250, 400, and 800 m/min) cutting speeds. However, increasing the pearlite content of CGI from (70-80%) to (>95%) at nodularity (5-10%) enhanced the tool life in milling. Although, pearlite content shows an effect in CGI machinability, it is important not to relate it just for pearlite content.

The actual reason for this machinability improvement was basically due to lower nodularity percentage (<5%) in the (70-80%) pearlite range, compared to (5-10%) nodularity in the (50-60%) pearlite range. In addition, increasing the cutting speed improved machinability in milling, but had a negative effect on turning. he reported that the low pearlite alloys are too soft and deformable for easy cleavage and chip formation during milling while the high pearlite alloys are too hard and abrasive for continuous cutting. Figure 3.1 shows the optimized cutting parameters for different machining operation (milling, turning and boring) of CGI with different cutting tools.

Sahm et al. [49] conducted CGI machining tests on CGI at low cutting speeds (about 100 m/min) with coated carbide tools and measured tool wear and tool life. However, during CGI boring of CGI at low cutting speeds by using PCBN cutting tools, the tool life decreases drastically (by 10 to 20 factor). Also, during continuous cutting operation of CGI with PCD (Polycrystalline diamond) tools, tool life has been increased in contrast with PCBN (Polycrystalline boron nitride) tools (increased by about 20 factors).

Pretorious et al. [50] found PCD tools to be more favorable for CGI milling than for CGI continuous cutting operations in their research. They claimed that during continuous cutting of CGI, high temperature rise accelerated thermal wear of PCD cutting tools. Nevertheless, PCD tools and PCBN tools are highly expensive than carbide tools which normally are used in turning operations.

Gabaldo et al.[51], studied performance comparison in milling of 98% pearlitic CGI using coated carbide inserts; (TiCN, Al_2O_3 and TiN on the flank face) and Si_3N_4 (Sialon)-based ceramic tool. Milling operation have been conducted in different cutting speeds (140, 220, 280, and 340 m/min) and without cutting fluids. Carbide's tool life did not show a significant decrease when cutting speed increased to 420 m/min. At higher cutting speeds, at 680 and 850 m/min, carbide inserts presented significant decrease in tool life tendency. According to research, at same cutting conditions carbide inserts have showed more tool life than ceramic cutting tools. Experimental study on determining the wear mechanisms of CBN (cubic boron nitride) tools for CGI machining was first conducted by Gastel et al. [7]. The mechanisms which realized during the tool wear were oxidation and diffusion. However, they did not show the solutions for CGI machining improvement by using PCBN tools.

Diamini et al. [52] studied CGI's machinability by using PCBN inserts in turning operation to achieve a desired optimization. In the experiment dry turning of 5% nodularity, 70% pearlitic compacted graphite iron was selected to study flank wear of tool and finish surface of workpiece. During the study cutting speed was in the range of 400-800m/min, and the tool had a negative rake angle of -6°, flank angle 6°, and a lead angle of 45°. They reported that tool wear at high cutting speed (600 – 800 m/min) was dominated by crater wear. Decreasing the cutting speed prolonged the tool life and wear was mainly on the flank surface. Other researchers have been lead to innovative techniques and methods of CGI machining. Multiple insert tool usage was one of these techniques. Although, they revealed better productivity, they were expensive, complex and hard to maintenance [5]. Rotary-insert boring tools were used and enabled machining of CGI at cutting speeds comparable to cast irons. However, machine tool rigidity and accuracy were the problems [53].

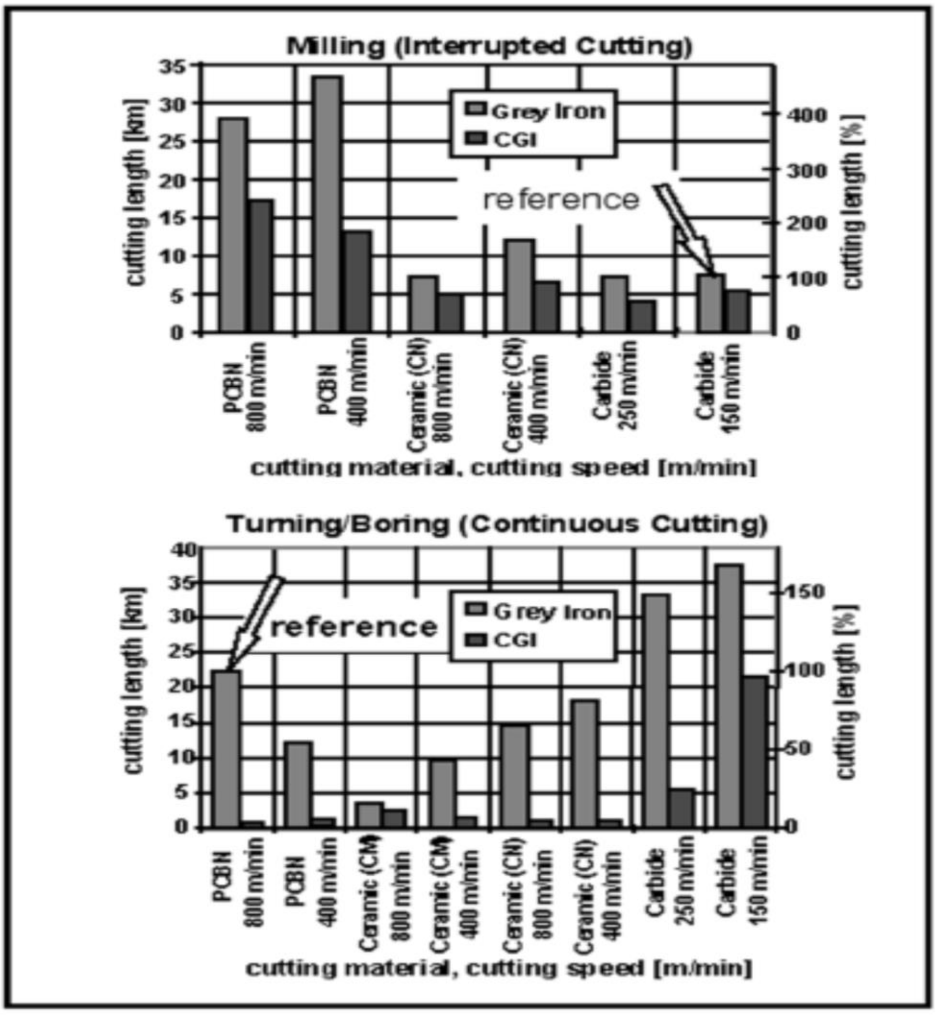

Figure 3.1 : Tool life for different tool materials in interrupted and continuous cutting of 70-80% pearlitic CGI and gray iron.

Abele et al. [6] declared CO_2 cryogenic coolant system increase the tool life of PCD cutting inserts in CGI machining. They claimed these improvements were directly related with diamond grain size, the binder material, and the cutting parameters.

Skvarenina et al. [10] used Laser Assisted Machining (LAM) technique for compacted graphite iron machining. LAM was effective and cost saving, but it was laboratory based technique and hard to be established in a factory based setting.

Moreover, the process was economically useful only at low cutting speeds (100-120 m/min) which was in the same success rate of carbide tools. So, usage of LAM in low cutting speed was an expensive and complex alternative in comparison with carbide cutting tools.

Mohammad et al [3,54] studied the microstructure of CGI for modeling the machining process and its effect on tool wear, cutting forces and chip formation. They modeled segmental chips which were produced during CGI machining and by the means of cohesive zone elements graphite-matrix interface have been studied. In order to validate their finite element model, they have compared simulated chips and force trends with experimental findings. They investigated the effect of cutting forces, cutting speeds and cutting temperature on tool wear during CGI machining for finding an optimized technique of CGI machining and tool material selection. Their work gathered different cutting conditions and selective tool material for automotive and locomotive industries are of significant need to date. Their experiments were at 100, 200, and 400 m/min, cutting speeds and feeds of 0.05, 0.1, and 0.2 mm/rev each. Although, their comprehensive work helped to understand chip microstructure, cracked behavior of segmented chips, cutting forces and tool wear, it was assumed to be orthogonal cutting condition and the work was focused on modeling not to improve CGI machinability.

Moecellin et al. [11] reported an 83% tool life improvement during the drilling of CGI and cause the machinability advancement which was similar to gray cast iron. The tests were performed using 10 mm diameter solid carbide drills from class K35, TiAlN single layer coated (3000 HV). However, the reported data were valid for drilling only and may not be applicable to other machining processes as admitted by

Moecellin.His paper clarified the machinability improvement with the aid of external Minimum Quantity Lubrication system during drilling.

Oliveira et al. [55] studied the effect of cemented carbide coated with TiAlN tool geometry during drilling of CGI. They investigated maximum flank wear (V_{Bmax}) as a function of tool life and machinability performance of CGI. He reported the geometry with tip radius obtained the best results and higher tool life was obtained. Also, in their observations better surface roughness of holes were announced. Their optimized tool geometry for CGI drilling could be used as a reference in engine block production.

Heck et al. [56] investigate the wear behavior of cutting tools used for CGI machining. They reported that the main reason in poor machinability of CGI is related to the lack of MnS layer and in order to solve this problem they suggested reducing cutting speed and increasing feed rate in the same amount as decreasing the cutting speed. Also, replacing single insert tools with multiple insert tools has shown effective in productivity. Furthermore, in this study the analytical MnS layer thickness value for other cast irons were measured and compared with CGI.

Alves et al. [44] investigated improvements in CGI drilling achieved through the use of cutting fluids with EP (extreme pressure) additives. Cutting parameters in the study were kept constant by a cutting speed of 110 m/min, feed velocity of 350 mm/min and hole-depth of 20 mm. He reported an improvement due to a layer comprised of sulphur (EP additive) and metal. The use of EP (extreme pressure) additives leads to the formation of protective layers upon high loading in the friction process. Also, as a result, adhesion was avoided and the friction and wear behavior of cutting tool was improved.

Abele et al. [57] studied the tool wear mechanism of CGI machining and MnS layer relation with tool life. Also, different cylinder boring in different cutting speeds (10-800 m/min) with PCBN inserts has been examined. They used different cutting tools (PCBN-CBN-ceramic and carbide) for caparisoning grey cast iron and CGI machinability in turning and boring operations.

Nayyar et al. [58] investigated the machinability of flake, compacted and spheroidal graphite iron in continuous machining operations. Cutting temperatures, cutting forces, tool life, deformed chip thickness and contact length in different continuous machining operations (turning- boring and face turning) were measured for different cast iron grades.

During their examinations, face turning tests were performed in both dry and wet conditions to see the importance of cutting fluids for different grades of cast iron. They have reported that during CGI and SGI machining, usage of cutting fluids is useful. In order to measure tool life during CGI turning; cutting speed, feed and depth of cut was kept constant as 300m/min,0.2mm/rev and 1.5mm respectively.

Evans et al. [59] studied the machining properties of CGI, and the metalworking fluid properties and composition which impact and potentially extend tool life in CGI drilling and reaming operation. Machinability studies were made by measurement of the cutting forces, tool wear occurring and torque (as a function of friction) during the operation. In order to achieve a machinability rate as in gray cast iron and to assess the validity and effectiveness of process, a sulfur based additive was incorporated into the same metalworking fluid were used and for the same machining conditions, drilling and reaming operations were performed. As a result, the incorporation of the sulfur based additive has a significant effect on reducing cutting forces and tool's flank wear. While it is necessary to cast CGI with minimal sulfur content, it was shown that lubricating sulfur based additives can be utilized in the machining fluid to compensate for the lack of sulfur in the metal. Figure 3.2 shows the reamed hole finish surface roughness and effect of additive on the hole quality.

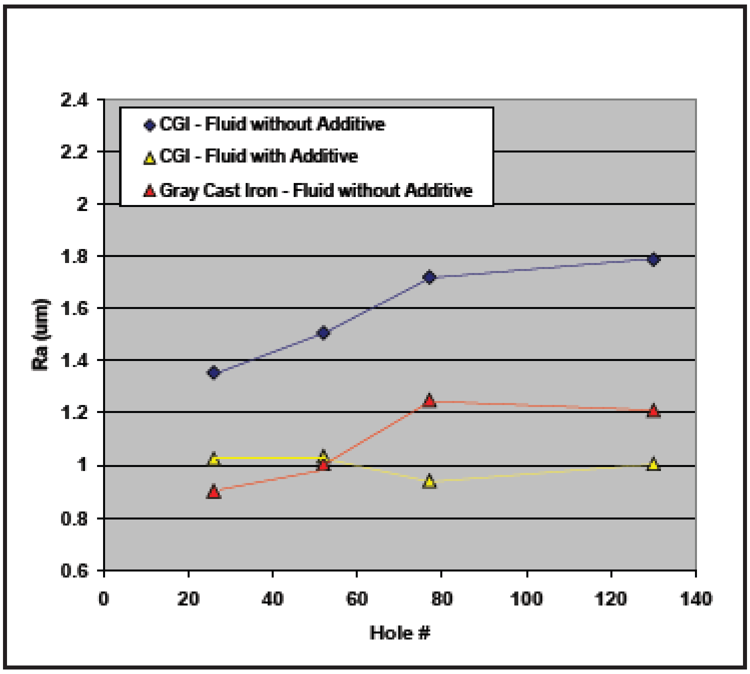

Figure 3.2 : Sulfur additive effects in CGI reaming.

There have been little investigations over the performance of CGI machining under any lubricant action. This is because of additional costs during CGI and other cast irons machining. So, it is preferred to be machined in dry conditions. Moreover, the costs in machines with rotary tools or multiple-insert tools (for improving CGI machinability) would be more than using lubricants. In addition, several researchers have shown the poor machinability of CGI is related to the absence of a lubricating (MnS) layer during high speed cutting [5,7,56]. Thus, Minimal Quantity Lubrication (MQL) system is investigated in this study to see whether the absence of this layer's effect could be rejected by other means such as cutting fluid action in MQL form. Also, during CGI machining, discontinuous chips are produced and by the means of cutting fluid penetration to the cutting zone and cooling the interface area, machinability development could be achieved [60].

Minimum quantity lubrication (MQL) has increasingly found its way into the area of machining and, in many areas, has already been established as an alternative to conventional wet processing. In contrast to flood lubrication, minimum quantity lubrication uses only a few drops of lubrication in machining.

Today, the enormous cost-saving potential resulting from doing almost entirely without Metalworking fluids in machining production is recognized and implemented by many companies, primarily in the automotive industry. By using MQL in the framework of highly automated large volume production, most of automotive industry parts like cylinder heads, crankcases, camshafts and numerous other components made of common materials – such as steel, cast iron and aluminum, could be produced economically.

Minimal Quantity Lubrication (MQL) is a near dry lubrication technique that has been recently used as an alternative for wet machining and also dry machining operations. In MQL small amount of lubricant (mostly oil), in atomized form, is mixed with compressed air and spray over the tool-workpiece contact area for coolant means. This action causes friction reduction between tool and chip contact area. Also, this process effectively reduces disposal fluid management and by the help of compressed air, cooling achieves [60]. Although, this lubrication system is in the category of near-dry process, it has achieved success through most of machining operations like sawing, turning, milling, drilling, and tapping in the means of adequate cooling, less pollution and effective lubrication.

Ford motor company reported a 13% decrease in the process costs via MQL by the means of tool life improvement, and water waste elimination [61]. In addition, chips produced are devoid of cutting fluid coating, enabling easier recycling. Several investigators have found MQL to be superior to dry and flood machining in terms of surface roughness, tool wear and cutting forces under certain cutting conditions [62,63,64]. Machining with MQL thus presents a perfect alternative to both dry machining and machining under flood lubrication.

Weinert et al. [13] investigated dry and MQL machining in different cutting conditions and analyzed cutting parameters, cutting tools, machine tools and the production environment during MQL machining. Although, a comprehensive study over MQL systems and its equipments were shown in this study, suitable operations and work materials with internal and external MQL systems were presented. Also, selective MQL fluids, dry and MQL process for different machining operations, optimized cutting parameters have been conducted in this paperwork.

Thamizhmanii et al. [65] studied Inconel 718 (steel) machining by applying MQL system. In the research vegetable based oil was applied by MQL in milling operation. They reported that MQL helps to use limited supply of coolant in order to minimize waste and it is environmental free. Also, their study showed that super cobalt tool has given more life by MQL than dry milling. Furthermore, better surface roughness in high cutting speeds was achieved by the means of MQL.

Silva et al. [66] investigated behavior of the MQL technique under different lubrication and cooling conditions when grinding ABNT 4340 Steel. They studied various types of lubricants for MQL system in order to determine the best lubricant and compressed air flow. Cutting forces, surface roughness, grinding wheel's diametric wear and residual stresses were measured. They reported that the MQL technique could be applied efficiently in the grinding process, providing environmentally friendly and technologically relevant gains. Also, surface roughness, tangential cutting forces and tool wear values were reduced by MQL usage.

Park et al. [67] studied the droplet sizes and the droplet distribution after MQL oil has been sprayed onto a polished silicon wafer. Also, droplet distribution has been investigated in this study to determine the MQL optimal nozzle–workpiece distance and the nozzle discharge pressure.

Droplets in several distances from target and different pressures were examined in this study for finding droplet velocity, size estimation and distribution behavior during machining operations with MQL systems.

Tasdelen et al. [68] investigated the contact length during minimum quantity lubrication (MQL) machining. They used uncoated and TiN coated inserts in the orthogonal turning tests. The examination conditions for both dry and MQL machining were same and contact length, chip morphology and engagement time were compared for both circumstances. They reported that MQL and compressed air lowers the contact length compared to dry cutting at short and longer engagement times. Although, the contact length was almost same for MQL and compressed air machining operation, the difference was in sliding region with the shorter engagement times. As a result, it was shown that MQL is a suitable method for short engagement time machining.

Ali et al. [69] studied the effect of MQL on cutting performance of medium carbon steel during turning operation at different speed-feed combinations. The paper investigated the role of MQL on chip ratio thickness, cutting forces, cutting temperature, tool wear and surface roughness in medium carbon steel turning by uncoated carbide inserts. Different cutting velocity (68-266 m/min) and feed rates (0.1-0.2mm/rev) were used in this examination for both dry and MQL turning conditions. Upon their results, a reduction in cutting zone temperature, surface roughness, tool wear and dimensional inaccuracy were achieved by the means of MQL. They reported that a productivity improvement and cost saving could be reached by implementing MQL systems in dry machining operations.

Heisel et al. [70] carried out extensive studies on applications of MQL in cutting processes. They described the possibilities of MQL applications in turning, milling and broaching experiments with geometrically defined cutting edges. All the investigations in turning and milling processes were using TiN-coated carbide inserts. They announced that certain surface quality and economical tool life depending on the machining operation and technology could be obtained with minimum quantity lubrication. Although, MQL could be applied to various machining operations, the volume of the cooling lubricant and the number of nuzzles are effecting the cutting operation. So, these factors should be used in optimized values during cutting of different materials.

Lugscheider et al. [35] MQL in reaming process of gray cast iron and aluminum alloy with coated carbide tools. During high speed cutting (250m/min), dry cutting was not possible in the reaming operation. By the aid of PVD layers and MQL, cutting process of gray cast iron were realized by twice the speed of dry cutting.

They concluded that it caused a reduction of tool wear when compared with the completely dry process and, consequently, an improvement in the surface quality of the holes.

Dhar et al. [34] conducted an experiment on the influence of minimum quantity of lubrication (MQL) on cutting temperature, chip formation and dimensional accuracy in AISI-1040 steel turning operation. They compared results with dry machining and machining with soluble oil as coolant in different cutting velocities (64, 80, 110 and 130 m/min) and feed rates (0.10, 0.13, 0.16 and 0.20 mm/rev).

Due to experimental results they noted that MQL enables substantial reduction in the cutting temperature, dimensional inaccuracy depending upon the levels of the cutting velocity and feed rate.Furthermore, under MQL cutting condition chip formation and chip-tool interaction zone become more favorable than dry machining. By the means of MQL, discontinuous chips with smaller length were produced. Thus, in selective cutting speed-feed combinations, it appears that MQL not only provides environment friendliness but can also improve the machinability characteristics. Their dimensional deviations results are shown in figure 3.3.

The drilling of aluminum–silicon alloys is one of those processes where dry cutting is impossible. Braga et al. [71] used MQL system and diamond coated tool in the drilling of aluminum–silicon alloys. Their results showed an irregular wear in the surface of the diamond coated drill and a decrease in the quality of the hole made by it, compared to the uncoated drill. They reported that the performance of the process by considering cutting forces, tool wear and holes roundness when using MQL, was same as using very high amount of soluble oil, for both coated and uncoated drills. In addition, MQL was more economical than wet machining and could be used in aluminum-silicon alloy’s drilling operation.

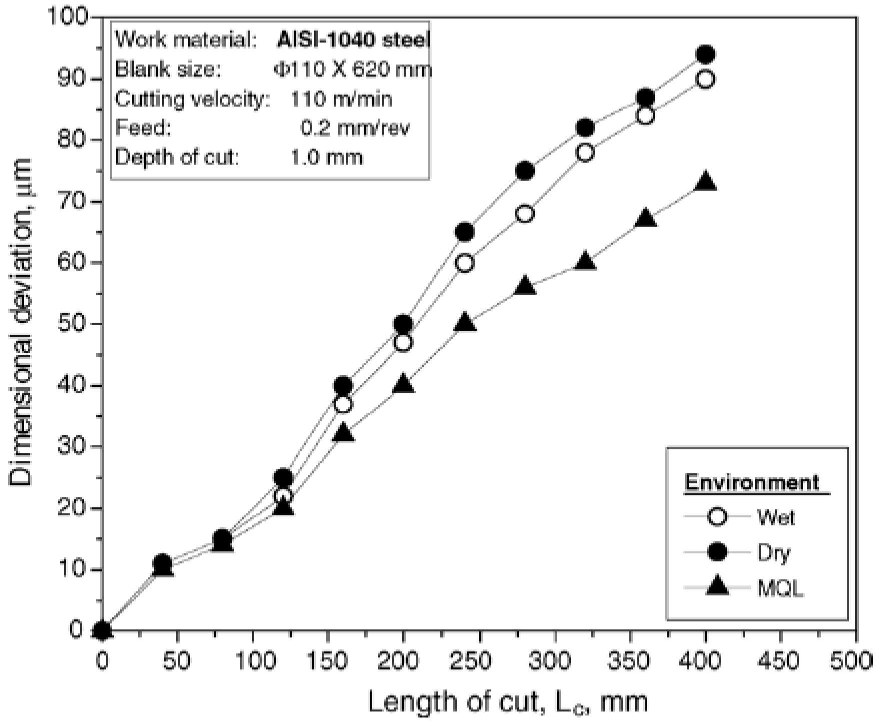

Figure 3.3 : Dimensional deviations observed under dry, wet and MQL conditions.

Rahman et al. [72] studied the effect of minimum quantity lubrication (MQL) in drilling commercially used steels. He reported that due to the high ductility of some cast irons, without cooling and lubrication, the chip sticks to the tool and breaks it in a very short cutting time and more crater wear and adhesion wear of tool will happen, which reduces the tool life and increases the production costs. Therefore, in drilling process a good alternative is the use of the MQL technique.

Da silva et al. [73] analyzed coated cemented carbide insert wear in milling of medium carbon steel by using different lubrication systems. Although MQL has shown its effectiveness during the operation, it was not suitable for high machined length conditions and for these circumstances wet machining with the applying method of reduced flow rate will be favorable. They measured flank wear and surface roughness for dry, wet and MQL machining in order to comparison their effects on the process as shown in figure 3.4 and 3.5.

N.R.Dhar et al. [106] studied the effect of MQL on tool wear and surface roughness during the turning operation of AISI 4340 steel. By this mean, the examined in three circumstances as dry, wet and MQL machining and claimed that MQL machining has better cutting performance than dry and wet machining due to reserving tool sharpness and reducing the cutting temperature. Because tool tip has less damage, better surface roughness is achieved. Figure 3.6 shows the average flank wear and surface roughness in these circumstances.

Attanasio et al. [74] investigated effect of MQL on tool wear in turning operation of normalized 100Cr6 steel. MQL was applied to the rake and flank face of a triple coated carbide tool (TiN outer layer, Al2O3 intermediate layer and TiCN inner layer) with constant cutting speed (300m/min) and two feed rates (0.2, 0.26mm/rev). They reported that when MQL is applied to the tool rake, tool life is generally no different from dry conditions, but MQL applied to the tool flank can reduce flank wear and eventually increases the tool life. Although, MQL gives some advantages during the turning operation, it presents some limits due to the difficulty of lubricant reaching the cutting surface.

Varghese et al. [60] determined the effect of tool material, tool topography and minimal quantity lubrication (MQL) on machinability of CGI. Cutting tools used in this study were coated carbide, coated cermet inserts, and ceramic insert materials. He reported that flat coated carbide inserts provided higher cutting forces in dry and MQL conditions compared to grooved coated carbide inserts. However, machining under MQL conditions at low speed (250 m/min) caused an increase in the cutting forces when flat coated carbide and grooved coated cermet inserts were tested. Reduction in cutting forces under MQL conditions was in the grooved coated carbide and flat ceramic inserts. At higher cutting speed (400 m/min), machining under MQL conditions increased the cutting forces for all cutting inserts. Hence, several useful techniques and studies have been conducted over CGI machining in different cutting operations.

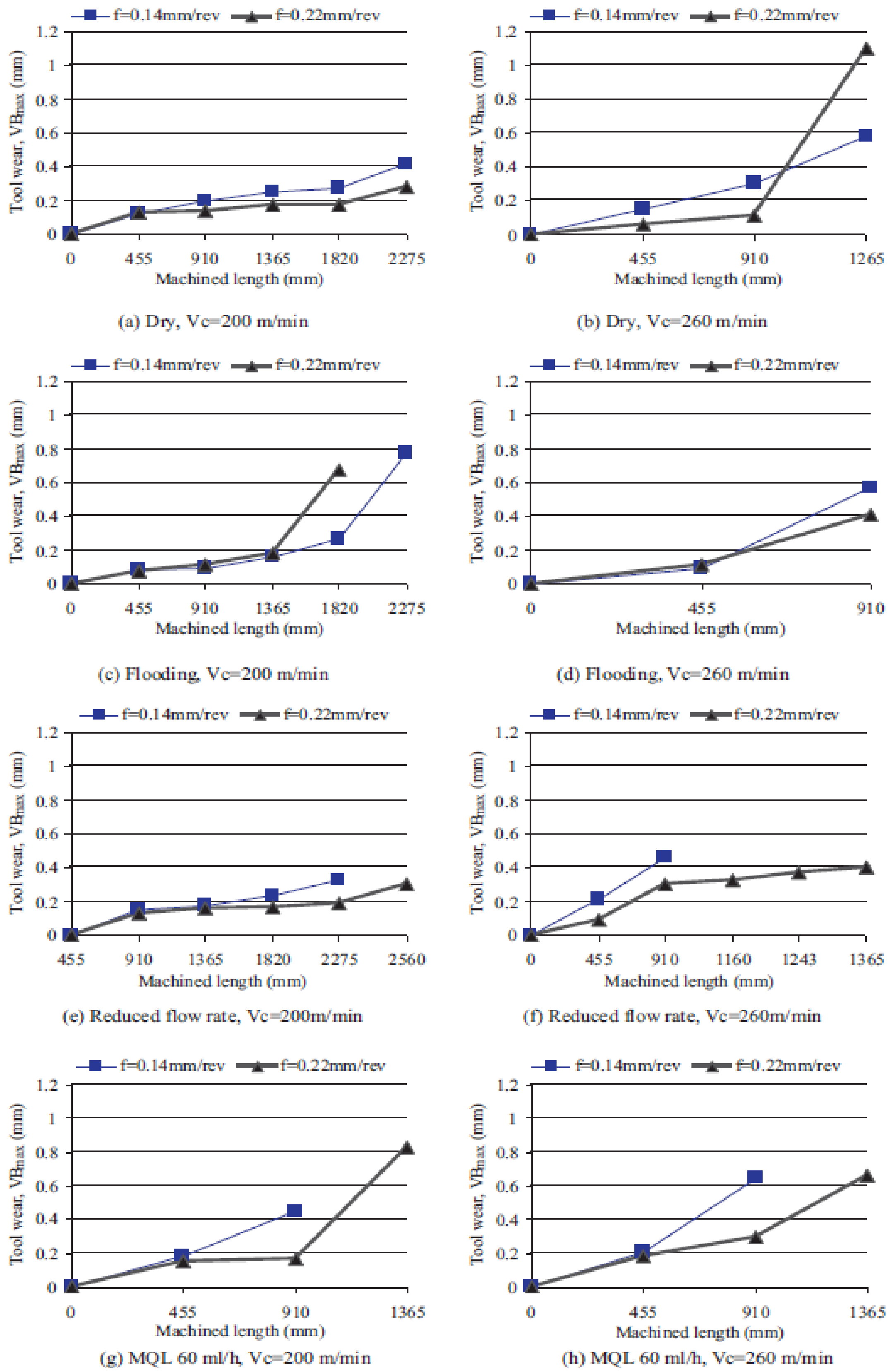

Figure 3.4 : Tool wear (VBmax) curves versus machined length when machining AISI 1047 steel under various cutting conditions.

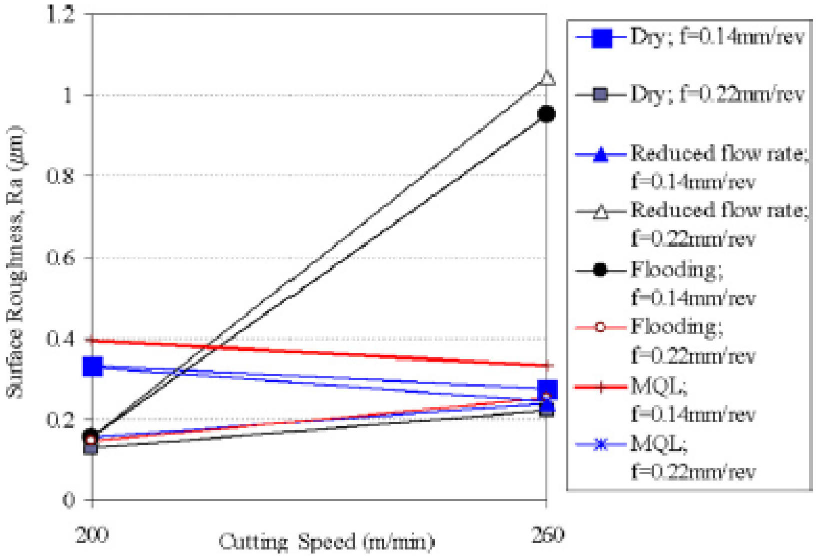

Figure 3.5 : Surface roughness recorded after milling AISI 1047 steel versus cutting speed and under various machining lubrication/cooling systems.

As mentioned before CGI's favorable mechanical properties like high tensile strength, good fatigue resistance, good damping capacity, fair shock resistance and low shrinkage characteristics, persuaded automotive industry to use it as a trend material in reducing motor block weight.

Despite CGI's poor machinability, innovative techniques for diminishing this effect needs to be economical. By this means, MQL seems to be a desirable solution for high speed continuous cutting of CGI (boring/turning operations) and other dry machining circumstances. These investigations still remain elusive, in using MQL system for CGI turning and perusing its effect in cutting conditions (tool wear, cutting forces, surface roughness, cutting temperature and chip morphology). So, further studies in this area are needed [75].

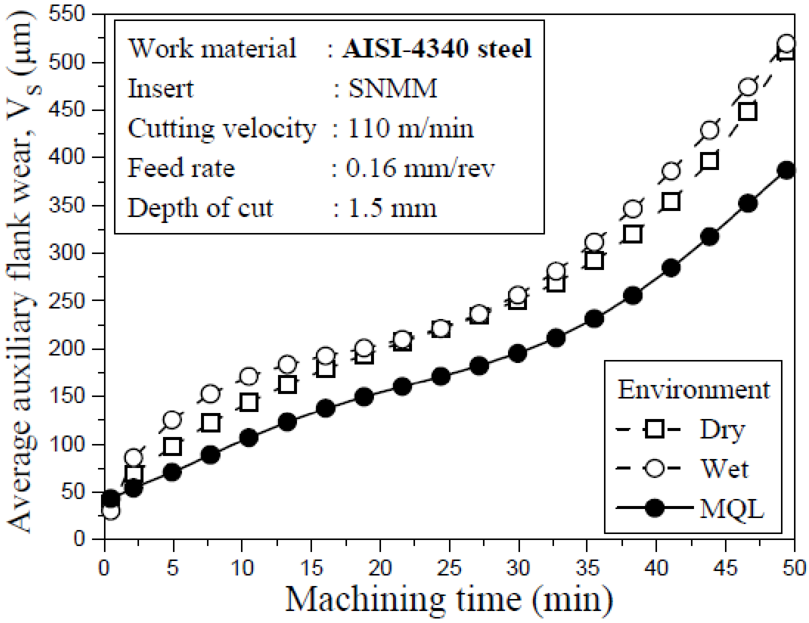

Figure 3.6 : Auxiliary flank wear, with time under dry, wet and MQL conditions.

4. EXPERIMENTAL PROCEDURE

The primary aim of the current work is to investigate machinability of compacted graphite iron (CGI) in dry and minimum quantity lubrication (MQL) machining circumstances. However, such goal should be scrutinized and validated to give valuable results for manufacturing societies. Also, the work has to be applicable to the poor CGI machinability problem and economically should be favorable. Compacted graphite iron (CGI) is becoming popular material for automotive industries and is used as cylinder block material for diesel motors. The worthiness of adopting CGI as a new material in designing automotive and locomotive components has to be comparable to the conventional cast iron types. Literally, CGI machining is a challenging issue and restricts its application in manufacturing. Accordingly, this paperwork will conduct experiments over CGI machinability in dry and MQL conditions with different cutting parameter combinations and will evaluate cutting forces, tool wear, surface roughness and chip morphology of both.

4.1 Testing Methods

Compacted graphite iron basically consists of nodular and flake graphite particles with pearlite and ferrite phases in microstructure. Figure 4.1 shows the microstructure of CGI with nodular and flake graphites as A and B respectively. The pearlite phase makes the material brittle and nodular compacted graphite protects the crack initiation and consequently the strength of CGI becomes higher than gray cast iron. White parts which are around the graphite are ferrite phases. Microstructure micrographs of CGI were taken by a microscope (Nikon SMZ 800). The samples were polished and cleaned to remove any surface contamination. The samples were etched with 2% Nital. They were exposed to Nital for an appropriate time (5-10 seconds) and then washed off under a stream of water to stop the etching process. Later washed with alcohol (methanol or ethanol) and dried by air.

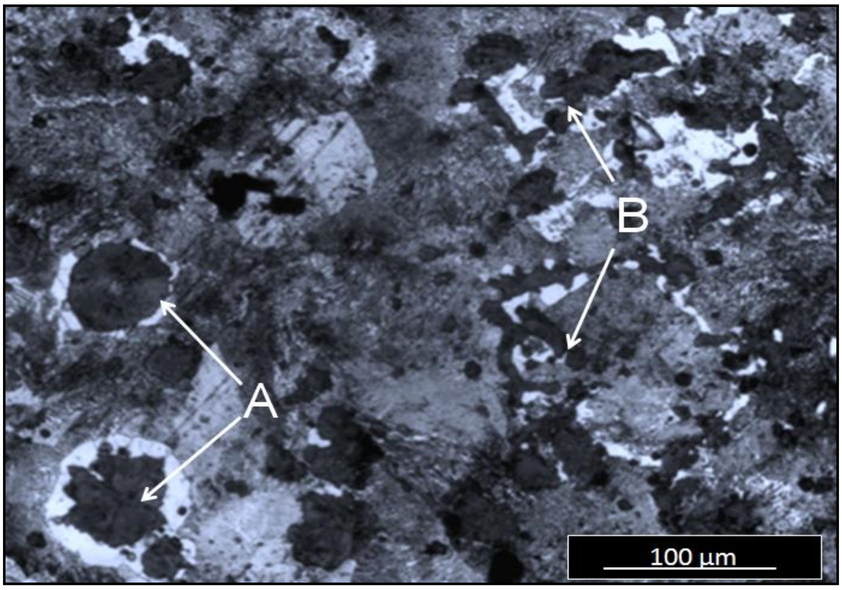

Figure 4.1 : Microstructures of workpiece material.

The ISO 16112 standard for CGI grades ranging from 300 MPa to 500 MPa of tensile strength is showed in Table 4.1 [76]. EN-GJV-300 grade is fully ferritic and the GJV 500 grade is fully pearlitic due to application demands [77].

Table 4.1 : CGI Grades – German Standard VDG Merkblatt W50 (2002).

Grade	UTS (MPa)	YS (MPa)	E (%)	HB 30 (typical results)
EN-GJV-300	300-375	220-295	1.5	140-210
EN-GJV-350	350-425	260-335	1.5	160-220
EN-GJV-400	400-475	300-375	1.0	180-240
EN-GJV-450	450-525	340-415	1.0	200-250
EN-GJV-500	500-575	380-455	0.5	220-260

In order to determine the mechanical properties of our workpiece, three samples were tested by tensile test at room temperature. The obtained test results were given in table 4.2. Also figure 4.2 shows the stress-strain curve of three samples.

Table 4.2 : Mechanical properties of CGI samples.

Mechanical properties	Value
Yield Strength (MPa)	345-365
Tensile Strength (MPa)	435-495
Elongation (%)	1.2-1.6
Hardness (HB)	190-200

In this study YCM GT200A CNC turning machine with 7.5 kW spindle power and a maximum spindle speed of 6000 rpm was used. The CNC lathe can be seen in Fig 4.3.

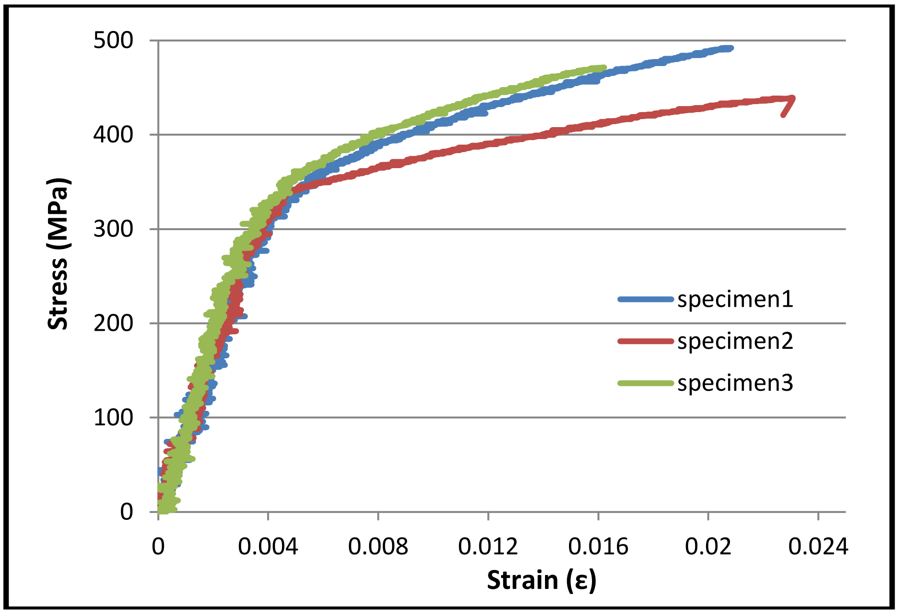

Figure 4.2 : Stress- strain curve of tensile samples.

In order to measure cutting forces the CNC machine was equipped with a 3-axis force dynamometer Kistler 9257BA on the turret and the used software for analyzing the data of cutting forces was CUT PRO. MQL experimentations were conducted by Werte DKN-25 MQL system in order to mix the oil with compressed air and spray it periodically via nozzle.

Also, the supply rate of MQL during the machining was 17.28 ml/h. The schematic representation of experimental set-up was given in Figure 4.4. The uncoated SSangYong SZ200 ceramic inserts without chip breaker of ISO code CNGN 120708 E040 were used during the cutting experiments. The ceramic inserts are mostly used because of their hardness and wear resistance at higher temperatures.

These inserts are consisting of the Alumina (AL_2O_3) and Zirconia (ZrO_2) mixture. Zirconia causes the hardness and toughness behavior of cutting tool and Alumina bond with it for its hot hardness properties. The hardness of insert is 1800 Hv and the fracture toughness of ceramic insert is 4, 5 MPa $m^{1/2}$. The CCLNR 2020 K 12 S type tool holder was used in throughout the work.

Figure 4.3 : CNC lathe.

Figure 4.5 shows the CNGN inserts actual geometry which were obtained from SSangYoung catalogue. The surface quality of machined work pieces were measured by MITUTOYO SJ.201P surface roughness measurement machine.

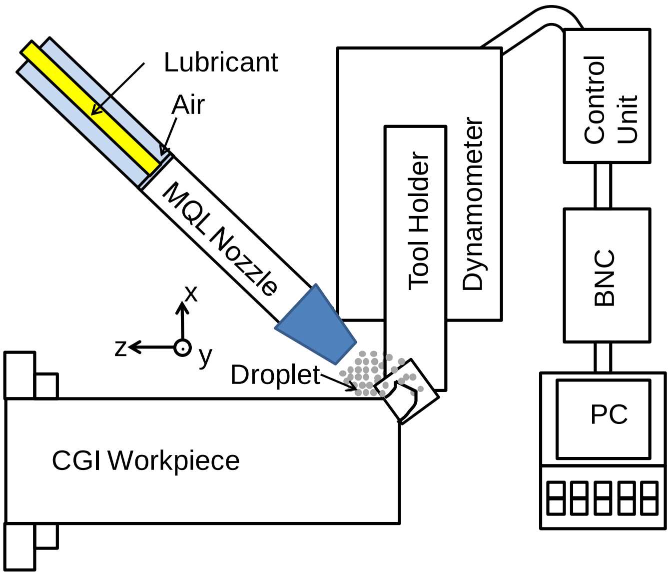

Figure 4.4 : Schematic representation of test set-up.

Cutting speed (V_c) and feed (f) were selected as 200 m/min and 0.3 mm/rev, respectively in order to understand the effect of MQL on tool wear mechanisms during CGI turning with ceramic insert. Depth of cut was kept constant as 1 mm. In order to comparison the effect of MQL on CGI machinability, three different cutting speeds and feed rates were selected which are given in Table 4.3.

The cutting forces, surface roughness, tool wear and chip morphology were investigated according to these cutting parameters. During all experiments, depth of cut was kept constant as 1 mm. The cutting parameters for both machining conditions (dry and MQL) were same and each case was repeated twice for improving the statistical errors. In order to keep cutting speed constant a G code algorithm was developed. Dry and MQL turning tests were carried out on the prepared samples of about 150mm length. Theses samples were machined in the length of 120mm each time. During the experiment the chips were collected and the microstructure and fracture behavior was investigated.

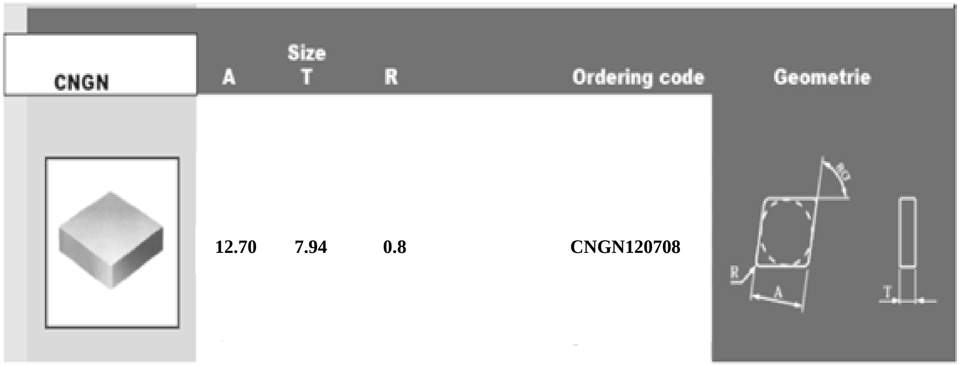

Figure 4.5 : CNGN inserts actual geometry.

Chip samples were cold mounted and polished to reach the middle plane of the chip. chip samples mounted on an examination stub and SEM chip images were taken. Also, flank and rake face of ceramic tools was examined by optic microscope and scanning electron microscope (SEM). The measured responses of tool wear included crater wear, flank wear, notch wear and oxidation zone length.

Table 4.3 : Cutting parameters.

“ Vc ” Cutting speed (m/min)	“ f ” feed (mm/rev)
100	0.1
200	0.2
300	0.3

For wear comparison, tests were conducted on cutting velocity of 200 m/min and feed of 0.3 mm. A fresh cutting edge was used for each test condition. In the event of rapid tool wear, the test was stopped to avoid catastrophic failure.

For wear progression, all tests were conducted until tool reached a flank wear value of 0.3 mm. The worn tools were viewed under SEM and optical microscope to measure tool wear values.

5. RESULTS AND DISCUSSION

Machinability tests were conducted with reference to surface roughness, cutting forces, tool wear and chip morphology criterions. In order to achieve favorable purpose, the surface roughness (R_a), cutting forces, tool wear values were recorded during turning CGI specimens via CNC machine. The procedure contained selective cutting velocity, feed rate and depth of cut to comparison MQL and dry machining circumstances.

5.1 Tool Wear

In order to produce parts with desired surface finish and dimensional tolerances, the cutting tool edges must be in favorable life cycle with monitoring the tool wear and breakage. Otherwise, if the tool reached its life limit it should be replaced with new one [14]. Tool wear is related to cutting parameters, tool and workpiece materials and coolant circumstances. It increases gradually as the cutting proceeds. Because of its importance in mass production and directly relation to manufacturing costs, understanding the wear mechanisms with longer tool life achievement is needed during the machining operations.

In this study, tool wear of CGI was measured in order to comprehend the influence of MQL on tool life. Although flank wear (V_B) is the most important wear type in tool life expectancy, crater wear (V_{cr}), notch wear (V_{Bmax}) and oxidation zone (V_{OX}) was measured. Tool life was considered by the machining distance in which the flank wear reaches a limited value of 300 µm. Xavier et al. [78] reported that adhesion and abrasion are the two main wear mechanisms of CGI machining. Adhesion occurs while two materials interact with each other under high pressure and temperature conditions [79], and abrasion is related to the mechanical wearing due to hard particles which are chips in machining process. These phenomena could be decreased with the aid of lubricant.

MQL is a newly known near dry lubrication method which decreases the friction coefficient as a result, the effect of adhesion and abrasion wear mechanisms diminish. SEM micrographs of different kinds of tool wears are shown in Figure 5.1. Flank wear occurs as a result of friction between the tool flank and machined surface of workpiece. The higher amount of flank wear could cause the tool failure and high surface roughness due to cutting force growth. The flank wear was measured by the width of wear land (V_B). The excessive local plastic deformation on insert faces leads to notch wear. Notch wear is a special type of combined flank and rake face wear which occurs adjacent to the point where the major cutting edge intersects the work surface. It was measured by the maximum width of wear length at flank face (V_{Bmax}). Crater wear is related to friction between chip and rake face of insert. The crater wear in the cutting edge, weakens the rake and the contact area which could cause chipping.

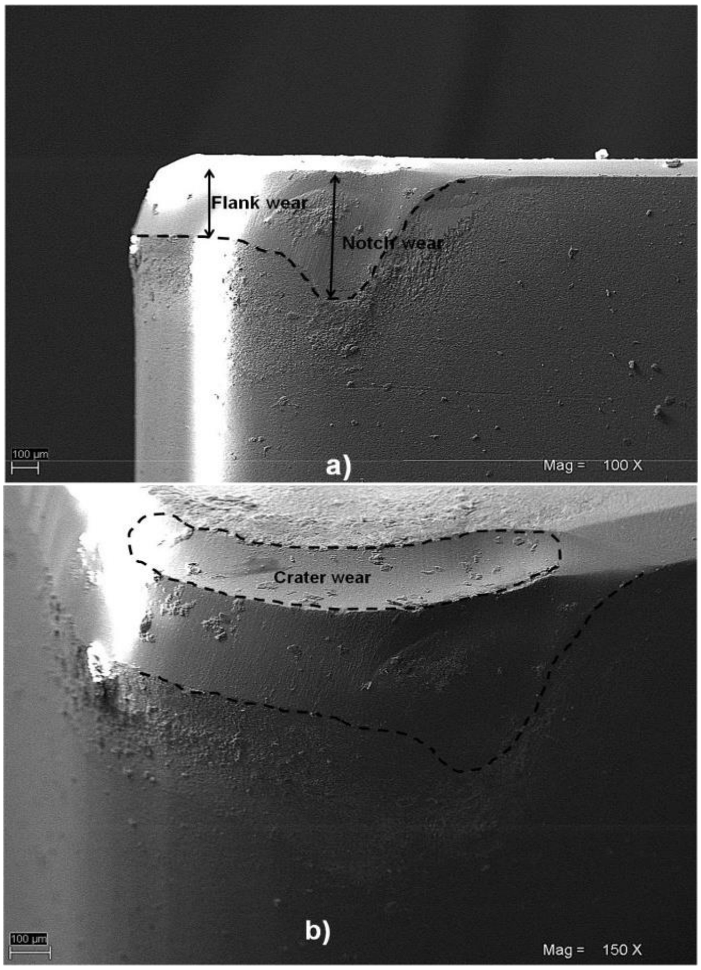

Figure 5.1 : Typical wear types of CGI under dry cutting conditions a) Flank and Notch Wear b) Crater Wear (Vc=200 m/min, f=0,2 mm/rev).

The flank wear curves for the turning of CGI are shown in Figure 5.2. Flank wear curve of MQL and DRY cutting conditions were almost similar. The effect of MQL on flank wear was gradually observable while the cutting distance is increased. By the means of MQL, limited value of flank wear 0,3 mm was obtained with more cutting distances corresponding to DRY cutting conditions. These observations could be attributed to cutting temperature or abrasive and adhesion reduction via oil particles.

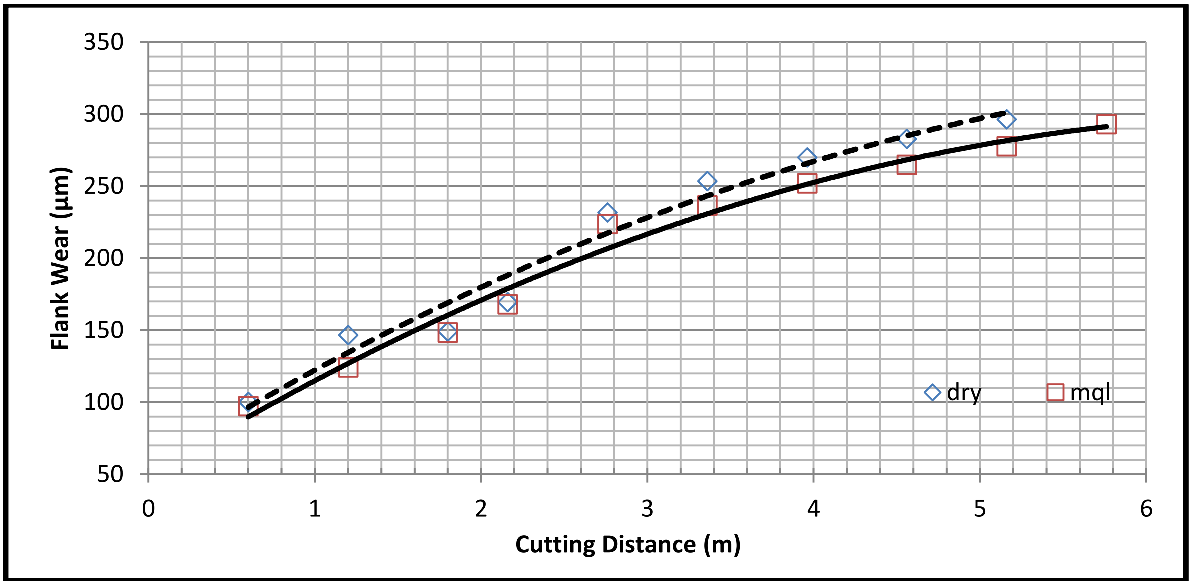

Figure 5.2 : Flank wear vs cutting distance under VC=200 m/min, f= 0.3 mm/rev.

Figure 5.3 shows the relation between notch wear and cutting distance. The notch wear under dry cutting condition was lower than MQL at the beginning of the graph. However notch wear under MQL condition reached 300 µm at higher cutting distance because the wear rate of MQL was lower than dry cutting condition.

As shown in Figure 5.3, distinguishable role of MQL was not observed for notch wear excelling. Nevertheless, few development of notch wear at higher cutting distances could be explained by reduction in abrasion wear through MQL. The oxidation zone on the rake face and crater wear of ceramic insert were measured by optical microscope as shown in Figure 5.4.

In this figure, Vox and Vcr represent oxidation length and crater width, respectively. Figure 5.5 shows crater wear vs cutting distance graph. Observations of rake face of the tool revealed the fact that, the crater width increases as the cutting distance grows for both DRY and MQL conditions.

Although, in low cutting distances crater wear with MQL is higher, gradually MQL becomes effective in crater wear at the high cutting distance. It could be attributed less adhesive wear and less cutting temperature and deposits on the cutting tool via oil droplets. The use of lubricant and its penetration between the chip and tool reduces the friction and cutting temperature and eventually the crater wear reduces.

The oxidation zone measurement which was explained at previous paragraph is given in Figure 5.6 according to the cutting distance. As the cutting distance increases, length of oxidation zone progressively grew larger. The larger oxidation zone on the rake face of insert could weaken the cutting edge and consequently tool life.

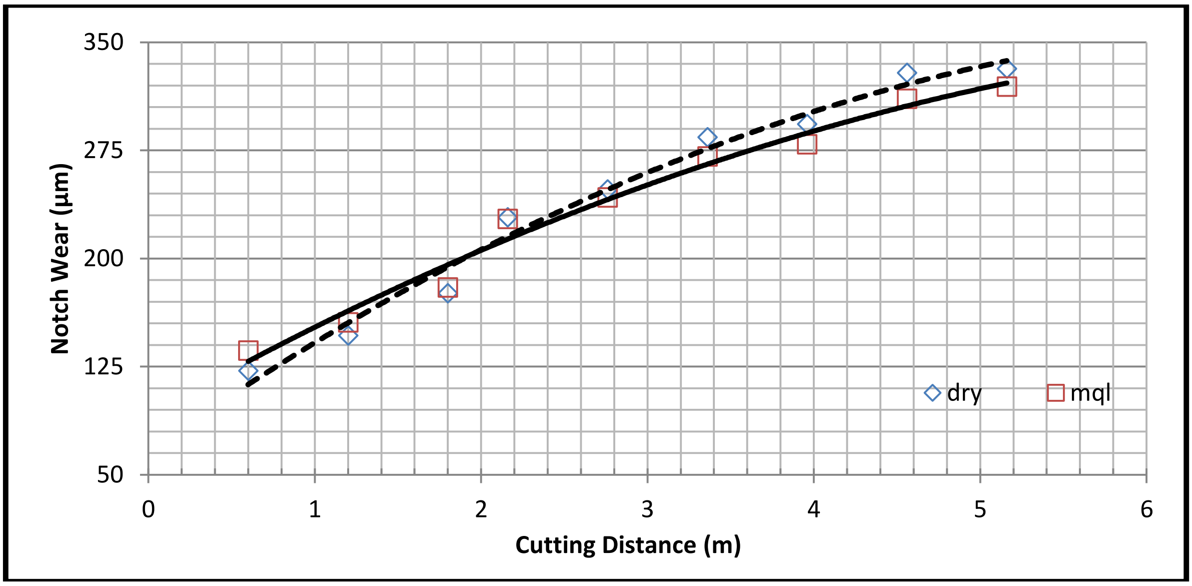

Figure 5.3 : Notch wear vs cutting distance under VC=200 m/min, f= 0.3 mm/rev.

During machining with MQL, oxidation area was reduced in comparison with DRY machining. One objective of MQL is decreasing cutting temperature and oxidation dispersion which cause machining stability. Also, MQL could reduce the effect of oxidation via less tool-chip contact length and chip spreading mechanisms in cutting edge. Accordingly, compressed air assists chip evacuation from the cutting zone so the contact length between chip and flank surface decreases. SEM photos of inserts which show the wear types of CGI turning for DRY and MQL cutting conditions were taken in Figure 5.7.

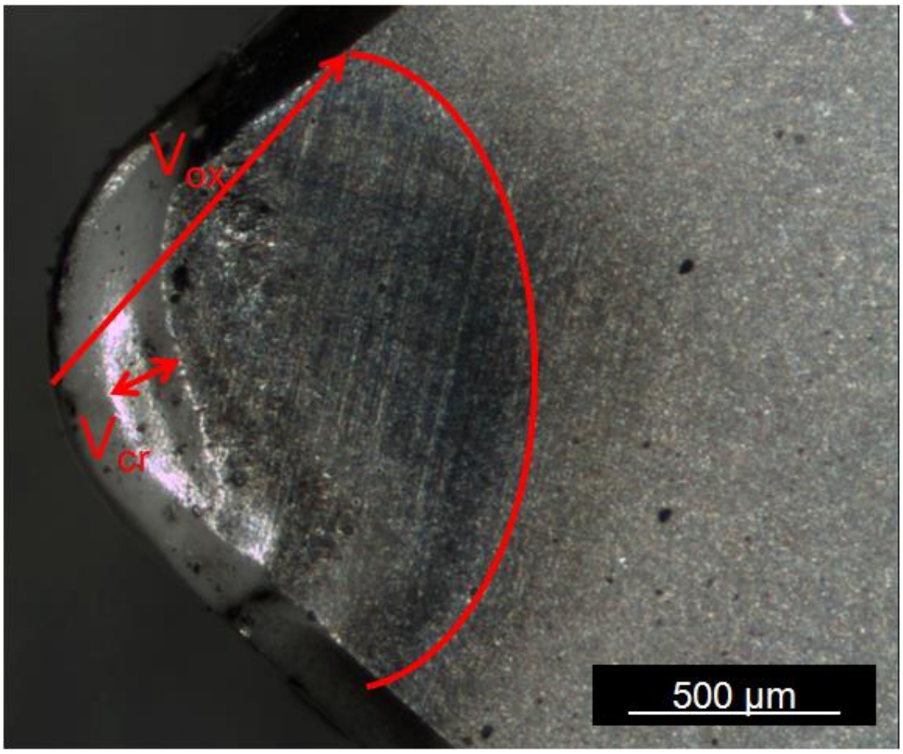

Figure 5.4 : The oxidation zone on the rake face and crater wear width.

Figure 5.5 : Crater wear vs cutting distance in VC=200 m/min, f= 0.3 mm/rev.

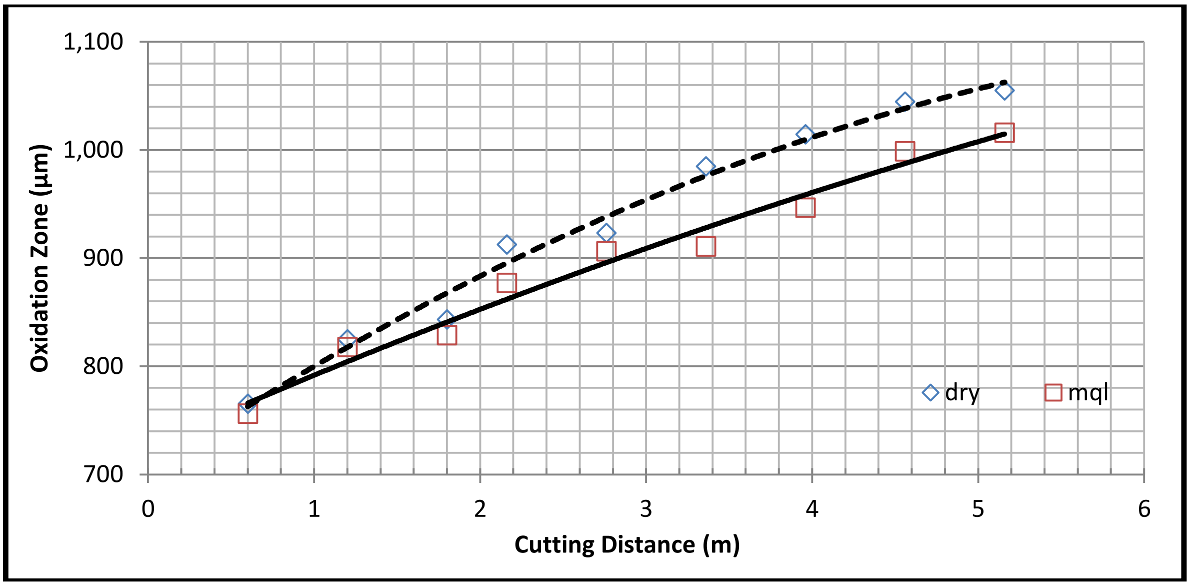

Figure 5.6 : Oxidation zone vs cutting distance under V_c=200 m/min f= 0.3 mm/rev.

MQL does not prevent the wear of tool but it decrease the abrasion and adhesion effect. Obviously the main role of MQL development was seen at crater wear and oxidation zone.

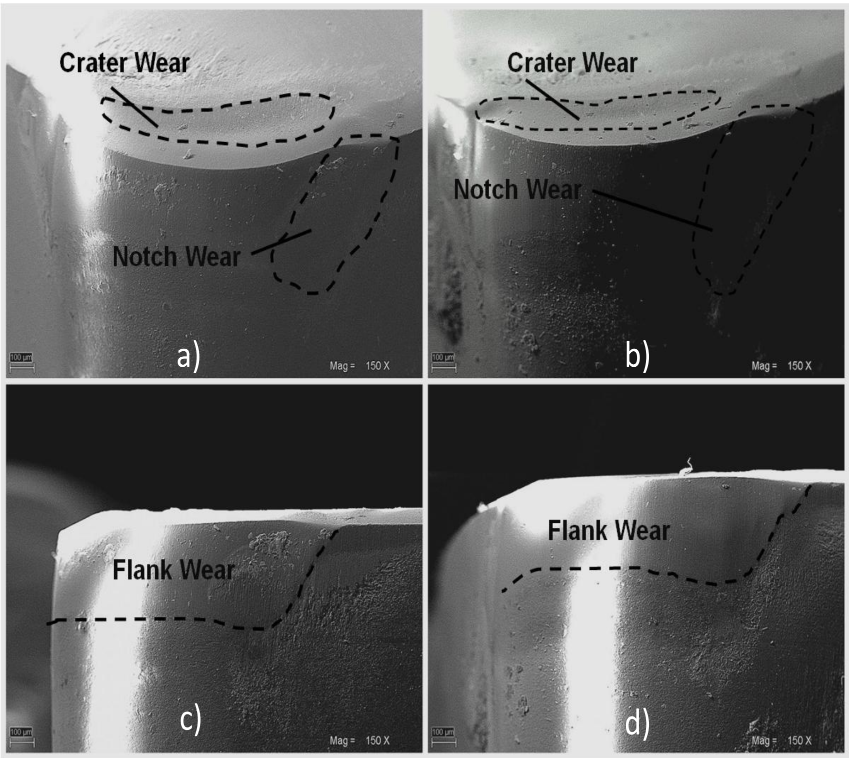

Figure 5.7 : SEM cutting edge photo a, c) DRY b, d) MQL.

5.2 Cutting Forces

During the machining operation, high stresses acting on cutting tool could cause tool failure, and high friction stresses in chip forming action and high machine vibration [80]. Turning test of CGI were performed in dry and MQL machining conditions to evaluate the cutting force components and resultant cutting forces.

Cutting forces were measured to see if any improvement and consequently, cutting force reduction could be achieved by using MQL or not. These tests were conducted with worn and fresh cutting tools both for dry and MQL circumstances for comparison mean. Experiments were conducted on CNC turning machine in order to measure 3 cutting force components in dry and MQL machining. The cutting forces at three axes were given in Figure 3 for both machining conditions.

Minimum cutting force value was 146 N which measured under Vc=100m/min, f=0.1mm/rev through MQL method as the y-axis force component. Also the maximum cutting force value was 685N measured under Vc=100m/min, f=0.3mm/rev through MQL method as he x-axis force component.

Furthermore it can also be seen that during the experiment F_x is always the highest among other force components. Although all the three force components are seen to increase with feed rate, cutting forces in machining with MQL system were a little bit less (about 2%) than dry machining in same cutting conditions. This kind of behavior could be explained through small layer of oil in tool-workpiece cutting interface which cause less vibration in CNC machine and wet area helps the chip to slide over tool more sufficiently. Also ductile and brittle cutting removal could be effective criteria. In some cases, the usage of MQL under these cutting conditions could affect cutting temperature and heat transfer between chips and oiled tool and eventually cause some disturbance which sometimes makes more cutting force at MQL cutting procedure. Figure 5.8 shows components of cutting force on ceramic inserts. The value of cutting forces is an important factor for machine parts deformability, tool life, vibration, finished surface of parts, machinability of workpiece and other cutting parameters.

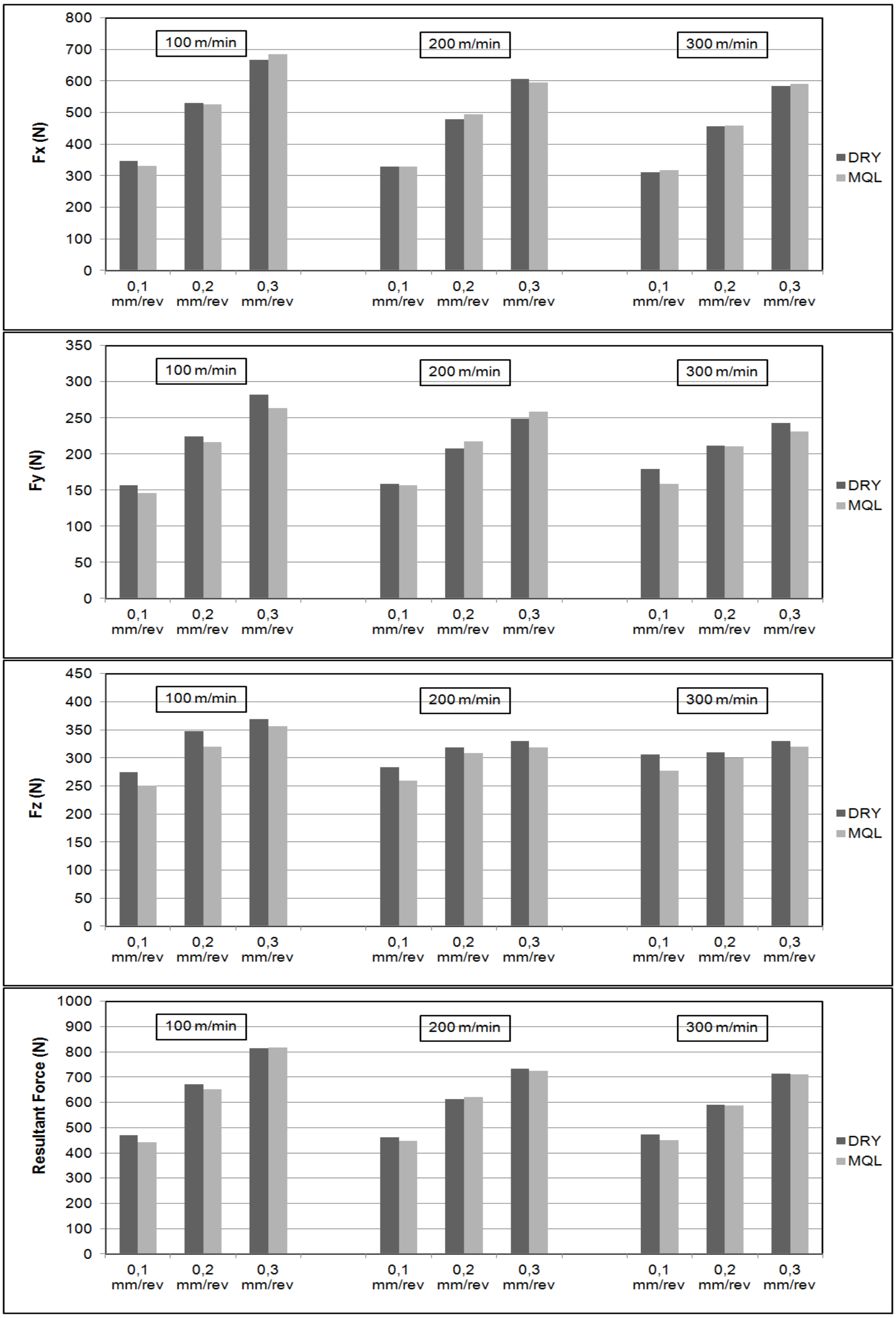

Figure 5.8 : Cutting forces components for both conditions.

As shown in figure 5.9, F_x always has the highest value among other cutting force components. Cutting force, during machining operation by the means of MQL were a little bit less (about 2%) but not enough to be tangible in CGI machining considerations. Also, machining with worn cutting tool caused higher cutting forces in both conditions.

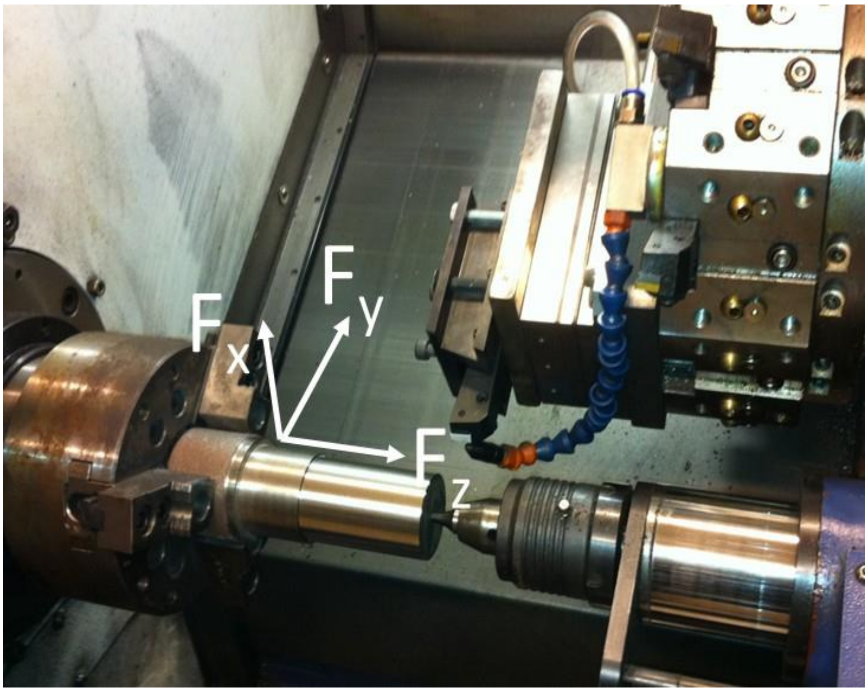

Figure 5.9 : Components of cutting force on ceramic inserts.

It is assumed that the small layer of oil in contact area and air compressing cause less vibration and easier slide of chips over tool rake face and this procedure is the key to little improvement in MQL using.

However, this reduction is not in considerable rate and the cutting force components and resultant force are about the same value. Because the cutting temperature during dry machining is higher than machining with MQL, CGI tends to be softer. On the other hand MQL causes friction coefficient reduction in tool-workpiece interface. These two conflicting behavior compensate each other in a way that MQL has not an effective role in cutting force decreasing.

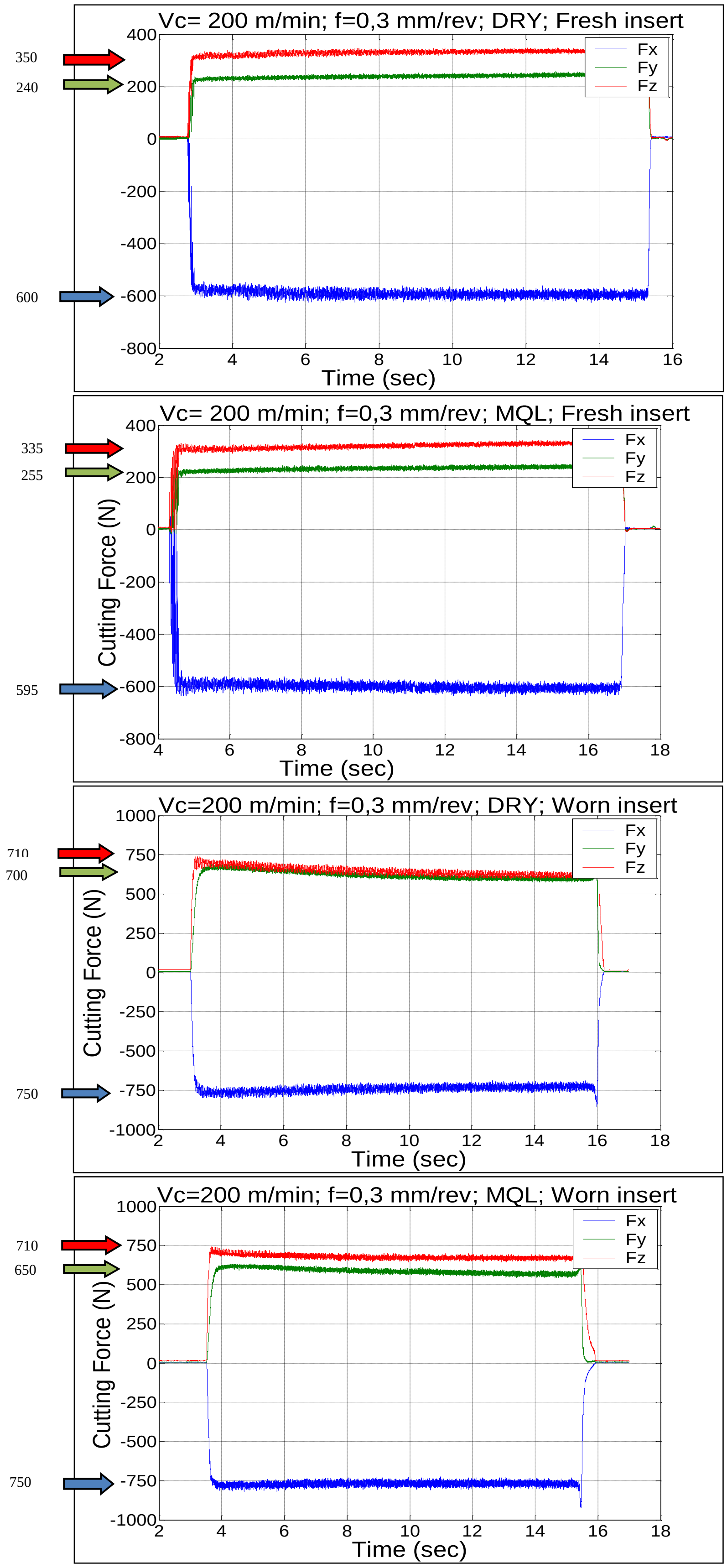

Figure 5.10 : Cutting Force components at Vc=200 m/min, f=0,3 mm/rev in time domain fresh insert: a)DRY b)MQL wear insert: c)DRY d)MQL.

5.3 Surface Roughness

Surface roughness is one of the most important machinability indexes in manufacturing industries. It effects the life cycle, micro crack generation on the machined surface and performance of components. Figure 5.11 illustrates the average surface roughness values of the samples with different feed rates and cutting speeds. The comparisoning figure reveals that the effect of feed rate on surface roughness is clear in dry condition. Surface roughness increases as feed rate increase for all cutting speeds. The maximum surface roughness occurred in highest feed rate value, 0.3 mm/rev at the speed of 300 m/min. In contrast influence of feed rate on surface roughness is not obvious for the evaluated range of cutting in MQL condition. Recorded Ra values regardless of parameter increases, reduces or no change.

During the examinations, samples were examined three times in each steps in order to get the average values and determine the deferences for dry and MQL cutting. The average surface roughness values vary between 4-6 μm for dry, 3-5μm for MQL condition. It was observed that surface roughness of workpieces which have been machined via MQL method is better than dry those in same cutting parameters except two circumstances which were under slow cutting velocity (100 m/min). The best response of near dry machining in surface roughness decrease was at Vc =300 m/min and f=0.2 mm/rev condition.

These results confirmed that MQL has 25% lower surface roughness than that of dry condition in CGI turning. MQL method's improvements on surface roughness can be explained through lower cutting temperature and vibration due to the better lubrication conditions.

MQL				
	Ra1	Ra2	Ra3	Average Ra
Vc=100 m/min				
F=0,1 mm/rev	2,23	3,30	3,07	2,87
F=0,2 mm/rev	3,50	4,37	4,18	4,02
F=0,3 mm/rev	5,36	4,69	5,71	5,25
Vc=200 m/min				
F=0,1 mm/rev	2,97	3,08	2,76	2,94
F=0,2 mm/rev	2,84	4,23	4,70	3,92
F=0,3 mm/rev	2,77	2,74	3,58	3,03
Vc=300 m/min				
F=0,1 mm/rev	3,32	2,03	3,61	2,99
F=0,2 mm/rev	1,85	3,01	3,81	2,89
F=0,3 mm/rev	4,45	3,20	3,98	3,88
DRY				
	Ra1	Ra2	Ra3	Average Ra
Vc=100 m/min				
F=0,1 mm/rev	1,17	0,91	0,92	1,00
F=0,2 mm/rev	3,80	3,63	5,78	4,40
F=0,3 mm/rev	5,22	4,92	5,27	5,14
Vc=200 m/min				
F=0,1 mm/rev	5,98	4,09	3,18	4,42
F=0,2 mm/rev	5,20	6,00	4,08	5,09
F=0,3 mm/rev	6,10	5,71	3,74	5,18
Vc=300 m/min				
F=0,1 mm/rev	3,12	3,42	3,00	3,18
F=0,2 mm/rev	5,95	5,16	5,66	5,59
F=0,3 mm/rev	5,58	4,98	6,38	5,65

Table 5.1 : Surface roughness values for DRY and MQL machining.

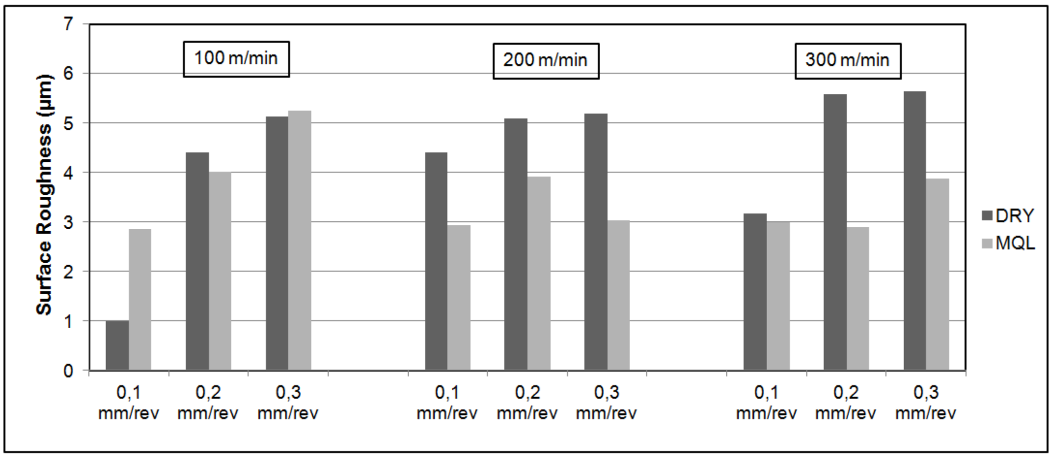

Figure 5.11 : Surface Roughness for both conditions under cutting parameters Vc= 100, 200, 300 m/min and f= 0,1, 0,2, 0,3 mm/rev.

5.4 Chip Morphology

Machining chips in both MQL and dry condition were collected and optical micrographs of typical chips are given in Fig 5.12. During the turning of compacted graphite iron, segmented chips have been observed both in MQL and dry conditions due to the fracture characteristics of CGI.

Segmented chip lengths were affected by cutting velocity in both conditions. Higher the velocity causes lower the chip length. Effect of serrated chip formation in tool wear will be discussed in succeeding section. This kind of chip is consisting of low and high shear strain zones. The geometric shapes of the chips are mostly caused by CGI's brittle behaviour and fracture characteristics. Also all chips were easy to break by hand.

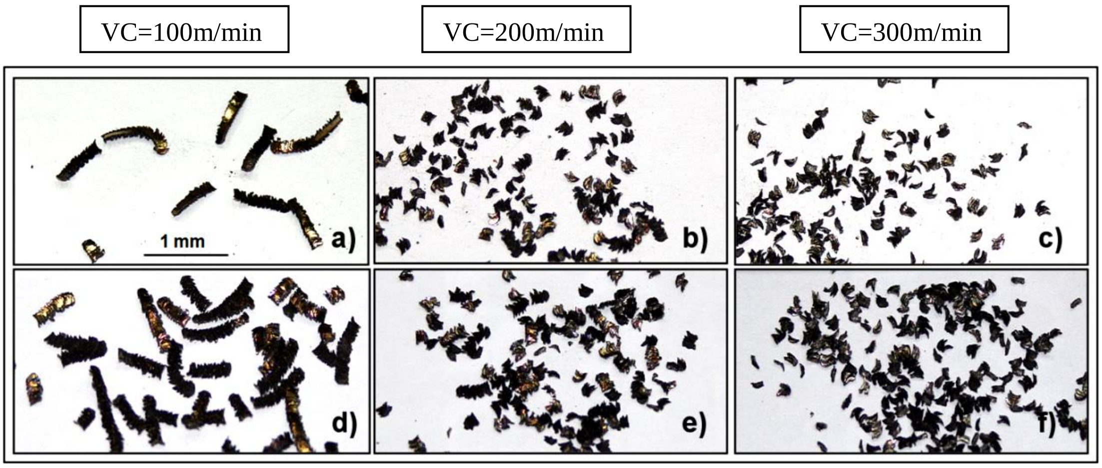

Figure 5.12 : The optical micrographs of chips at constant feed of 0,2 mm/rev. a),b),c) for DRY condition; d),e),f) for MQL condition.

Chip lengths are affected mainly with cutting velocity. Moreover under both DRY and MQL conditions, cutting velocity increment cause chips length reduction. Fig 5.13 shows the SEM micrograph of the cross-sectional morphology of the serrated chips, which are mounted in bakallite for both dry and MQL conditions. Saw tooth shape forms of chips due to the sequential high and low shear strain formation can be seen clearly in Fig 5.13 (a) and (b). Graphite particles, which are allocated randomly in CGI's matrix, cause the crack initiation on segmented chip. However, as can be seen in both figures, Fig 5.13 (a) and (b), all along the chip width segmentation does not follow-up specific pattern, they are irregular size and geometries due to the random dispersion of graphite's throughout the matrix. Fig 5.14 shows the single serrated chip, which has been magnified in Fig 5.15.

The micrograph belongs to 100 m/min cutting speed and 0.3 mm/rev feed conditions on MQL used test.

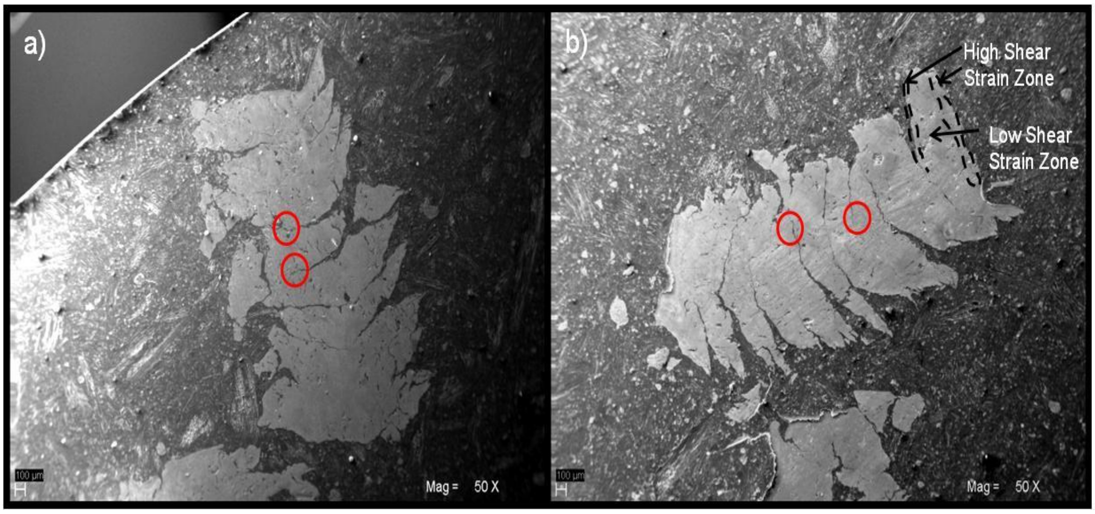

Figure 5.13 : Micrograph of chips under a) DRY and b) MQL conditions .

The asymmetric segmentation of chip form and inhomogeneous deformation can be seen clearly in Figure 5.15 (a). The close up view of "Y" section was given in Figure 5.15 (b). In this Figure, cleavage steps and stacked shear planes which is the proof of the cleavage fracture, is shown.

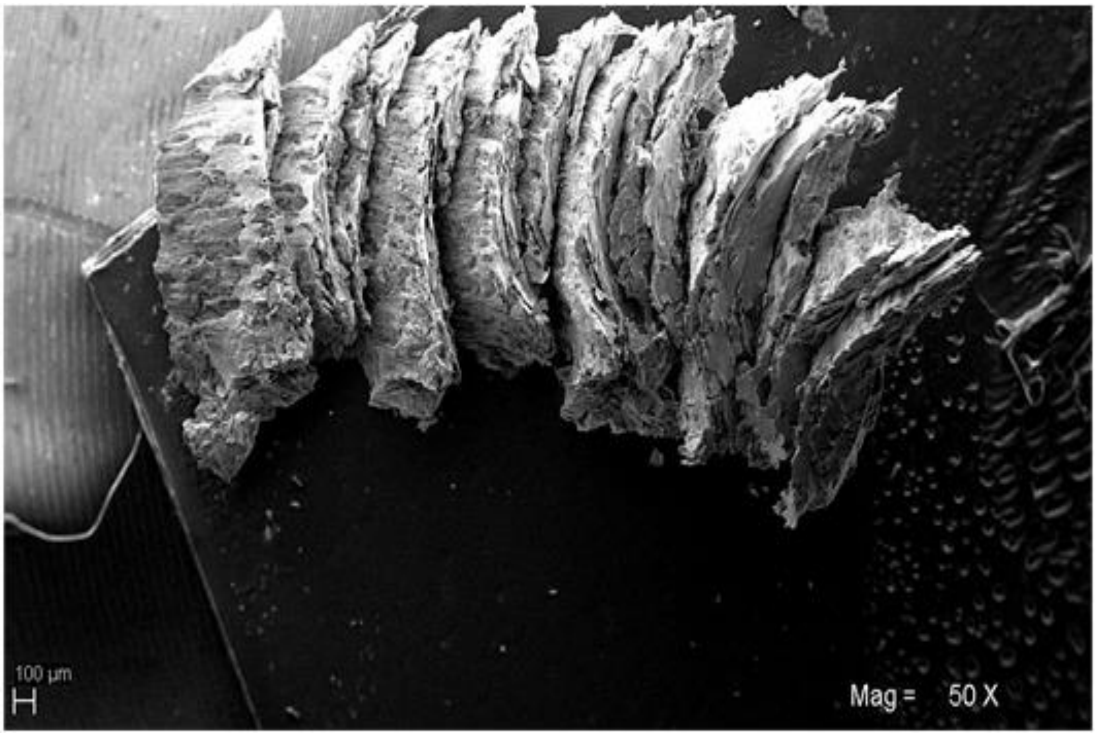

Figure 5.14 : SEM micrograph of chip under Vc=100m/min and f= 0.3mm/rev.

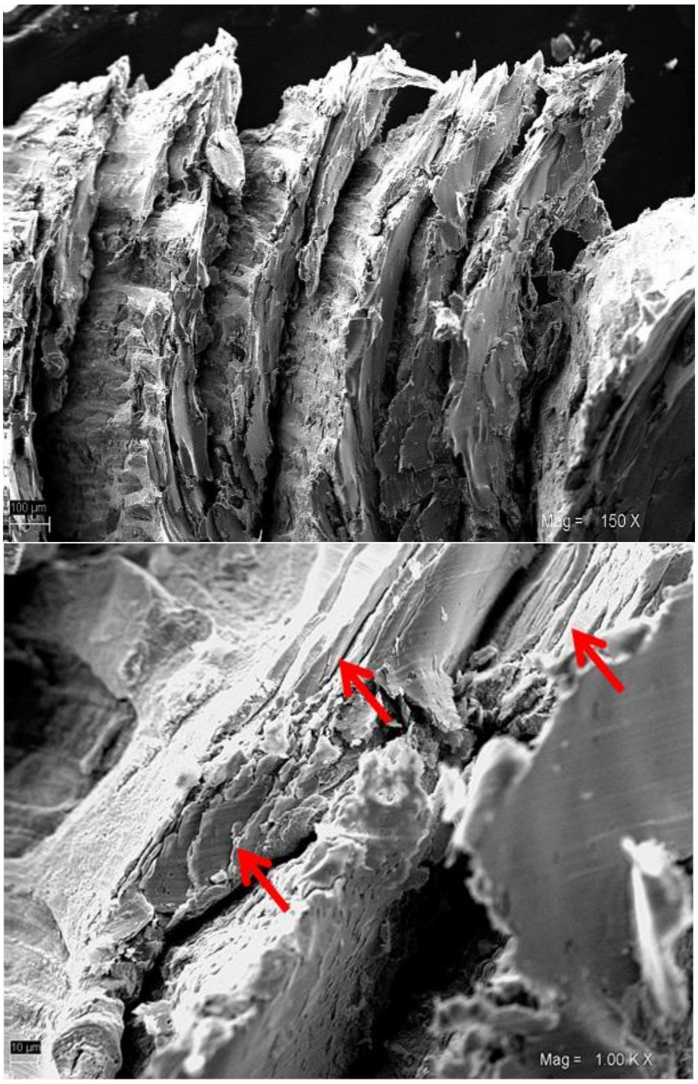

Figure 5.15 : a) The close up view of X   b) The close up view of Y.

6. CONCLUSIONS AND RECOMMENDATIONS

In the current work, compacted graphite iron (CGI) machinability, in dry machining and minimum quantity lubrication (MQL) machining have been investigated. The previous chapters presented a detailed representation and discussion of the examinations conducted on CGI turning in order to gain insight into the MQL's effect on the machinability factors.

Throughout the experimental observations in this paper, a comprehensive study of different types of tool wear, cutting forces measurement, surface roughness and chip morphology were conducted in both cutting conditions. Available literature in the area of CGI turning operation with ceramic cutting inserts in both dry and MQL machining, fails to provide a detailed understanding of tool wear mechanisms, cutting force components, finished surface quality and chips produced in both conditions. This lack caused to study CGI machinability in more detailed form.The current chapter concludes the main findings of the study. Also, it suggest some recommendations for future work in the area. In order to evaluate the effect of MQL in CGI turning, cutting force, surface roughness, chip morphology and tool wear were analyzed. The results are summarized as follows:

1- Cutting forces were measured by the means of piezoelectrical dynamometer and package software of CUTPRO. The examinations on cutting forces revealed that MQL has not considerable effect in cutting force reduction due to its conflicting behavior in less friction coefficient and less cutting temperature which cause less softer workpiece during machining. However, the effects of MQL in higher feed rates were negligible. Under MQL conditions, the results are inconclusive to point out a trend in the measured forces. Furthermore, Varghese et al. [60] studied the cutting forces in machining with grooved tool for dry and MQL conditions. He claimed that the grooved tool caused a 3-12% reduction under dry conditions and 9-20% in MQL when tangential cutting force were measured. The difference for other force component was not in considerable rate. Also he claimed that the usage of MQL at low cutting speed, reduces the cutting forces. However, at high cutting speed it has reverse effect and increses the measured cutting forces.

2-The positive effect of feed rate on surface roughness was clear in dry condition. R_a values increased as feed rate increase for all cutting speeds. The influence of feed rate on surface roughness was not obvious for the evaluated range of cutting in MQL condition. Recorded R_a values regardless of parameter, increased, reduced or did not change.

The average surface roughness measurement results confirmed that MQL generated 25% lower surface roughness than that of dry condition.

3- During the turning of compacted graphite iron, serrated chips have been observed both in MQL and dry conditions. Serrated chips were long length and had accordion shape due to the excessive inhomogeneous plastic.

4- Tool wear analysis result indicated that MQL provides 10% less flank wear, 30% less crater width than that of dry condition. Silva et al. [66] claimed that by using MQL technique during the grinding process of 4340 steel, a 13 to 50% reduction in diametral wear has been achieved. Also, Ali et al. [69] stated that MQL reduces the flank wear and surface roughness in turning of medium carbon steel. They said that this process reduces deep notching and grooving. By this mean better surface finish is achieved. Thamizhmanii et al. [65] studied Inconel 718 (steel) MQL machining and said that by comparisoning dry machining, tool life has been increased 43.75%.

Although MQL has less improvement in reduction of flank wear and notch wear, its considerable development in crater wear and oxidation zone decreasing was observed during the examinations. Under constant cutting speed and feed, all wear types show an increase in amount as the cutting distance grows. However, with the effect of MQL this increase is less. And flank wear reaches the limited value of 0.3mm in more cutting distance by using MQL which could cause longer tool life.

6.1 Recommendations for Future Work

As the current work is a foundation to possible future perfection, the following recommendations can be provided on the field of this study:

1- Acording to data available from progressive tool wear, the machining model to include different cutting tool materials, geometries and configurations (angles, edge preparation, chip breaking, etc), coatings at different machining conditions (cutting speeds, feed rates, dry/coolant condition simulation) to study the effect of all variables on machining outputs can be investigated. Developing tool wear models can reduce the experimantal time, effort and raw material costs. Also, these models could provide new cutting tools in manufacturing industries.

2- During the experimental investigations in this paper work oxidation zone length were studied. Application of lubricant during machining can affect the chemicalwear type on the tool rake face. In addition, lubricant could affect the materials microstructure during machining operation. An investigation of MQL effects on the lubricants chemical content and oxidation zone could be useful.

3- Due to prior studies, absence of a manganese sulphide (MnS) layer on CGI microstructure and cutting tools interface zone at high cutting speeds results in high tool wear and machinability reduction.

Some researchers report this layer as a protector/lubricator during the process. A fundamental study on the nature of this layer over tools and its effect on machinability and possible improvement by the means of specific lubricants or other aspects could be useful.

4- This study provides information about CGI turning. Study on CGI's machining with other machining operations (milling, drilling, and grinding ...) in dry, MQL and wet machining could persue the automotive industry in CGI's mass production.

REFERENCES

[1] **Murthy V.SR., Seshan, S., Seshan, K.** (1985). Vermicular graphite cast iron current state of the art. In: Sadhana-Academy Proceedings in Engineering Sciences: 361-372.

[2] **Murthy V.SR., Seshan, S., Seshan, K.** (1984).Vermicular graphite cast iron--current state of the art Department of Mechanical Engineering, Indian Institute of Science, Bangalore 560 012, India MS received 8 May 1984; revised 7 August 1984.

[3] **Mohammed, W., M., Ng, E., Elbestawi, M.a**.,,. (2012). Modeling the effect of compacted graphite iron microstructure on cutting forces and tool wear, CIRP Journal of Manufacturing Science and Technology ,5 : 87-101.

[4] **Berhane, Mulugeta.** (2011). Optimization of cutting parameters in machining of Compacted Graphite Iron (CGI). (KTH, School of Industrial Engineering and Management (ITM), Production Engineering) May 26, 2011.

[5] **Dawson, S., Hollinger, I., Robbins, M., Daeth, J., Reuter, U., Schulz, H.,** (2001), The Effect of Metallurgical Variables on the Machinability of Compacted Graphite Iron, Society of Automotive Engineers Inc . Paper no. 2001-01-0409.

[6] **Abele, E., Burkhard, S.,** (2008), Using PCD for Machining CGI with a CO2 Coolant System, Production Engineering 2 :165-169.

[7] **Gastel, M., C., Konetschny, U., Reuter, C., Fasel,H.,Schulz, R., Riedel,** (2001), Investigation of the Wear Mechanism of Cubic Boron Nitride Tools Used for the Machining of Compacted Graphite Iron and Grey Cast Iron, International Journal of Refractory Metals and Hard Materials : 287–296.

[8] **Philip Varghese.** (2008). MACHINING OF COMPACTED GRAPHITE IRON (CGI) AND SPHEROIDAL GRAPHITE IRON (SGI): A FUNDAMENTAL STUDY OF TRIBOLOGICAL ISSUES AND PROGRESSIVE CUTTING TOOL WEAR By K. A dissertation submitted to the faculty of The University of Utah in partial fulfillment of the requirements for the degree of Doctor of Philosophy Department of Mechanical Engineering The University of Utah December 2008.

[9] **J. Destefani**,. (2002). Old Tool Design Takes Off, Manufacturing Engineering, One SME Drive, Dearborn, Michigan 48128 Society of Manufacturing Engineers, 2002.

[10] **S. Skvarenina, Y.C. Shin.,** (2006). Laser-assisted machining of compacted graphite iron, International Journal of Machine Tools and Manufacture 46 (2006) 7–17.

[11] **Mocellin, F., Melleras, E., Guesser, W.L., Boehs, L.,** (2004), Study of the Machinability of Compacted Graphite Iron for Drilling Process, Journal of the Brazilian Society of Mechanical Science & Engineering, XXVI/1: 22–27.

[12] **Citing Websites,** Improving Tool Life with Minimum Quantity Lubrication. Technical report of UNIST co., retrieved 02.19.2012 from: **Url-1** <unist.com/news/24/193/ Improving-Tool-Life-with-Minimum-Quantity-Lubrication.html.>
[13] **K. Weinert, I. Inasaki, J. W. Sutherland, T. Wakabayash.** (2004), Dry Machining and Minimum Quantity Lubrication. CIRP Annals - Manufacturing Technology Volume 53, Issue 2, Pages 511–537
[14] **Altintas, Y.,** (2012), Manufacturing automation: metal cutting mechanics, machine tool vibrations, and CNC design, Cambridge University Press, Cambridge.
[15] **J.Krystof.** (1939). Berichte uber Betriebswissenschaftliche Arbeiten, Bd., 12. VDI Verlag, 1939.
[16] **E.H.Lee and B.W.Shaffer.** (1951). Theory of plasticity applied to the problem of machining. Journal of applied Mechanics, Vol. 18: 405-413, 1951.
[17] **M.E.Merchant.** (1945). Mechanics of the cutting process. Journal of Applied physics, vol.16:318-324, 1945.
[18] **E.J.A.Armarego and R.C.Whitfield.** (1985). Computer based modeling of popular Machining operations for force and power predictions. Annal of the CIRP, 34:65-69.
[19] **E.Budak, Y.Altintas, and E.J.A.Armarego.** (1996). prediction of milling force coefficients from orthogonal cutting data. Trans. ASME Journal of Manufacturing Science and Engineering, vol. 118:216-224.
[20] **G.V.Stabler.** (1964). The chip flow law and its consequences. Advances in Machine tool design and research, pages: 243-251.
[21] **W.Konig and K.Essel.** (1975). New tool materials wear Mechanism and Application. Annals of the CIRP, 24/1:1-5.
[22] **F.W.Taylor.** (1907). On the Art of cutting Metals. Transactions of the ASME,28.
[23] **Fritz Klocke** Manufacturing Processes 1 Cutting
[24] **Ernst, H., Merchant, M.E.** (1941). Chip Formation, Friction, and High Quality Machined Surfaces. Surface Treatment of Metals. ASM (Cleveland, OH) 29, 299.
[25] **Childs, T.H.C.; Maekawa, K.; Obikawa, T.; Yamane, Y**. Metal Machining - Theory and Applications
[26] **YE. Bangyan, XU Jin, WU Weijie, ZHAO Xuezhi, LIU Xiaochu.**Study of the forming mechanism of serrated chips in high speed turning for carbon steel
[27] **Reardan, Arthur c.** (2011). metallurgy for the non-metallurgist (2nd edition) ASM international (2011).cast irons, 269-270.
[28] **Raymond aurelius higgins.** (1983). engineering metallurgy part 1 . applied physical metallurgy.R.E.Krieger pub.co., 1983 . 559 (cast irons and alloy cast irons).
[29] **K.H.Buschow.** (2001). Encyclopedia of materials: science and technology, 2. Vol. Elsevier. 1009.
[30] **Dr. Steve Dawson.** (1999). Compacted Graphite Iron: Mechanical and Physical Properties for Engine Design . Based on a paper presented at: Werkstoff und Automobilantrieb (Materials in Powertrain VDI (Verein Deutscher Ingenieure) Dresden Germany 28-29.

[31] **J. Destefani,.** (2002). Old Tool Design Takes Off, Manufacturing Engineering, One SME Drive, Dearborn, Michigan 48128 Society of Manufacturing Engineers,.

[32] **Nourredine Boubekri, Vasim Shaikh.** (2012). Machining Using Minimum Quantity Lubrication: A Technology for Sustainability. International Journal of Applied Science and Technology . Vol. 2 No.1 : Jan. 2012 **.**

[33] **U.S Department of Health and Human Services**. (1998). "Occupational Exposure to Metal Working Fluid" , NIOSH Publication No. 98-102.

[34] **N.R. Dhar, M.W. Islam, S. Islam, M.A.H. Mithu,.** (2006). 'The influence of minimum quantity of lubrication (MQL) on cutting temperature, chip and dimensional accuracy in turning AISI-1040 steel'. Journal of Materials Processing Technology, vol : 171 , : 93–99.

[35] **E. Lugscheider, O. Knotek, C. Barimani, T. Leyendecker, O. Lemmer, R. Wenke**, (1997). Investigations on hard coated reamers in different lubricant free cutting operations, Surf. Coat. Technol. 90. pp: 172–177.

[36] **Walid M. Mohammad El Sabagh.** (2011) .' THE EFFECT OF THE MICROSTRUCTURE OF COMPACTED GRAPHITE IRON ON FRACTURE AND MACHINING.' McMaster University . P.H.D thesis.

[37] **Steve Dawson**, (2008). SinterCast, Sweden. Compacted graphite iron – A material solution for modern diesel engine cylinder blocks and heads. Pp.243-244 overseas foundary.

[38] **M. Bazdar, H.R. Abbasi∗, A.H. Yaghtin, J. Rassizadehghani,.** (2009). 'Effect of sulfur on graphite aspect ratio and tensile properties in compacted graphite irons' journal of materials processing technology. pp.1701–1705.

[39] **I. Riposan, M. Chisamera, R. Kelley, M. Barstow, R. L. Naro** – (2003). "Magnesium-Sulfur Relationships in Ductile and Compacted Graphite Cast Irons as Influenced by Late Sulfur Additions'. AFS Transactions 03-093.

[40] **J. Warrick Robert,G. Ellis Gerald,C. Grupke Clifford,R. Khamseh Amir,H. McLachlan Theodore, and Gerkits Carrie**. (2008). "Development and Application of Enhanced Compacted Graphite Iron for the Bedplate of the New Chrysler 4.7 Liter V-8 Engine", World of Science, Engineering and Technology 24.

[41] **K.P. Cooper, and C.R. Loper.** (1978), "A critical evaluation of the production of compacted graphite cast iron", American Foundary Society, 86, 267-272.

[42] **E. Campomanes, and R. Goller.** (1975), "Production of cast iron containing intermediate forms of graphite", Transactions of the American Foundrymen's Society, 83, Compendex, 55-62.

[43] **C.M.Ecob and C.Hartung, Elkem**. ASA, Norway 'An Alternative Route for the Production of Compacted Graphite Irons' pp.9-11.

[44] **Salete Martins Alves , Rolf Bertrand Schroeter, Júlio Celso dos Santos Bossardi Cássio Luiz Francisco de Andrade .** (2011). 'Influence of EP Additive on Tool Wear in Drilling of Compacted Graphite Iron' J. of the Braz. Soc. of Mech. Sci. & Eng , Vol. XXXIII, No. 2 / 197-202.

[45] **J. V. C. Souza,M. C. A. Nono,O. M. M. Silva, and M. V. Ribeiro**. (2008). "Comparative study on turning CI and CGI using silicon nitride

cutting tools". In: Salgado L., filho F.A., editors. Advanced Powder Technology Vi. Stafa-Zurich: Trans Tech Publications Ltd, 572-577.

[46] **N. Pretorius, and T. Toomey.** (2007), "Evaluation of different cutting tool materials for the interrupted machining of compacted graphite cast iron", Industrial Diamond Review, 67, Compendex, 41-44+47-48.

[47] **S. D. Rosa,A. E. Diniz,C. L. F. Andrade, and W. L. Guesser.** (2010), "Analysis of Tool Wear, Surface Roughness and Cutting Power in the Turning Process of Compact Graphite Irons with Different Titanium Content", Journal of the Brazilian Society of Mechanical Sciences and Engineering, 32, 3, 234-240.

[48] **Phillips, C.W.,** (1981), "Machinability of CGI," American Foundry Society Transactions, Paper no.81-179, pp. 47-52.

[49] **Sahm, A., Abele, E., and Schulz, H.,** (2002), "Machining of Compacted Graphite Iron (CGI), Spanende Bearbeitung von Gusseisen mit Vermiculargraphit (GJV)," Matwiss.U. Werkstofteck, 33, pp. 501-506.

[50] **Pretorius, N., Howard, T. P., Bowler J. J., and Toomey T.,** (2006), "Evaluation of Different Cutting Tool Materials for the Machining of High Strength Cast Irons," .Industrial Diamond Review, 66(2), pp. 33-37.

[51] **S. Gabaldo, A. E. Diniz, C. L. F. Andrade, and W. L. Guesser.** (2010), "Performance of Carbide and Ceramic Tools in the Milling of Compact Graphite Iron - CGI", Journal of the Brazilian Society of Mechanical Sciences and Engineering, 32, 5, 511-517.

[52] **Niniza S. P. Diamini, Iakovos Sigalas, and Andreas Koursaris,** (2008),. "Cutting tool wear and mechanisms of chip formation during high-speed machining of compacted graphite iron", 2007 ASME/STLE International Joint Tribology Conference, IJTC 2007, October 22, 2007 - October 24, 2007, San Diego, CA, United states, American Society of Mechanical Engineers, PART B, 701-703.

[53] **Ezugwu, E. O.,** (2005), "Key Improvements in the Machining of Difficult-to-Cut Aerospace Superalloys," International Journal of Machine Tools and Manufacture, 45, pp. 1353-1367.

[54] **Mohammed, W., M., Ng, E., Elbestawi, M.a.,,** (2011), Modeling the effect of the microstructure of compacted graphite iron on chip formation, International Journal of Machine Tools and Manufacture, Volume 51, Issues 10–11 : 753-765.

[55] **V.V. de Oliveira, P.A. de C. Beltrao, G. Pintaude.,** (2010), Effect of tool geometry on the wear of cemented carbide coated with TiAlN during drilling of compacted graphite iron, International Journal on the Science and Technology of Friction, Lubrication and Wear, volume 271 (2011): 2561– 2569.

[56] **M. Heck , H.M. Ortner , S. Flege , U. Reuter , W. Ensinger .**, (2007), Analytical investigations concerning the wear behaviour of cutting tools used for the machining of compacted graphite iron and grey cast iron, International Journal of Refractory Metals & Hard Materials 26 (2008) :197–206.

[57] **E. Abele, A. Sahm, H. Schulz,** (2002). Wear Mechanism when Machining Compacted Graphite Iron, CIRP Annals- Manufacturing Technology Volume 51, Issue 1, : 53-56.

[58] **Varun Nayyar, Jacek Kaminski, Anders Kinnander and Lars Nyborg.**, (2012) , An Experimental Investigation of Machinability of Graphitic Cast Iron Grades; Flake, Compacted and Spheroidal Graphite Iron in Continuous Machining Operations, 5th CIRP Conference on High Performance Cutting (2012): 488 – 493.

[59] **R. Evans, F. Hoogendoorn, & E. Platt,** (2011). Lubrication & Machining of Compacted Graphite Iron, Quaker Chemical Corporation, Metalworking Division Laboratory. Society of Tribologist and Lubrication Engineers. (STLE).

[60] **K. P. Varghese, and A. K. Balaji.** (2007), "Effects of tool material, tool topography and minimal quantity lubrication (MQL) on machining performance of compacted graphite iron (CGI)", International Journal of Cast Metals Research, 20, 6, 347-358.

[61] **Walker, T.**, (2012), Improving Tool Life with Minimum Quantity Lubrication Report courtesy, UNIST Technical Report.

[62] **Wakabayashi, T., Sato, H., and Inasaki, I.,** (1998), "Turning Using Extremely Small Amounts of Cutting Fluids," JSME International Journal, Series C: Mechanical Systems, Machine Elements and Manufacturing, 41(1), pp. 143-148.

[63] **Popke, H., Emmer, Th., and Steffenhagen, J.,** (1999), "Environmentally Clean Metal Cutting Processes - Machining on the Way to Dry Cutting," Proceedings of the Institution of Mechanical Engineers, Part B, 213, pp. 329-332.

[64] **Rahman, M., Senthil Kumar, A., and Manzoor-Ul-Salam,** (2001), "Evaluation of Minimal Quantities of Lubricant in End Milling," International Journal of Advanced Manufacturing Technology, 18(4), pp. 235-241.

[65] **S. Thamizhmanii, Rosli, S.Hasan,** (2009). A study of minimum quantity lubrication on Inconel 718 steel, Archives of Materials Science and Engineering 39/1 38-44.

[66] **L. R. Silva, E. C. Bianchi, R. E. Catai, R. Y. Fusse, T. V. França,P. R. Aguiar. ,** (2005). ‘Study on the Behavior of the Minimum Quantity Lubricant – MQL Technique under Different Lubricating and Cooling Conditions When Grinding ABNT 4340 Steel’. Journal of the Brazilian Society of Mechanical Sciences and Engineering., vol.27, n.2, pp. 192-199.

[67] **Kyung-Hee Park , JorgeOlortegui-Yume , Moon-ChulYoon , PatrickKwon.** (2010).‘A study on droplets and their distribution for minimum quantity lubrication (MQL)’ International Journal of Machine Tools & Manufacture. 50: 824–833.

[68] **B. Tasdelena, H. Thordenberg, D. Olofsson ,.** (2008).‘An experimental investigation on contact length during minimum quantity lubrication (MQL) machining’. journal of materials processing technology , volume 2 0 3,: 221–231.

[69] **Ali, S.M; Dhar, N.R. ; Dey, S.K ; .** (2011).‘ Effect of Minimum Quantity Lubrication (MQL) on Cutting Performance in Turning Medium Carbon Steel by Uncoated Carbide Insert at different speed-feed combinations’ . Advances in Production Engineering& Management . volume 6 , pp: 185-196.

[70] **Uwe Heisel; Marcel Lutz; Dieter Spath; Robert Wassmer; Ulrich Walter.** (2010) ‘Application of Minimum Quantity Cooling Lubrication Technology in Cutting Processes’. Universities of Stuttgart and Karlsruhe, Institute for Machine Tools I Institute for Machine Tools and Production Science. opus publication.

[71] **D.U. Braga, A.E. Diniz, G. Miranda, N.L. Coppini,** (1999). Minimal lubrication in the drilling process of aluminum–silicon alloy-A356 (SAE 323), in: Proceedings of the Third International Machining and Grinding Conference (SME), vol. 1, Cincinnati, USA, pp. 683–697.

[72] **K.M. Rahman,** (2004). Effect of minimum quantity lubrication (MQL) in drilling commercially used steels, M. Eng. Dissertation, BUET, Bangladesh.

[73] **R.B. Da Silva, J.M. Vieira, R.N. Cardoso, H.C. Carvalho, E.S. Costa, A.R.** (2011). ‘Tool wear analysis in milling of medium carbon steel with coated cemented carbide inserts using different machining lubrication/cooling systems’. International Journal on the Science and Technology of Friction, Lubrication and Wear. Vol :271, pp. 2459–2465.

[74] **A. Attanasio, M. Gelfi, C. Giardini, C. Remino ;** (2006).‘Minimal quantity lubrication in turning: Effect on tool wear’ . International Journal on the Science and Technology of Friction, Lubrication and Wear. Vol :260, pp. 333-338.

[75] **Dawson, S., and Schroeder, T.,** (2004), "Practical Applications for Compacted Graphite Iron," American Foundry Society Transactions, Paper no. 04-47(05).

[76] **ISO 16112:2006** Specifies Five Grades Of Compacted (Vermicular) Graphite Cast Irons.

[77] **Citing Websites**, Compacted Graphite Iron- Material Data Sheet, Retrieved Feb 5, 2013, from http://www.sintercast.com/library/technical-publications, .

[78] **Xavier, F.A,.** (2009) . ‘ Study of Wear Mechanisms in Si_3N_4 Tool Applied in Machining of Compactef Graphite and Grey Cast’, Doctoral Thesis, Federal University of Santa Catarina, Florianopolis, Brazil, 308 p. (In portuguese).

[79] **Groover, M., P.,** (2010), Fundamentals of Modern Manufacturing: Materials, Processes, and Systems, 4th Edition, ,Wiley & Sons.

[80] **Childs, T.H.C.; Maekawa, K.; Obikawa, T.; Yamane, Y.,** (2000), Metal Machining - Theory and Applications, London; New York: Arnold ; John Wiley & Sons,.

[81] **Ruff, G. F., and Doshi, B. K**., 1980, "Relation between Mechanical Properties and Graphite Structure in Cast Irons Part - 2," *Modern Casting*, July, pp. 70-74.

[82] **Komanduri, R., and Brown, R. H.,** 1981, "On the Mechanics of Chip Segmentation in Machining," *Journal of Engineering for Industry*, 103, pp. 33-42.

[83] **Wakabayashi, T., Sato, H., and Inasaki, I.,** 1998, "Turning Using Extremely Small Amounts of Cutting Fluids," *JSME International Journal, Series C: Mechanical Systems, Machine Elements and Manufacturing*, 41(1), pp. 143-148.

[84] **Popke, H., Emmer, Th., and Steffenhagen, J.,** 1999, "Environmentally Clean Metal Cutting Processes - Machining on the Way to Dry Cutting," *Proceedings of the Institution of Mechanical Engineers, Part B,* 213, pp. 329-332.

[85] **Luo, X., Cheng, K., Holt, R., and Liu, X.,** 2005, "Modeling Flank Wear of Carbide Tool Insert in Metal Cutting," *Wear*, 259, pp. 1235-1240.

[86] **Shahabi, H. H., and Ratnam, M. M.,** 2008, "In-Cycle Monitoring of Tool Nose Wear and Surface Roughness of Turned Parts using Machine Vision," *International Journal of Advanced Manufacturing Technology*, DOI 10.1007/s00170-008-1430-8.

[87] **Chattopadhyay, A. K., and Chattopadhyay, A. B.,** 1989, "Mechanism of Crater Wear Growth of Coated Carbides in High Speed Machining," *Journal of the Institution of Engineers (India),* Part PR, Production Engineering Division. 70(1), pp. 19-26.

[88] **Kato, S., Yamguchi, K., and Yamada, M.,** 1972, "Stress Distribution at the Interface between Tool and Chip in Machining," *Transacation of ASME, Journal of Engineering for Industry*, 94, pp. 683-689.

[89] **Doyle, E. D., Home, J. G., and Tabor, D.,** 1979, "Frictional Interactions between Chip and Rake Face in Continuous Chip Formation," *Proceedings of Royal Society of London,* A366, pp. 173-183.

[90] **Davis J.R.** ,1998, "Metals Handbook, Desk Edition.", West Conshohocken, PA, ASM International Handbook Committee.

[91] **ASTM Standards A247-67."**Standard Test Method for Evaluating the Microstructure of Graphite in Iron Castings".. West Conshohocken, PA: ASTM International, (1971).

[92] **BCIRA,** (1981), "Effect of Some Residual or Trace Elements on Cast Iron",

[93] **Yih-Hsun Shy,Cheng-Hsun Hsu,Shen-Chih Lee, and Chih-Yuan Hou.** (2000), "Effects of titanium addition and section size on microstructure and mechanical properties of compacted graphite cast iron", Materials Science and Engineering A, 278, Compendex, 54-60.

[94] **G. F. Ruff, and T. C. Vert.** (1979), "Investigation of Compacted Graphite Iron Using a High Sulfur Gray Iron Base", AFS Transactions, 87, 459-464.

[95] **F. Martinez, and D. M. Stefanescu,** (1983),"Properties of compacted/vermicular graphite cast irons in the Fe-C-Al system produced by ladle and in-mold treatment", Transactions of the American Foundrymen's Society, Proceedings of the Eighty-seventh Annual Meeting, Rosemont, IL, USA, AFS, 91, 593-606.

[96] **M. Konig.** (2010), "Literature review of microstructure formation in compacted graphite Iron", International Journal of Cast Metals Research, 23, 3, 185-192.

[97] **A. Velichko,C. Holzapfel, and F. Mucklich.** (2007), "3D Characterization of Graphite Morphologies in Cast Iron", Advanced Engineering Materials, 9, 1-2, 39-45.

[98] **Torsten Sjogren,Peter Vomacka, and Ingvar L. Svensson.** (2004), "Comparison of mechanical properties in flake graphite and compacted graphite cast irons for piston rings", International Journal of Cast Metals Research, 17, Compendex, 65-71.

[99] **G.F. Sergeant, and E.R. Evans.** (1978), "The Production and Properties of Compacted Graphite Irons", British Foundryman, 71(5), 115-124.

[100] **J.P. Hrusovsky.** "Formation, production and properties of compacted graphite iron",Ph.D. Thesis, Case western Reserve University, Cleveland; (1982).

[101] **M. Selin.** (2010), "Tensile and Thermal Properties in Compacted Graphite Irons at Elevated Temperatures", Metallurgical and Materials Transactions a Physical Metallurgy and Materials Science, 41A, 12, 3100-3109.

[102] **R. O. Marwanga,R. C. Voigt, and P. H. Cohen.** (1999), "Influence of graphite morphology and matrix structure on chip formation during machining of gray irons", Transactions of the American Foundrymen's Society, 107, 595-607.

[103] **Niniza S. P. Diamini,Iakovos Sigalas, and Andreas Koursaris,** (2008),"Cutting tool wear and mechanisms of chip formation during high-speed machining of compacted graphite iron", 2007 ASME/STLE International Joint Tribology Conference, IJTC 2007, October 22, 2007 - October 24, 2007,

[104] **E. Ceretti,M. Lucchi, and T. Altan.** (1999), "FEM simulation of orthogonal cutting: serrated chip formation", Journal of Materials Processing Technology, 95, 1-3, 17-26.

[105] **R. G. Fenton, P L B Oxley,** (1968), "Mechanics of orthogonal machining allowing for the effects of strain rate and temperature on tool-chip friction," Proceedings of the Institution of Mechanical Engineers, 183, 417-438.

[106] **N. R. Dhar, M. Kamruzzaman, Mahiuddin Ahmed,** (2007), "Effect of Minimum Quantity Lubrication (MQL) on Tool Wear, Surface Roughness and Dimensional Deviation in Turning AISI-4340 Steel", Journal of Materials Processing Technology, 20(2): 23-32.

APPENDICES

APPENDIX A: Flank wear, for DRY, V_c = 200m/min and f= 0.3mm/rev
APPENDIX B: Flank wear, for MQL, V_c = 200m/min and f= 0.3mm/rev
APPENDIX C: Crater wear for DRY and MQL, V_c = 200m/min and f= 0.3mm/rev

APPENDIX A

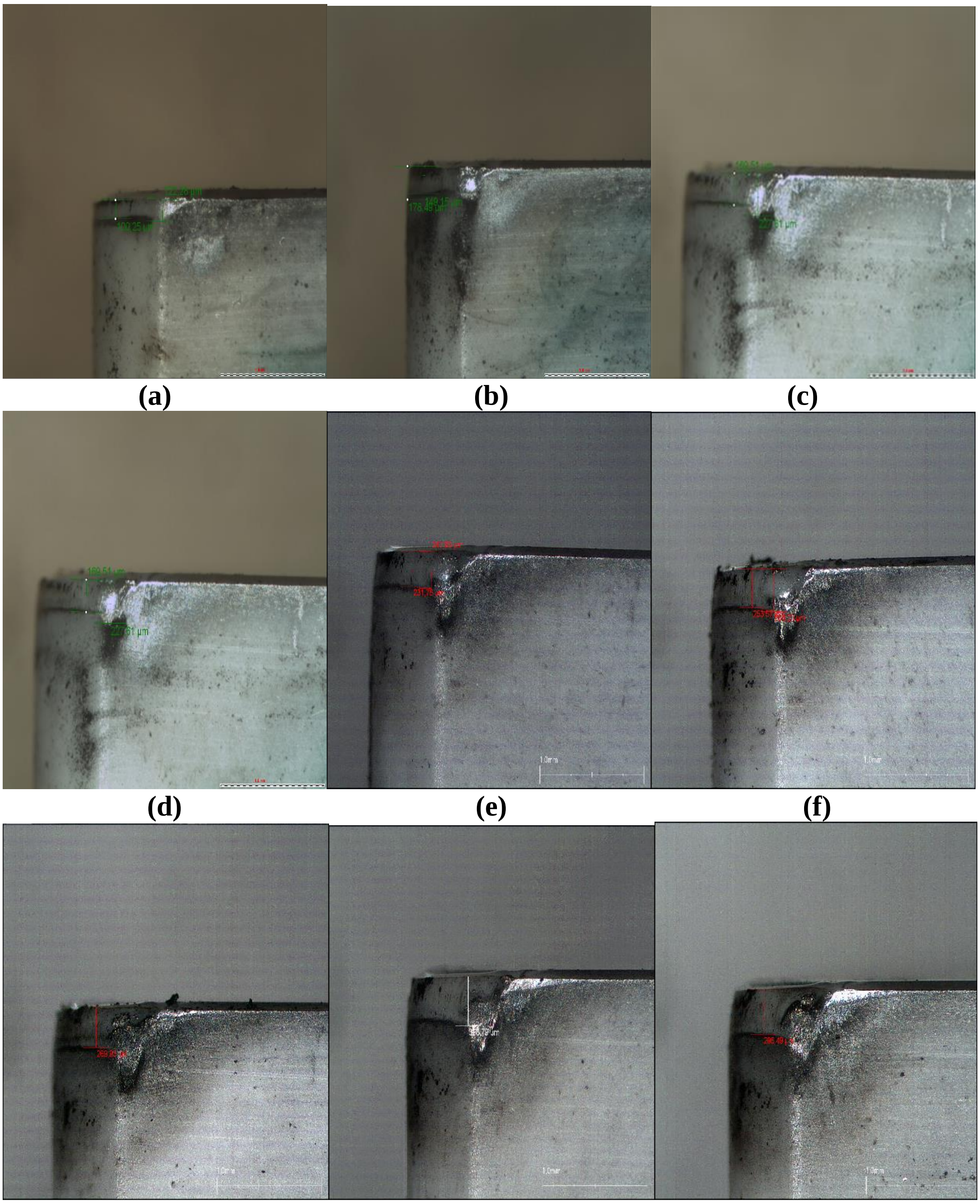

(a) (b) (c)

(d) (e) (f)

(g) (h) (i)

Figure A.1 : Flank wear, for DRY machining, Vc = 200m/min and f= 0.3mm/rev: (a)5th pass. (b)10th pass. (c)15th pass. (d)18th pass. (e)23th pass. (f)28th pass. (g)33th pass. (h)38th pass. (i)43th pass.

APPENDIX B

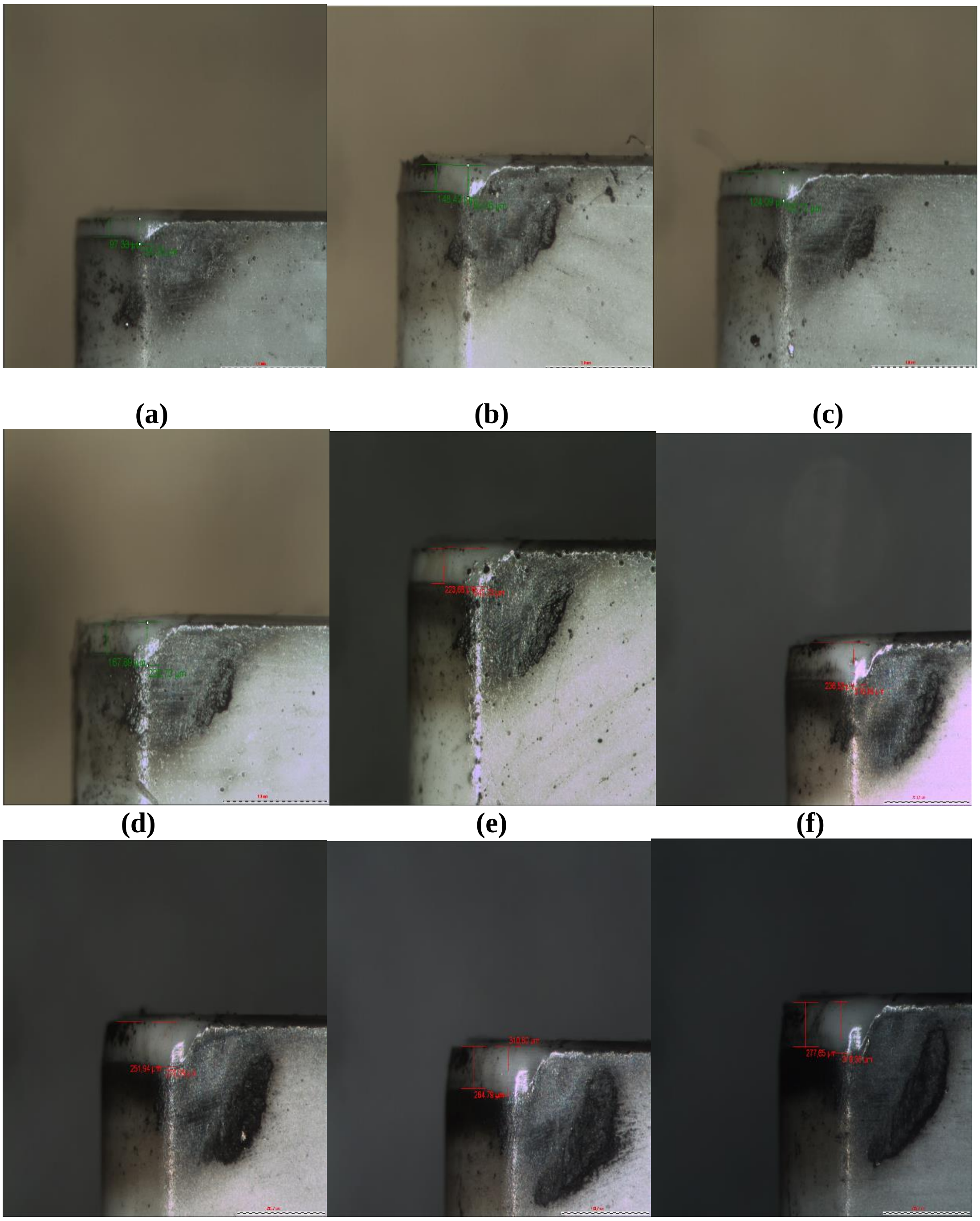

(a) (b) (c)

(d) (e) (f)

(g) (h) (i)

Figure B.1 : Flank wear, for MQL machining, V_c = 200m/min and f= 0.3mm/rev: (a)5th pass. (b)10th pass. (c)15th pass. (d)18th pass. (e)23th pass. (f)28th pass. (g)33th pass. (h)38th pass. (i)43th pass.

APPENDIX C

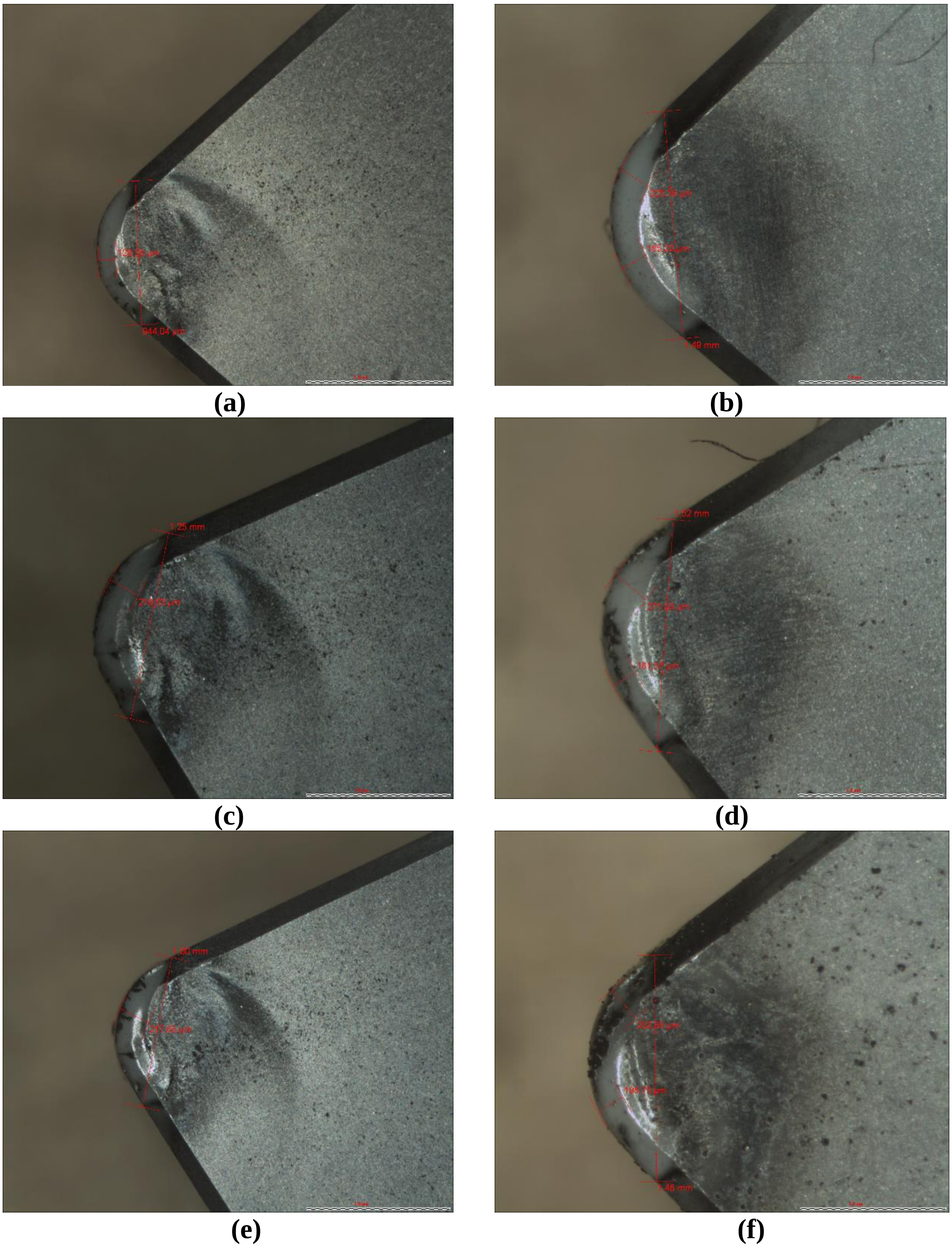

Figure C.1 : Crater wear, for DRY machining, V_c = 200m/min and f= 0.3mm/rev: (a)5th pass. (c)10th pass. (e)15th pass., Crater wear, for MQL machining, V_c = 200m/min and f= 0.3mm/rev: (b)5th pass. (d)10th pass. (f)15th pass.

CURRICULUM VITAE

Name Surname: Armin Bijanzad

Place and Date of Birth: Tabriz – Iran / 03/23/1987

Address: Bakırköy/ Istanbul

E-Mail: feb.301@gmail.com

B.Sc.: **University of Tabriz, Mechanical Engineering (Manufacturing and Production program)**

M.Sc.: **Istanbul Technical University, Mechanical Engineering (Materials and Manufacturing program)**

List of Publications and Patents:

PUBLICATIONS/PRESENTATIONS ON THE THESIS

- **A.Bijanzad,** A.T.Kuzu, M.Bakkal, 2013: " Influence of MQL on tool wear in CGI turning ", 7th International Conference and exhibition on design and production of machines and dies/molds. Antalya, Turkey, June 2013.
- **A.Bijanzad,** A.T.Kuzu, M.Bakkal, 2013: " Experimental study of minimum quantity lubrication effect on compacted graphite iron machining ", 11th Global Conference on Sustainable Manufacturing. Berlin, Germany, September 2013.
- Kuzu, A.T., **Bijanzad, A.,** Bakkal, M., 2013: "Experimental Evaluation on the Effect of Minimum Quantity Lubrication in CGI turning", Journal of Mechanical Working Technology. 2013 (In review procedure).